

平成 27 年度 修士論文

Evaluation of the Weight Perception With a  
Control Based on the Modification of the  
Relation between the Human and the Reaction  
Force

指導教員 池浦 良淳

博士前期課程 機械工学専攻  
システム設計研究室

Rodríguez Martínez Itzel Jared

三重大学大学院 工学研究科

---

# Acknowledgments

---

I would like to thank all the people who contributed in some way to the work described in this thesis. First and foremost, I thank my academic advisor, Professor Ikeura Ryojun, for accepting me into his group. During my tenure, he contributed to a rewarding graduate school experience by giving me intellectual freedom in my work, supporting my attendance at various conferences, engaging me in new ideas, and demanding a high quality of work in all my endeavors.

I would like to express my gratitude to Sawai Hideki, who contributed greatly to this project with his support and all his practical knowledge and who spend many days with us devising, creating and testing the system.

I am also very grateful to the Japanese Ministry of Education, Culture, Sports, Science and Technology (Monbukagakusho: MEXT) for the funding sources that allowed me to pursue my graduate school studies

I would be remiss if I did not thank Fujiwara Akiko, who deserves credit for providing much needed assistance with administrative tasks, impending deadlines, and keeping our work running smoothly.

I would like to acknowledge the Department of Mechanical Engineering at Mie University. My graduate experience benefitted greatly from the courses I took, the opportunities I had to serve as a teaching assistant, and the seminars that the department organized. Within Mie University, I would also like to thank all the help and opportunities provided by the Center for International Education and Research, who made all the possible for this experience to be successful and to run.

I should as well address the help and support of fellow labmates who made the long hours at the laboratory fun and who bared with my interminable questions.

Last but not least, I want to acknowledge my family, blood related or not, who supported me even from afar.

---

# Table of Contents

---

Acknowledgments .....	II
List of Figures.....	V
List of Tables .....	VII
List of Abbreviations .....	VIII
Chapter 1 Introduction .....	1
1.1 Research Motivations .....	1
1.2 Research Objectives.....	1
1.3 Outline of this Thesis .....	2
Chapter 2 Background.....	4
2.1 Weight Perception .....	4
2.2 Power Assist Devices.....	5
2.3 Previous experiments.....	5
2.4 Phases of the Lifting .....	6
Chapter 3 Methodology for the Weight Perception's Modification .....	7
3.1 Relationship between the Reaction Force and the Human Force .....	7
3.2 Control Algorithm.....	13
Chapter 4 Experimental System.....	14
4.1 Objects .....	14
4.2 Experimental Device.....	15
4.3 Electronics of the System .....	17
Chapter 5 Experimental Method .....	22
5.1 Subjects.....	22
5.2 Lifting Method.....	22
Chapter 6 Experimental Results.....	25
6.1 Subjective Results.....	25
6.2 Data from the Sensors.....	32

Table of Contents	IV
Chapter 7 Discussion and Conclusions .....	45
7.1 Discussion.....	45
7.2 Conclusions.....	47
7.3 Future Work .....	48
Appendices .....	50
A. Accelerometer's Specifications.....	50
B. Gap Sensor's Specifications.....	51
C. PIC18F4455's Specifications .....	52
D. Comparisons between the PW and the Recorded Forces ( $m_d=0.45$ kg, $w_d=4.41$ N, Time Length: Entire Lifting).....	53
E. Comparisons between the PW and the Recorded Forces ( $m_d=0.45$ kg, $w_d=4.41$ N, Time Length: Detaching Phase).....	55
F. Comparisons between the PW and the Recorded Forces ( $m_d=0.55$ kg, $w_d=5.39$ N, Time Length: Entire Lifting).....	57
G. Comparisons between the PW and the Recorded Forces ( $m_d=0.55$ kg, $w_d=5.39$ N, Time Length: Detaching Phase).....	59
References .....	61
Publications Based on the Contents of this Thesis .....	63

# List of Figures

Fig.3.1 Body Diagram of the Free Object .....	7
Fig.3.2 Imaginary Modification of the Relation between HF and RF.....	8
Fig.3.3 Process of Creation of the New Functions .....	9
Fig.3.4 Peaks by Position .....	10
Fig.3.5 Peaks by Amplitude.....	10
Fig.3.6 Plots of the Possible Peaks .....	12
Fig.3.7 Body Diagram of the Object with PA Provided .....	13
Fig.4.1 Objects Lifted.....	14
Fig.4.2 Block Diagram of the Experimental System.....	15
Fig.4.3 Frontal View of the System .....	16
Fig.4.4 Isometric View of the System .....	16
Fig.4.5 Electronic Diagram for the RF's Load Cell and the Velocity.....	18
Fig.4.6 Electronic Diagram for the HF's Load Cells .....	19
Fig.4.7 Electronic Diagram for the PIC.....	21
Fig.5.1 Seat used during the Liftings (Left: Seat, Right: Posture for the Lifting).....	22
Fig.5.2 Grip used for the Liftings (Left: Upper View, Right: Side View).....	23
Fig.6.1 Perceived Weight and Position of the Peak (MI and MD, $m_d=0.45$ kg, $w_d=4.41$ N) .....	25
Fig.6.2 Perceived Weight and Amplitude of the Peak (MI and MD, $m_d=0.45$ kg, $w_d=4.41$ N) .....	26
Fig.6.3 Perceived Weight and Position of the Peak (Average, $m_d=0.45$ kg, $w_d=4.41$ N) .....	26
Fig.6.4 Perceived Weight and Amplitude of the Peak (Average, $m_d=0.45$ kg, $w_d=4.41$ N) .....	27
Fig.6.5 Perceived Weight and Position of the Peak (MI and MD, $m_d=0.55$ kg, $w_d=5.39$ N) .....	28
Fig.6.6 Perceived Weight and Amplitude of the Peak (MI and MD, $m_d=0.55$ kg, $w_d=5.39$ N) .....	29
Fig.6.7 Perceived Weight and Position of the Peak (Average, $m_d=0.55$ kg, $w_d=5.39$ N) .....	29
Fig.6.8 Perceived Weight and Amplitude of the Peak (Average, $m_d=0.55$ kg, $w_d=5.39$ N) .....	30

Fig.6.9 Position of the Peak and Difference between the Perceived Mass and the Desired Mass .....	31
Fig.6.10 Amplitude of the Peak and Difference between the Perceived Mass and the Desired Mass .....	31
Fig.6.11 Data from the Sensors ( $m_d=0.45$ kg, Entire Recorded Length).....	33
Fig.6.12 Data from the Sensors ( $m_d=0.45$ kg, $w_d=4.41$ N, Entire Lifting).....	33
Fig.6.13 PW and HF Arranged by the Position of the Peak ( $m_d=0.45$ kg, $w_d=4.41$ N, Lifting).....	34
Fig.6.14 PW and HF Arranged by the Amplitude of the Peak ( $m_d=0.45$ kg, $w_d=4.41$ N, Lifting).....	34
Fig.6.15 PW and (W-PA) Arranged by the Position of the Peak ( $m_d=0.45$ kg, $w_d=4.41$ N, Lifting).....	35
Fig.6.16 PW and (W-PA) Arranged by the Amplitude of the Peak ( $m_d=0.45$ kg, $w_d=4.41$ N, Lifting).....	35
Fig.6.17 Data from the Sensors ( $m_d=0.45$ kg, $w_d=4.41$ N, Detaching Phase).....	36
Fig.6.18 PW and HF Arranged by the Position of the Peak ( $m_d=0.45$ kg, $w_d=4.41$ N, Detaching Phase).....	37
Fig.6.19 PW and HF Arranged by the Amplitude of the Peak ( $m_d=0.45$ kg, $w_d=4.41$ N, Detaching Phase).....	37
Fig.6.20 PW and (W-PA) Arranged by the Position of the Peak ( $m_d=0.45$ kg, $w_d=4.41$ N, Detaching Phase).....	38
Fig.6.21 PW and (W-PA) Arranged by the Amplitude of the Peak ( $m_d=0.45$ kg, $w_d=4.41$ N, Detaching Phase) .....	38
Fig.6.22 Data from the Sensors ( $m_d=0.55$ kg, $w_d=5.39$ N, Entire Recorded Length).....	39
Fig.6.23 Data from the Sensors ( $m_d=0.55$ kg, $w_d=5.39$ N, Lifting) .....	40
Fig.6.24 PW and HF Arranged by the Position of the Peak ( $m_d=0.55$ kg, $w_d=5.39$ N, Lifting).....	40
Fig.6.25 PW and HF Arranged by the Amplitude of the Peak ( $m_d=0.55$ kg, $w_d=5.39$ N, Lifting).....	41
Fig.6.26 PW and (W-PA) Arranged by the Position of the Peak ( $m_d=0.55$ kg, $w_d=5.39$ N, Lifting).....	41
Fig.6.27 PW and (W-PA) Arranged by the Amplitude of the Peak ( $m_d=0.55$ kg, $w_d=5.39$ N, Lifting).....	42
Fig.6.28 Data from the Sensors ( $m_d=0.55$ kg, $w_d=5.39$ N, Detaching Phase).....	42
Fig.6.29 PW and HF Arranged by the Position of the Peak ( $m_d=0.55$ kg, $w_d=5.39$ N, Detaching Phase).....	43

Fig.6.30 PW and HF Arranged by the Amplitude of the Peak ( $m_d=0.55$ kg, $w_d=5.39$ N, Detaching Phase) .....	43
Fig.6.31 PW and (W-PA) Arranged by the Position of the Peak ( $m_d=0.55$ kg, $w_d=5.39$ N, Detaching Phase) .....	44
Fig.6.32 PW and (W-PA) Arranged by the Amplitude of the Peak ( $m_d=0.55$ kg, $w_d=5.39$ N, Detaching Phase) .....	44
Fig.D.1 PW and PA Arranged by the Position of the Peak ( $m_d=0.45$ kg, $w_d=4.41$ N, Lifting).....	53
Fig.D.2 PW and PA Arranged by the Amplitude of the Peak ( $m_d=0.45$ kg, $w_d=4.41$ N, Lifting).....	53
Fig.D.3 PW and RF Arranged by the Position of the Peak ( $m_d=0.45$ kg, $w_d=4.41$ N, Lifting).....	54
Fig.D.4 PW and RF Arranged by the Amplitude of the Peak ( $m_d=0.45$ kg, $w_d=4.41$ N, Lifting).....	54
Fig.E.1 PW and PA Arranged by the Position of the Peak ( $m_d=0.45$ kg, $w_d=4.41$ N, Detaching) .....	55
Fig.E.2 PW and PA Arranged by the Amplitude of the Peak ( $m_d=0.45$ kg, $w_d=4.41$ N, Detaching) .....	55
Fig.E.3 PW and RF Arranged by the Position of the Peak ( $m_d=0.45$ kg, $w_d=4.41$ N, Detaching) .....	56
Fig.E.4 PW and RF Arranged by the Amplitude of the Peak ( $m_d=0.45$ kg, $w_d=4.41$ N, Detaching) .....	56
Fig.F.1 PW and PA Arranged by the Position of the Peak ( $m_d=0.55$ kg, $w_d=5.39$ N, Lifting).....	57
Fig.F.2 PW and PA Arranged by the Amplitude of the Peak ( $m_d=0.55$ kg, $w_d=5.39$ N, Lifting).....	57
Fig.F.3 PW and RF Arranged by the Position of the Peak ( $m_d=0.55$ kg, $w_d=5.39$ N, Lifting).....	58
Fig.F.4 PW and RF Arranged by the Amplitude of the Peak ( $m_d=0.55$ kg, $w_d=5.39$ N, Lifting).....	58
Fig.G.1 PW and PA Arranged by the Position of the Peak ( $m_d=0.55$ kg, $w_d=5.39$ N, Detaching) .....	59

Fig.G.2 PW and PA Arranged by the Amplitude of the Peak ( $m_d=0.55$ kg, $w_d=5.39$ N, Detaching) .....	59
Fig.G.3 PW and RF Arranged by the Position of the Peak ( $m_d=0.55$ kg, $w_d=5.39$ N, Detaching) .....	60
Fig.G.4 PW and RF Arranged by the Amplitude of the Peak ( $m_d=0.55$ kg, $w_d=5.39$ N, Detaching) .....	60

---

# List of Tables

---

TABLE 3.1 POSSIBLE POSITIONS OF THE PEAK WITH THE AMPLITUDE AS REFERENCE .....	11
TABLE 3.2 POSSIBLE AMPLITUDES OF THE PEAK WITH THE POSITION AS REFERENCE .....	11
TABLE 5.1 TESTED POSITIONS AND AMPLITUDES OF THE PEAKS TESTED	24
TABLE 6.1 PERCEIVED WEIGHTS (MI AND MD, $m_d=0.45$ kg, $w_d=4.41$ N) .....	27
TABLE 6.2 PERCEIVED WEIGHTS (AVERAGE, $m_d=0.45$ kg, $w_d=4.41$ N) .....	28
TABLE 6.3 PERCEIVED WEIGHTS (MI, MD AND AVERAGE, $m_d=0.55$ kg, $w_d=5.39$ N) .....	30
TABLE 6.4 DIFFERENCE BETWEEN THE REAL MASS AND THE DESIRED MASS .....	32

# List of Abbreviations

---

In alphabetical order:

DOF	Degree Of Freedom
HF	Human Force
MD	Mass Decreasing
MI	Mass Increasing
PA	Power Assist
PAD	Power Assist Device
PAF	Power Assist Force
PW	Perceived Weight
RF	Reaction Force

---

# Chapter 1

## Introduction

---

### 1.1 Research Motivations

Our society has managed to extend the life expectancy of its population and with this comes an increased necessity of external help to perform the daily activities. This demographic phenomenon comes with a longer life expectancy and an elder working class. That in turns implies an increase of the need for assistance in the industry and at home. This need is more and more provided by automated systems and within them, power assist devices (PAD).

These devices are designed to work in cooperation with the users and that's why they need to be resistant enough to perform their task and at the same time supple enough to adapt to the characteristics of the humans they work with. This is a daunting task even for systems without human input: the need for the system to be able to perform their purpose, for the control to be stable, efficient, etc.

However, for systems that need to interact with humans, another problem that arises is that humans react according to their perception and this last one is susceptible to misinterpretations. Therefore any PAD designer must aim to understand the factors behind human perceptions.

So far, these perceptions have been studied mostly on psychological grounds, however, when these factors are not contemplated in the design of PA devices, the expectations of the users and the behavior of the system may mismatch. This results in malfunctions of the system, accidents or at least, discomfort. This in turn, makes the device useless and even dangerous.

This is why we consider vital to first determine the factors behind the weight perception and then, to apply this knowledge into the creation of PAD that can range from complex systems for industrial applications to more simple artifacts for domestic use.

### 1.2 Research Objectives

The overall objective of our research is to elucidate the factors that affect the weight perception when lifting objects with PA devices.

In our recent experiments, the lifting of an object has been divided in different phases. This division let us also separate the forces and factors that are in place at each

one of the different phases and measure their impact on the perceived weight (PW).

The focus of this research was on the first part of the lifting, when the object still have at least some contact with the surface that supports it. In this phase there few forces that react on the object, the subject isn't holding the entire weight of the object yet and the acceleration is basically null. This phase is interesting because it's when the first contact between the subject and the objects takes place. Therefore, the preliminary weight impressions are compared to the felling of the real object and corrections are made.

Considering the Laws of Motion, in non-altered circumstances, the reaction force (RF) from the support surface and the force applied from the subject to lift an object (human force HF) are linearly proportional.

However, our hypothesis was that modifying that linearity could have an impact on the weight perception.

Therefore, the objective of the experiments presented on this paper was to determine if our hypothesis was true or false. Since it has been reckoned that when working with haptic devices, the complexity of a multi degree of freedom (DOF) system may induce degradations in the sensing performance [1], a simple 1DOF device was found fitted for these experiments.

### **1.3 Outline of this Thesis**

Since our hypothesis was that modifying the HF-RF relation could have an impact on the weight perception, in this thesis research, a simple 1DOF (vertically up-down motion) PA device was developed for lifting objects and the object tied to the PA system was lifted by the human operator. In the control algorithm of the PA device, several functions representing the HF as a function of the RF were implemented

For the experiments, two desired masses, one 0.25 kg lighter than the actual mass of the object and other 0.15 kg lighter were tested. Moreover, the position and acceleration of the object, the RF and the HF were acquired via sensors implemented in the system. Additionally, the subjective PWs were registered.

Chapter 2 shows the background research for the current thesis. The background includes a brief explanation of what is the weight perception and of the PA devices. Also, the outline of previous experiments that leded to this research and the phases considered for the experiments are included.

Chapter 3 explains the theory behind the creation of the PA device. The relation between the RF and the HF is shown. Moreover, the proposed modifications to that relation and the resultant control algorithm are presented.

Chapter 4 describes the objects used for the experiments and the mechanical and electrical configuration of the experimental device.

Chapter 5 introduces the subjects that performed the experiments and explains the methodology followed on the experiments.

Chapter 6 shows the data obtained on the experiments. It includes both the subjective results from the subject's perception and the objective data obtained from the sensor implemented in the system.

Chapter 7 is the last chapter of this thesis paper. In it, a general discussion of the results and probable causes is performed. It also includes the concluding remarks and the future directions foreseeable for this research.

Afterwards, the appendices, references and a list of the publications based on the contents of this thesis are included.

---

# Chapter 2

## Background

---

Our society has managed to extend the life expectancy of its population and with it comes the necessity of external help to perform the daily activities. This demographic phenomenon implies a longer life expectancy and an elder working class, which in turns translates as an increased necessity of assistance, especially for lifting objects.

Nowadays, that help is progressively provided by machines and artificial systems. Due to the fact that their control is based on the cooperation between user and machine, is in that niche where PADs enter. However, in order to achieve a good symbiosis between the user and the device, comprehending the human response and the factors that affect it is vital.

### 2.1 Weight Perception

The human body has special cells called sensory receptors that can detect external factors as light or sound. When one of these sensory receptors detects a stimulus, it sends a signal to the brain. This reception represents sensation. How the brain interprets these sensations and makes them meaningful is called perception. Most of the times, the interpretation of the stimuli is consistent with it. However, sometimes this interpretation is incorrect. The name given to these misinterpretations is “illusions” [2].

The human response is affected by many illusions, among them in the weight perception. According to dictionary definitions, a weight illusion is when a sensory stimulus causes a distorted feeling or impression of the physical weight of an object. This definition encloses a series of illusions that are linked to the way that the misperception is produced, for example: due to the size of the objects, its temperature or material. The first one of these illusions to appear in the literature and one of the more researched is the Size-Weight or Charpentier Effect [3].

In several of these illusions, the sensory stimulus is opposed to the expectation of the subjects (for example: when the smaller object is perceived as heavier than a bigger one, both of them being actually of same mass). This contradiction between expectation and perception is called “Anti-Bayesian” [4] and implies that not only the physical sensations are implied, but also that there are psychological expectations that contribute to the illusion. There are many factors that allegedly contribute to the weight illusions, some of them psychological, others physical. But so far none of these factors alone can

fully account for the weight illusion [4]. However, since a research aiming to comprehend the human response tends to be challenged by the complexity that accompanies any human activity, the literature advises to first research each of the suspected factors by himself and then, to build a scenario integrating such factor with the rest of the previously researched ones [4].

Researches show that before lifting or even making contact with an object, using cues gathered through their senses and previous experiences, humans make an estimation of the force and characteristics needed to perform the lifting [5]. Due to the “uniqueness” of every person, narrowing down the factors that affect the weight perception is particularly difficult. Moreover, because after a few trials and even without being aware of doing so, users can modify the force that they apply to perform the lifting [6]. Although these subconscious corrections fix the force disparity, they don't prevent the weight illusion from happening [7].

## 2.2 Power Assist Devices

Unlike other devices, PA systems are designed to work in cooperation with the user, providing the power that humans lack to perform an action but without the stiffness that accompanies the mechanical systems. However, the advantages that characterize PA systems are also what make them difficult to devise, like the need for portability [8] or the desire for them to adapt to the user [9].

On one part, the system must be robust enough to fulfill its purpose, which in many cases involves lifting heavy objects and therefore, power elements. On the other part, the system must be safe and supple enough to cooperate on the task with the subject. Otherwise, the device may end up startling the user, being unstable or even causing accidents [10] [11].

Therefore, for this type of devices, it is not enough to comprehend the inherent factors of the task that affect the human perception, it is also necessary to research how the characteristics of the system can affect the perception of the user and even the way the user perceives the system.

On the other hand, some of the physical aspects of the system have been found to have an impact on the weight perception. The physical characteristics of the system have even been used to try to artificially produce the weight perception in virtual environments [12].

## 2.3 Previous experiments

In previous experiments at our Laboratory, some factors that affect the weight

perception have been researched. It has been found that the PW is affected by the lifting scheme, that is, that the PW of an object of same mass can be different depending if the object is lifted in an unimanual, bimanual or cooperative way [13].

Moreover, worst case scenarios have also been researched by determining the PW of lifting objects in tilted positions or without sight of those objects and comparing it to the PW of objects of same mass without such impediments [13].

Another factor that has been found related to the PW is the type of motion of the lifting, i.e. if the object was lifted using a simple linear vertical movement or using a harmonic repetitive movement [14].

Furthermore, other experiment determined the influence of the grip scheme on the PW. The grip scheme refers to the position of the hand relative to the object and to the surface of contact between the hand and the object at the moment of the lifting [15]. On that experiment, the system used was a 1 DOF PA device. Such a device constraints the object at the moment of the lifting and the effect on the PW of that restriction on the mobility was also reported [16]. What's more, in order to reduce the influence of that restriction on the PW when lifting an object with a 1 DOF PA device and comparing it with an unconstrained object, the best grip scheme was determined.

## 2.4 Phases of the Lifting

The results obtained in the previous experiments made us consider the lifting of an object as set of different phases and to consider independently within each of them, which factors affect the PW.

For this research, the lifting has been separated into two phases: one for the detaching of the object, that is, from the moment the object is fully supported on the surface until it is completely detached from it. This was considered the passive phase of the lifting because the subject doesn't hold yet the entire weight of the object, the position change of the object is minimal compared to the entire length of the lifting and so is the acceleration. Is at this phase when the subject enters in contact with the object, gets to see it, make a preliminary impression of its composition and weight, feel it for the first time and even to make small adjusts.

The other phase of the lifting is from the moment the object is fully detached from the surface that supports it until it is again completely on that surface, without any of its weight lifted by the subject. This was considered the active phase of the lifting, the acceleration being significant, without RF from the support surface and the entire weight of the object being lifted by the user and the PA device.

# Chapter 3

## Methodology for the Weight Perception's Modification

Three different concepts about the object were managed on this research. The first one was the real mass  $m$  [kg], which was the physical mass of the object without PA. The second one was the desired mass  $m_d$  [kg], which was the aimed mass for the subjects to perceive. The third one was the PW [N], which was the weight that the subjects expressed the object to be, after lifting it in the experiment.

For the design of the control algorithm, the lifting was separated into two phases. These phases are described on the previous chapter.

### 3.1 Relationship between the Reaction Force and the Human Force

The focus of this research was on the relationship between the Reaction Force (RF) and the Human Force (HF) at the detaching phase. During this phase, the acceleration was considered as null and therefore, the physical laws applicable were those for a static object. Fig.3.1 shows the forces applied in a lifting without PA.

In this case, the relation between RF and HF is given by Newton's First Law as shown in (1).

$$0 = F_h + R - mg \quad (1)$$

Where  $m$  was the mass of the object [kg],  $F_h$  the HF [N],  $R$  the RF applied on the object from the table [N] and  $g$  was the gravity constant [ $m/s^2$ ].

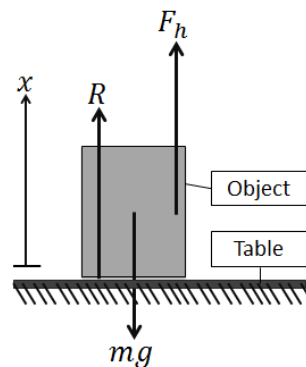


Fig.3.1 Body Diagram of the Free Object

Therefore, we can see that the RF and the HF have a linear correspondence as shown in (2).

$$F_h = mg - R \quad (2)$$

Since this research was based on the modification of the aforementioned relation between HF and RF, the HF was considered as a function of the RF, as stated in (3).

$$F_h = f(R) \quad (3)$$

To illustrate this, let's consider the example shown in Fig.3.2. In it, the blue line corresponds to the original relation of the HF and the RF. The green and the purple line correspond to imaginary modifications of that relation. The vertical axis represents the RF and the horizontal axis represents the HF. If we observe the blue line, we can see that the HF and the RF are straightforward and dependent of the weight of the object.

However, even if the green line starts and ends at the same points that the blue line, we can see that when the RF is at its maximum and as it decreases, the subject is required to proportionate not only more force but also to do it at an earlier stage than in the case of the blue line. For the example of the green line, most of the HF is suddenly required in the first quarter of the lifting and from that point, the HF rises slowly until it reaches its maximum and the RF is zero.

As for the purple line, it starts and ends also at the same points as the blue and the green lines, but the subject requires less force to lift the object from the support surface. Moreover, the HF is small for two thirds of the lifting (considering from the maximum of the RF until it becomes zero) and then suddenly rises until its maximum.

Therefore, this modification do change the force needed to lift the object and should modify also the PW from lifting it. Furthermore, the proportion and timing at which the HF is required are modified too.

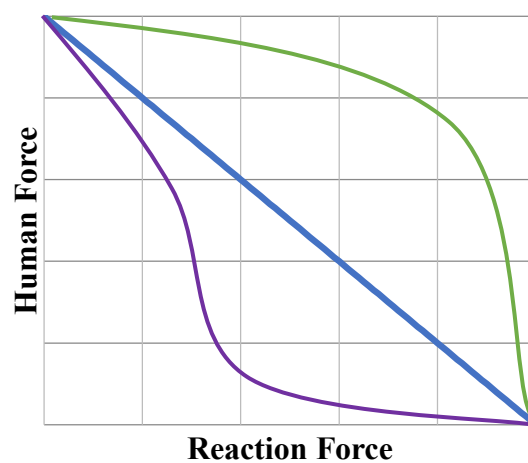


Fig.3.2 Imaginary Modification of the Relation between HF and RF

On the grounds that the experiment was to see if altering the aforesaid relation impacted on the PW, the proposed modification was that instead of a straight line, the new function would be two intersecting lines. The horizontal axis for this modification was the original straight line formed by the RF and the HF, rotated  $45^\circ$  in a trigonometric sense. Once the new function was determined, it was rotated back  $45^\circ$  in a clockwise sense for the original line to be in its original position and the new function still relative to it. This is shown in Fig.3.3.

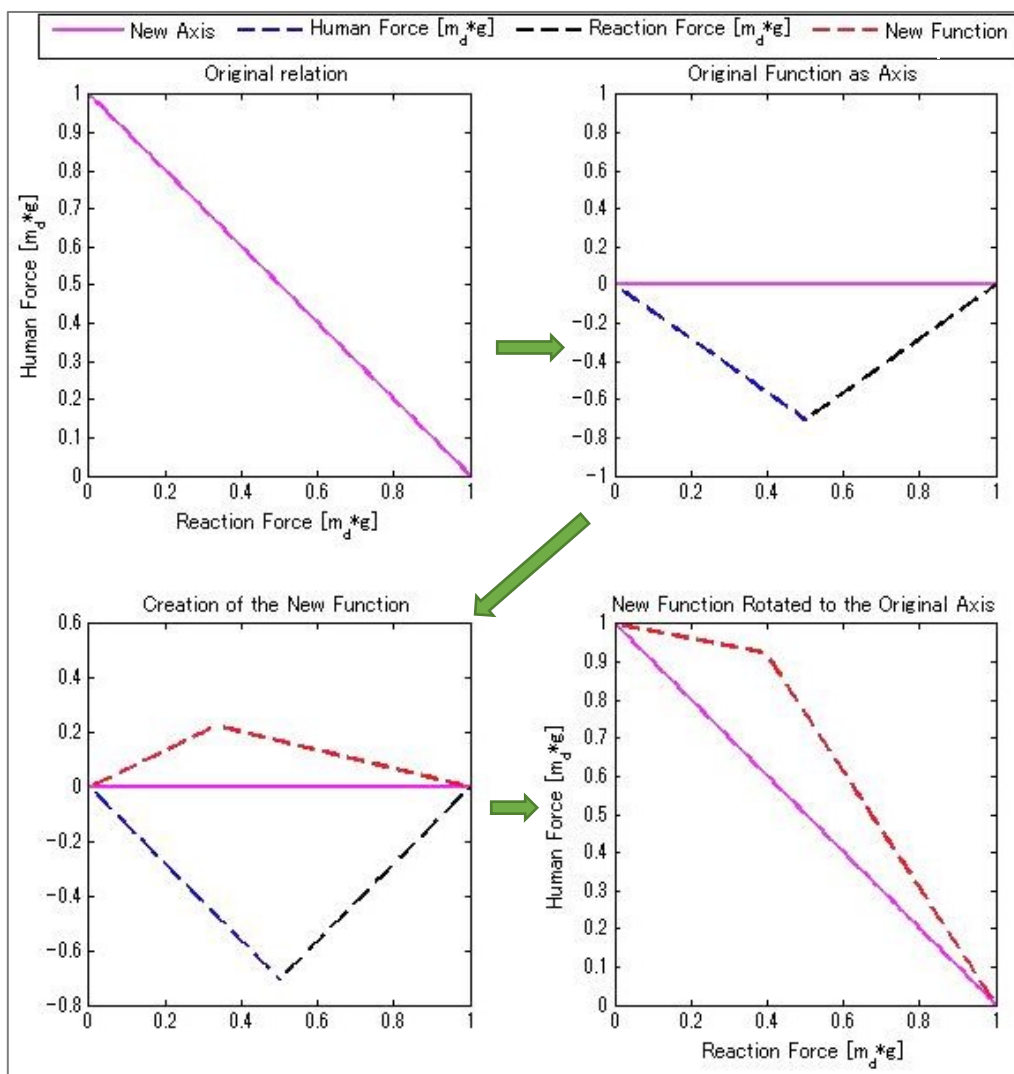


Fig.3.3 Process of Creation of the New Functions

The symmetric functions were also considered and for notation purposes, they were referred either as  $\{-1/4, -1/3, -1/2, -2/3, -3/4\}$  for the position of the peak or  $\{-1, -2, -2.5, -3, -4\}$  for the amplitude of the peak. This difference between position and amplitude of the peak is shown in Fig.3.4 and in Fig.3.5.

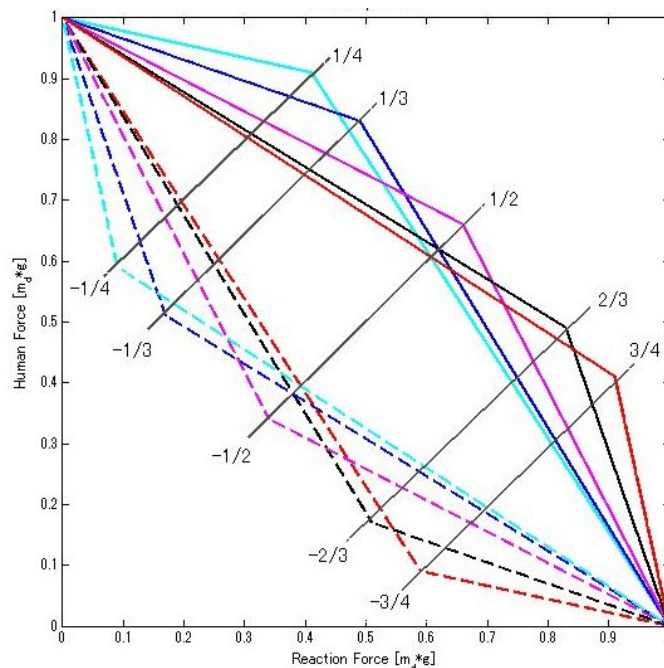


Fig.3.4 Peaks by Position

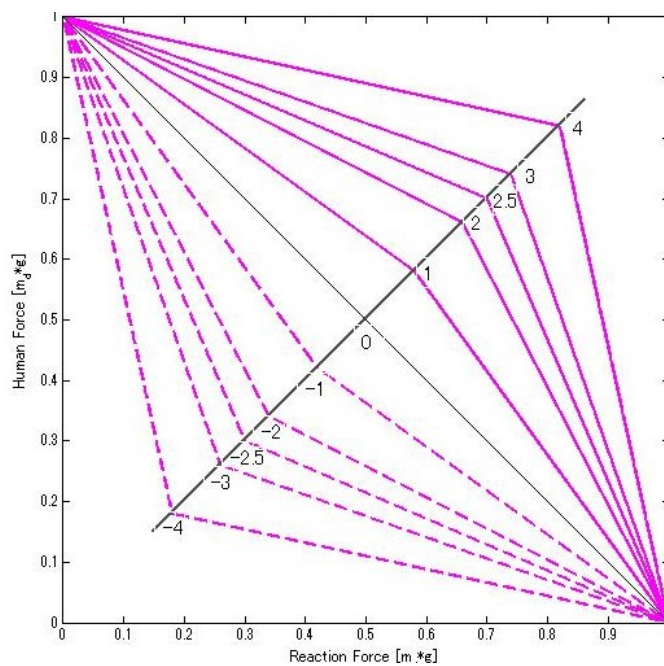


Fig.3.5 Peaks by Amplitude

Since one of the restrictions of the modification was for the function to be within the limits of the square formed by  $m_d \times m_d$ , not all the positions were compatible with all the amplitudes. The possible combinations of positions and amplitudes are shown in TABLE 3.1 and

TABLE 3.2, depending if the reference was the amplitude or the position of the peak. The plots of the possible functions are shown in Fig.3.6, where the vertical axes represent the HF and the horizontal axes represent the RF, the unit for both of the is the desired weight.

It is worth noticing that for the modification, the mass of the object was substituted for the desired mass of it in order for the PA to provide the rest of the force needed to lift the object and for the PW to be that corresponding to the desired mass.

TABLE 3.1 POSSIBLE POSITIONS OF THE PEAK WITH THE AMPLITUDE AS REFERENCE

Amplitude/ Position	-4	-3	-2.5	-2	-1	0	1	2	2.5	3	4
1/4				✓	✓		✓	✓			
1/3	✓	✓	✓	✓	✓		✓	✓	✓	✓	✓
1/2	✓	✓	✓	✓	✓	✓	✓	✓	✓	✓	✓
2/3	✓	✓	✓	✓	✓		✓	✓	✓	✓	✓
3/4				✓	✓		✓	✓			

TABLE 3.2 POSSIBLE AMPLITUDES OF THE PEAK WITH THE POSITION AS REFERENCE

Position/ Amplitude	-3/4	-2/3	-1/2	-1/4	1/4	1/3	1/2	2/3	3/4
0							✓		
1	✓	✓	✓	✓	✓	✓	✓	✓	✓
2	✓	✓	✓	✓	✓	✓	✓	✓	✓
2.5		✓	✓			✓	✓	✓	
3		✓	✓			✓	✓	✓	
4		✓	✓			✓	✓	✓	

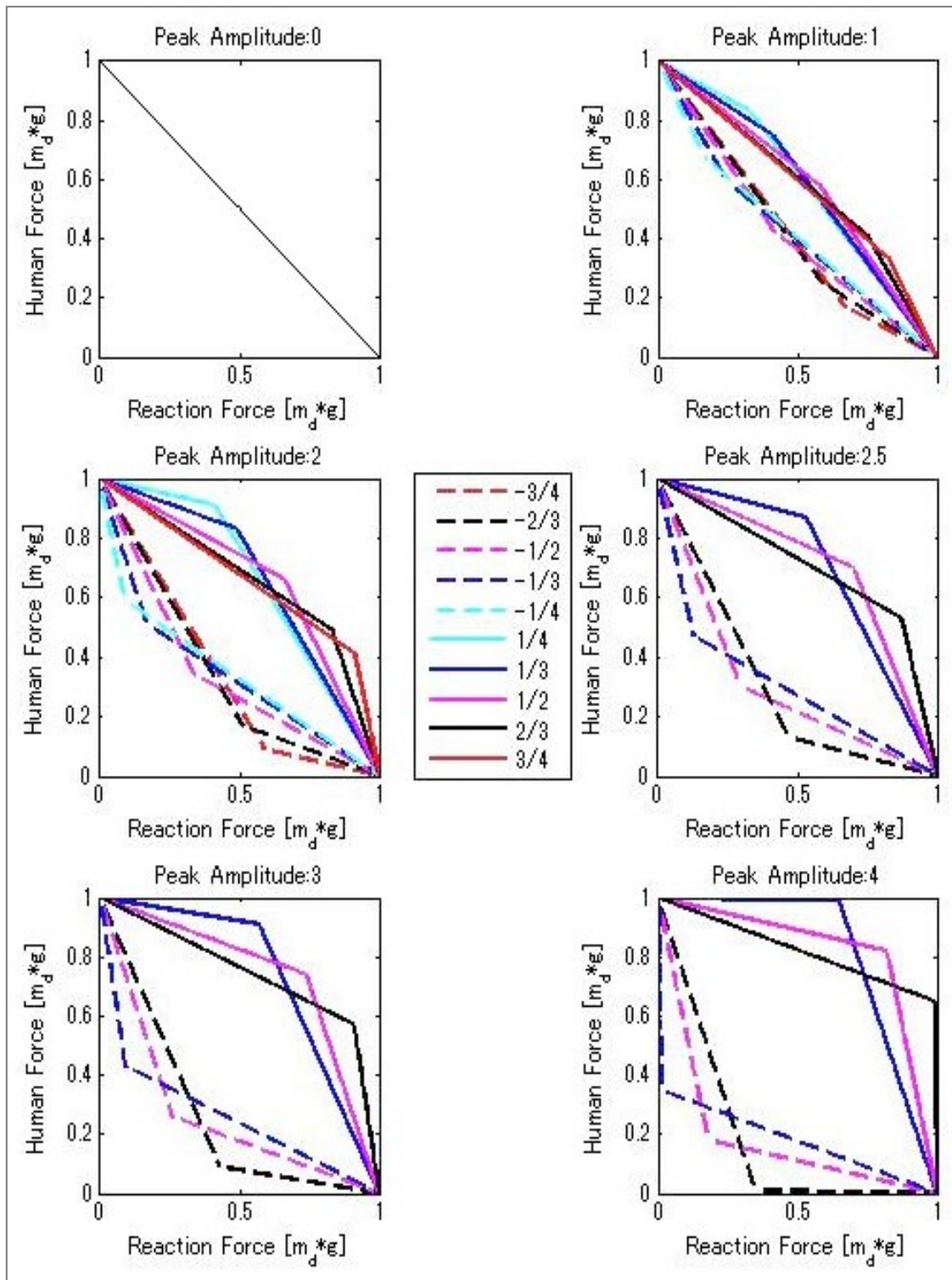


Fig.3.6 Plots of the Possible Peaks

### 3.2 Control Algorithm

As explained in Chapter 2, the lifting was separated into two phases, one for the detaching phase and the other for the rest of the lifting.

Fig.3.7 shows the forces applied on the object for the first phase with PA provided. The equation of motion was given by Newton's First Law as shown in (4).

$$0 = F_{PA} + F_h + R - mg \quad (4)$$

In order to test our hypothesis, the modification proposed in (3) was made to (4), which gave (5). This became the equation of the control for the detaching phase.

$$F_{PA} = mg - f(R) - R \quad (5)$$

On the second phase of the lifting, the object was considered in a dynamic state and therefore, the equation of motion was given by Newton's Second Law. First, the case without PA was considered. Its equation is (6).

$$m\ddot{x} = F_{PA} + F_h - mg \quad (6)$$

Where  $\ddot{x}$  was the acceleration [ $\text{m/s}^2$ ] of the object. On the other hand, considering the desired mass, the equation became (7).

$$m_d \ddot{x} = F_h - m_d g \quad (7)$$

Combining (6) and (7), we obtained (8), the equation of the control for the second phase of the lifting.

$$F_{PA} = (m - m_d)(\ddot{x} + g) \quad (8)$$

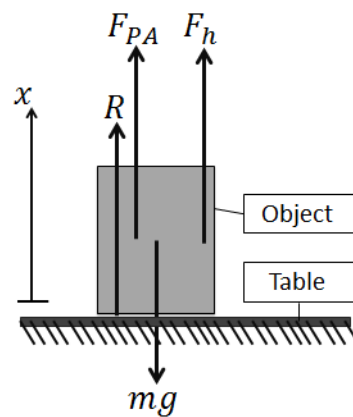


Fig.3.7 Body Diagram of the Object with PA Provided

---

# Chapter 4

## Experimental System

---

### 4.1 Objects

The mass of two objects was compared on the experiments. The first one was attached to the 1 DOF PAD and was denominated as the PA Object, as the name implies, this was the object that was lifted cooperatively between the subject and the system. The mass of this object was of 0.7 kg.

The other object was called the Guided Object, its mobility was restrained through a vertical ball bearing guide. The mass of this object was of 0.35 kg but could be raised by adding weights to the bottom of the guide. This was made because the center of gravity of the PAD was on the lower part due to its configuration and the objective was to replicate it as far as possible for comparison purposes.

In both cases, the objects were identical and made of a rectangular aluminum frame covered by plastic walls. The size of these objects was of 0.1m height and 0.05 m width. A plastic coating was applied to the objects in order to improve the adherence of the walls and improve the grip.

Fig.4.1 shows a snapshot of the object after the coating and without its lid, so all the layers are visible.



Fig.4.1 Objects Lifted

## 4.2 Experimental Device

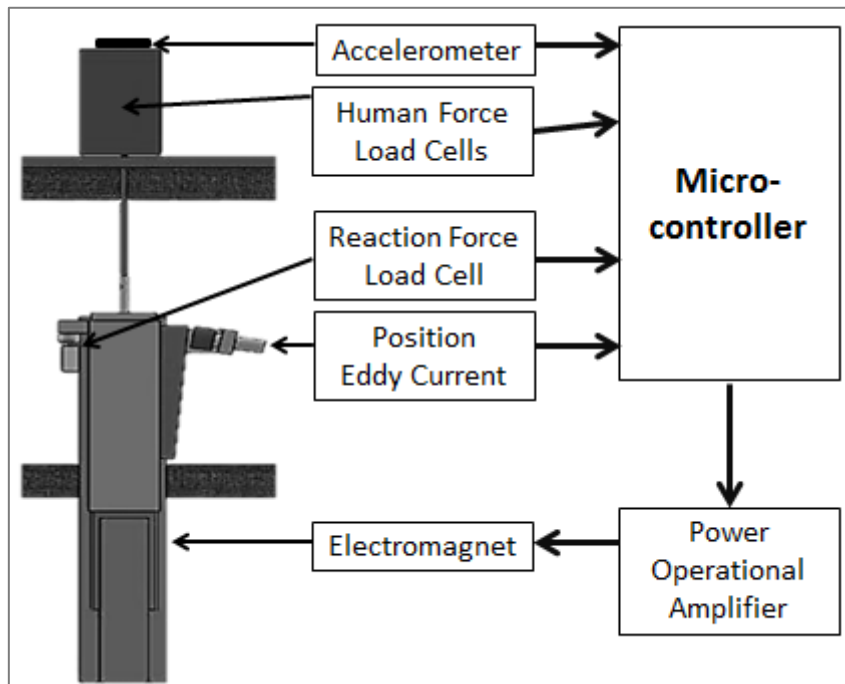


Fig.4.2 Block Diagram of the Experimental System

Fig.4.2 shows a block diagram of the experimental system. The PAD was a 1 DOF system that only allowed vertical displacement. The possible stroke was of approximately 0.07 m. This restriction in the mobility was implemented using a ball bearing slide placed on the bottom part of the system. A support surface was provided at a desktop height from the floor and the PA object was placed on top of it. This object was connected to the rest of the system through a transmission rod.

The acceleration was recorded using an accelerometer placed on top of the PA object. The RF from the support surface was measured through the bottom load cell and the HF via an X-Y load cell arrangement placed inside the PA object. An Eddy Current sensor placed at the side of the ball bearing slide recorded the position.

The data measured by the sensors was read using the ADC ports of the microcontroller that executed the control algorithm. The resultant signal was conditioned via a power operational amplifier and sent to the electromagnet which provided the power assist (PA) for the lifting.

On the support surface, the guided object was placed at approximately 0.2 m of the PA object. As mentioned before, the mobility of this object was also constrained, in this case using a roller ball guide. The restraining part of this object was placed below the support surface to imitate the configuration of the PAD and in this case, the object and the guide were also connected through a transmission rod.

Fig.4.3 and Fig.4.4 show a frontal and an isometric view of the PAD and the guided object.

The part of the system below the support surface was hidden from the sight of the subjects with a panel to avoid prejudices against either of the objects.

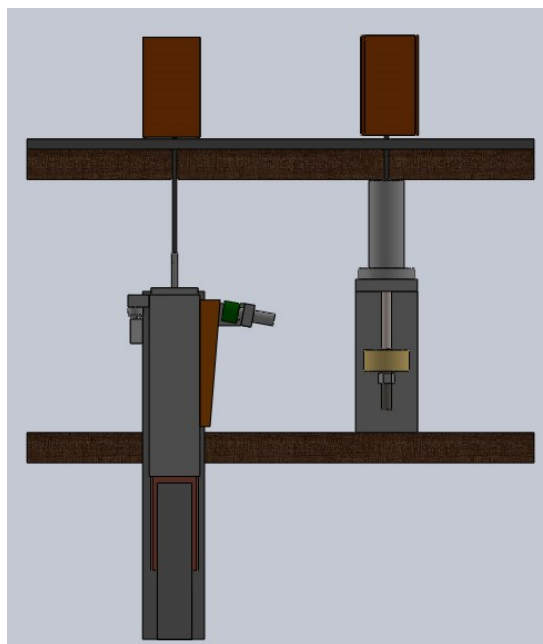


Fig.4.3 Frontal View of the System

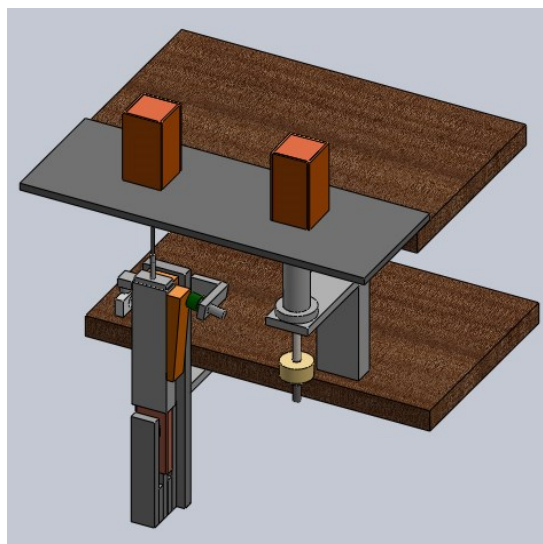


Fig.4.4 Isometric View of the System

### 4.3 Electronics of the System

This part explains the electronic circuits implemented to adapt the signals from the sensors, the microcontroller that performed the control and the coil to provide the PA.

The accelerometer was a general purpose performance accelerometer intended for instrumentation applications, an IC Sensors Model 3145. This sensor had its proper circuitry and it was set to be within the microcontroller's ADC range. The specifications of the accelerometer are in Appendix A.

For the position, an Eddy Current sensor was used. This selection was made thinking on the velocity of response needed for the system. This sensor was plugged to an AEC-55 Series Gap Sensor. A Gap-Sensor is a non-contacting measuring system, capable of measuring displacement, vibration, rotation and the gauging distance with high accuracy. The GAP-SENSOR may be used in numerous applications, such as large compressors of turbines as well as measurement of vibration levels in rotating and reciprocation equipment. Other applications include observation and measurement of motion, position, speed and thickness of conductive surfaces. The specifications of this sensor are in Appendix B.

The electromagnet was formed with a coil of  $6.5 \Omega$  of impedance, two pairs of magnets and an iron core. The ends of the coil were connected to a Power Operational Amplifier Shinko R1-0015. The settings made were for the coil to give a force of 1.5N/A.

Three PCBs were made for the system. The first one comprehended the electronic circuits for the RF's load cell and a circuit to calculate the velocity of the object from its position. Fig.4.5 shows the schematic for this PCB. The circuit for the load cell is composed by a Wheatstone bridge follow by op-amp configurations in series. The sequence one was: a Voltage Follower, next a Differential, then a Summing Amplifier and finally an Inversor that could be on or off. The circuit to determine the velocity of the object was also made using op-amp in the Derivator configuration.

The second PCB was for the X-Y array of load cells to determine the HF. Fig.4.6 shows the schematic of this PCB. Just like for the RF's load cell, the circuits for each load cell was formed by a Wheatstone bridge followed by configurations of op-amp. The sequence was the same as for the RF's load cell but a Summing Amplifier was added and joined the outputs of both load cells.

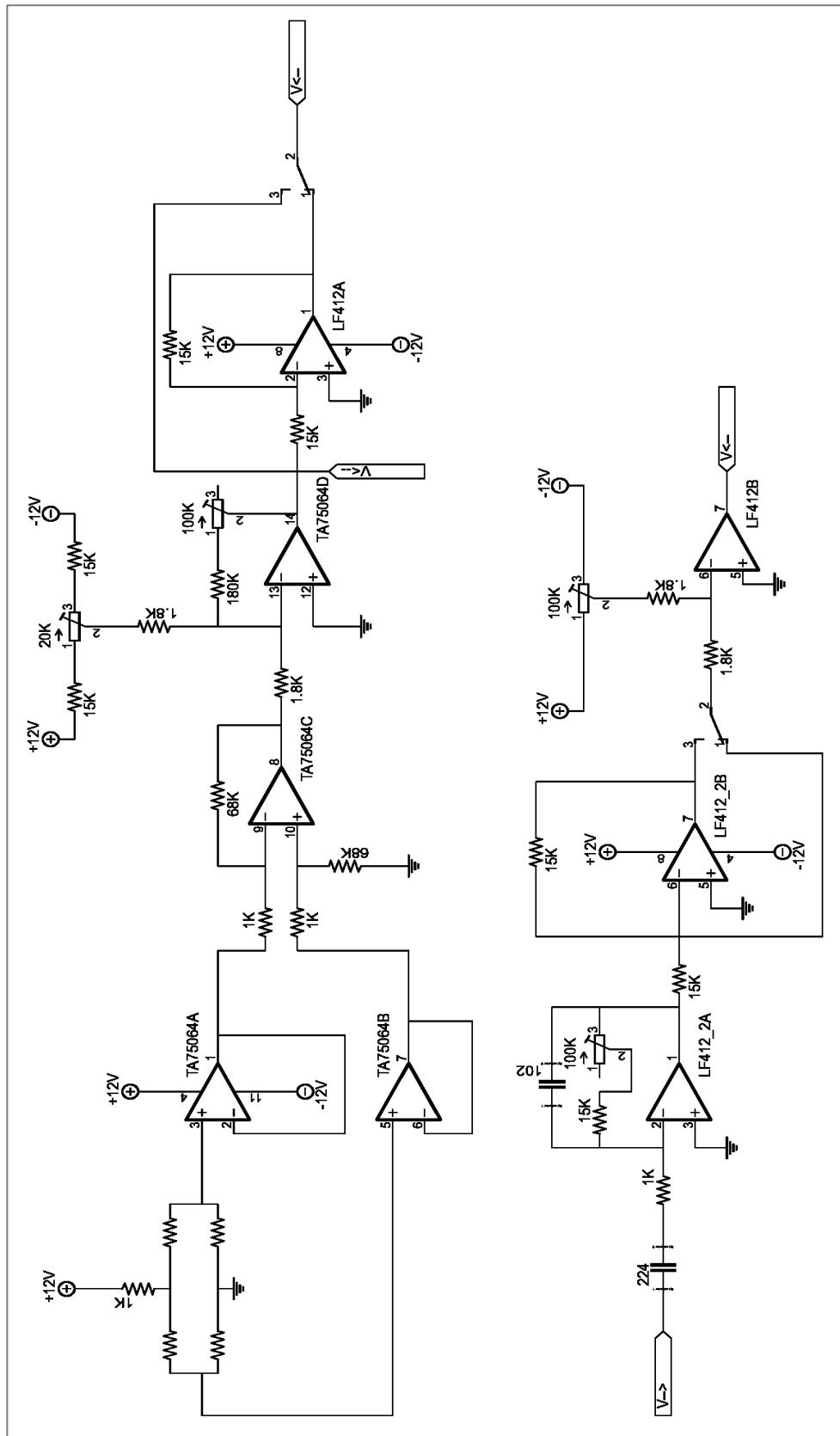


Fig.4.5 Electronic Diagram for the RF's Load Cell and the Velocity

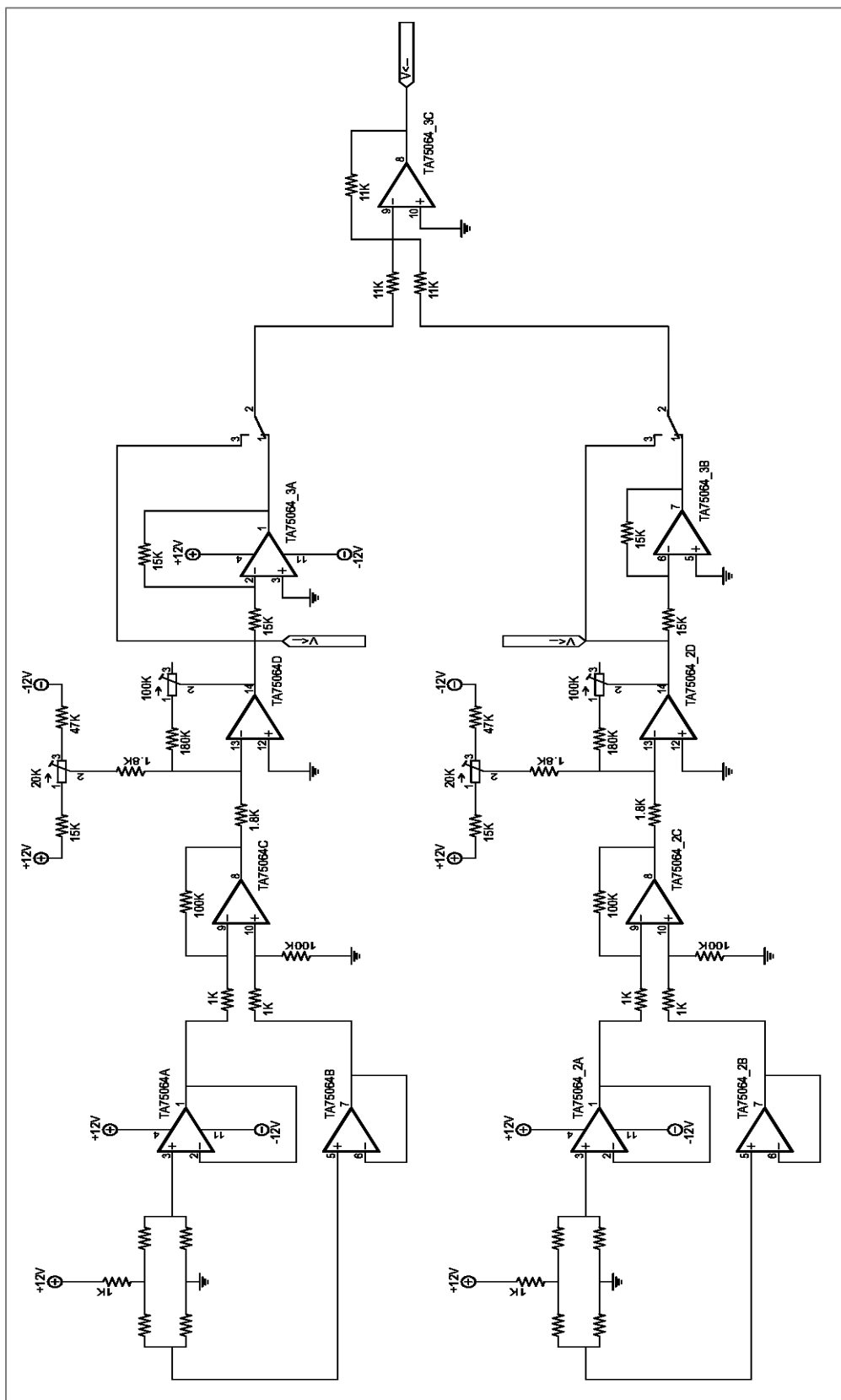


Fig.4.6 Electronic Diagram for the HF's Load Cells

The last PCB was for the microcontroller. The selected device was a Microchip's PIC18F4455. This chip was selected because it could run at a frequency of 48MHz. the specifications of this PIC are shown in Appendix C and Fig.4.7 shows the electronic diagram for the PCB. This circuit had a connection for in-circuit programming; the entries for the sensor signals had pull-down resistances and went directly to the ADC module of the PIC. A dip-switch was also connected to a port of the PIC, this gave us the opportunity of select the desired function without needing to reprogram the PIC. The PIC calculated the output of the control according to the equations shown in 3.2 Control Algorithm and this signal was send to an external DAC0800 that converted it from digital to analogic. The analogic signal was then send to a Current-Voltage configuration implemented through an op-amp, this was the output of this PCB and was also the entry of the Power Op-Amp for the coil.

All the exits of the sensors were set to within the range of [0,5]V in order for them to be readable by the PIC's ADC. Two generators were used for the circuitry, one in the range of  $\pm 12\text{V}$  for the PCB's and other one in the range  $\pm 24\text{V}$  for the power op-amp of the coil.

The signals corresponding to the RF, the HF, the position and acceleration of the object and the PAF (Power Assist Force) were recorded using an oscilloscope.

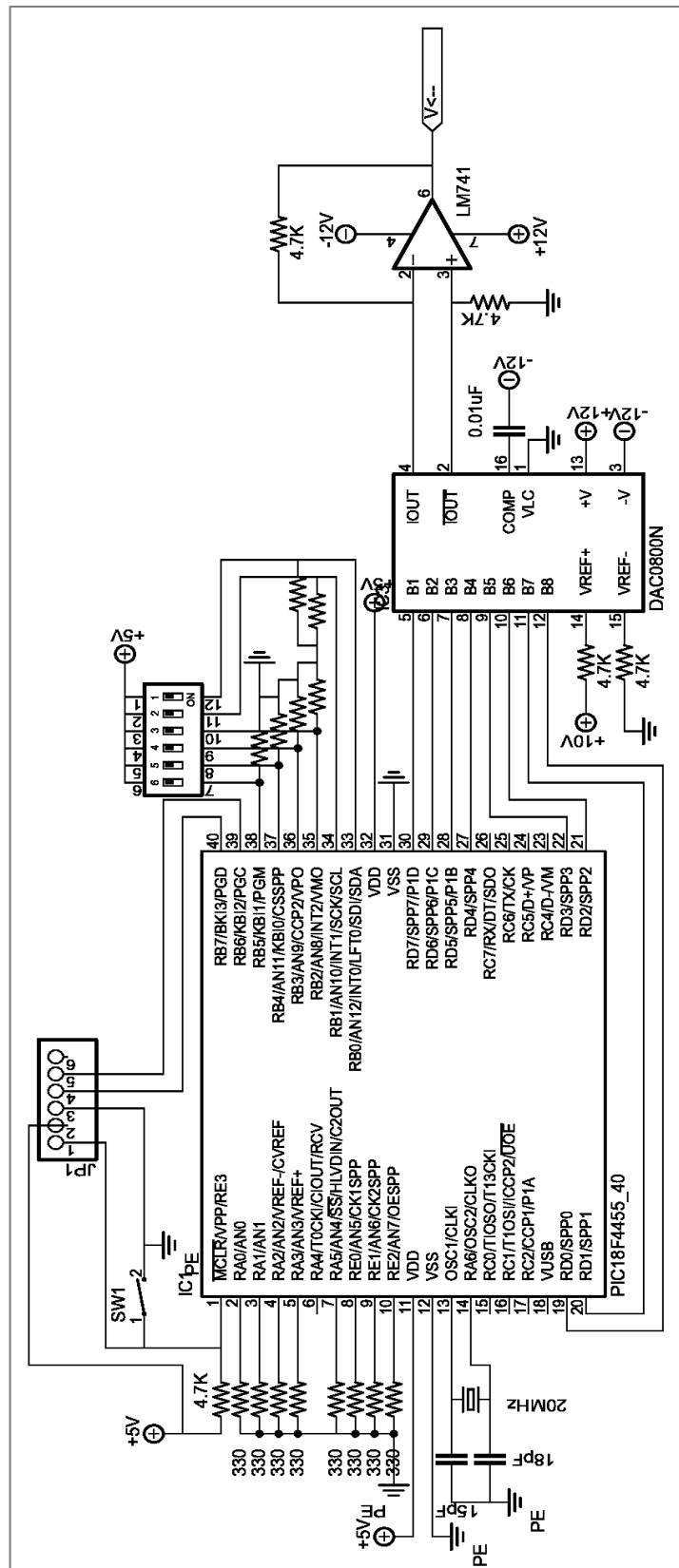


Fig.4.7 Electronic Diagram for the PIC

# Chapter 5

## Experimental Method

### 5.1 Subjects

The subjects for these experiments were 10 students in their 20's, four women and six men. They were presumed to be physically and mentally healthy and naive in expressing opinions. The subjects were not trained for the experiments but a demonstration was made by the researcher before each experiment.

### 5.2 Lifting Method

The seat provided to the subjects for the experiments had a rest for the right elbow. That support could be adjusted to create a 90° angle between the right upper arm and the forearm, therefore minimizing the influence of the triceps and the biceps on the lifting. The height of the seat could also be adjusted to the subjects comfort. Fig.5.1 shows this seat and the posture of the lifting.



Fig.5.1 Seat used during the Liftings (Left: Seat, Right: Posture for the Lifting)

For each of the control equations tested, two parts were performed. In one of them, the mass of the guided object was set at the desired mass plus 0.1 kg, this Mass Decreased (MD) by 0.01 kg at each trial. On the other part of the experiment, the mass of the guided object started at the desired weight minus 0.1 kg and its Mass Increased (MI) by 0.01 kg at each trial.

Once the subject was seated and the necessary adjustments have been made, he or she was asked to grab one of the objects. The subject was required to hold the object with his or her right hand from the object's middle-upper part, making full contact between the palm of his or her hand and the walls of the objects, as shown in Fig.5.2. This grip was required because in a previous research [15] this holding was found to minimize the influence of the mobility restriction consequent to the 1 DOF PAD. Then, the subjects were asked to lift the object approximately 0.005 m at their own rhythm and put it back down on the table. Afterwards, the subject was asked to lift the other object using the same grip and rhythm as with the previous object. After lifting both objects, the subject was asked by the researcher to declare if they felt both objects to be of same weight or not. This was the process performed for each trial of the experiment. If his or her response was affirmative, that part of the experiment was over. On the other hand, if his or her response was negative, the mass of the guided object was modified and the lifting of both objects was performed again.

On this research, two desired mass were tested: 0.45 kg and 0.55 kg. TABLE 5.1 shows the tested positions and amplitudes for each of these desired masses.



Fig.5.2 Grip used for the Liftings (Left: Upper View, Right: Side View)

TABLE 5.1 TESTED POSITIONS AND AMPLITUDES OF THE PEAKS TESTED

<i>md</i>	0.45 kg						0.55 kg					
Amplitude/ Position	0	±1	±2	±2.5	±3	±4	0	±1	±2	±2.5	±3	±4
1/4		✓	✓									
1/3		✓	✓	✓	✓	✓		✓	✓	✓	✓	✓
1/2	✓	✓	✓	✓	✓	✓	✓	✓	✓	✓	✓	✓
2/3		✓	✓	✓	✓	✓		✓	✓	✓	✓	✓
3/4		✓	✓									

The lifts were split into several sessions, each of them of approximately 30 minutes of duration. The sessions could be consecutive after a brief break or scheduled for a different day. As can be seen in TABLE 5.1, for the desired mass of 0.45 kg, 20 equations were tested and 16 equations for the 0.55 kg one; in both cases, the MI and the MD parts were performed. The order in which the equations were tested was completely random.

# Chapter 6

## Experimental Results

### 6.1 Subjective Results

For each of the trials of the experiment, the PW were recorded, that is, the weight of the guided object that was said to be of same PW as the PA object, was registered.

Fig.6.1 and Fig.6.2 show the average from all the 10 subjects for the desired mass of 0.45 kg (desired weight of 4.41N). The continuous lines correspond to the trials with MI and the dotted lines to the trials with MD. The vertical axes represent the weight of the guided object. For Fig.6.1 the horizontal axis represents the positions of the peaks tested, the amplitudes of the peaks being the different series. For Fig.6.2 the horizontal axis represents the amplitudes of the peaks tested, the positions of the peaks being the different series.

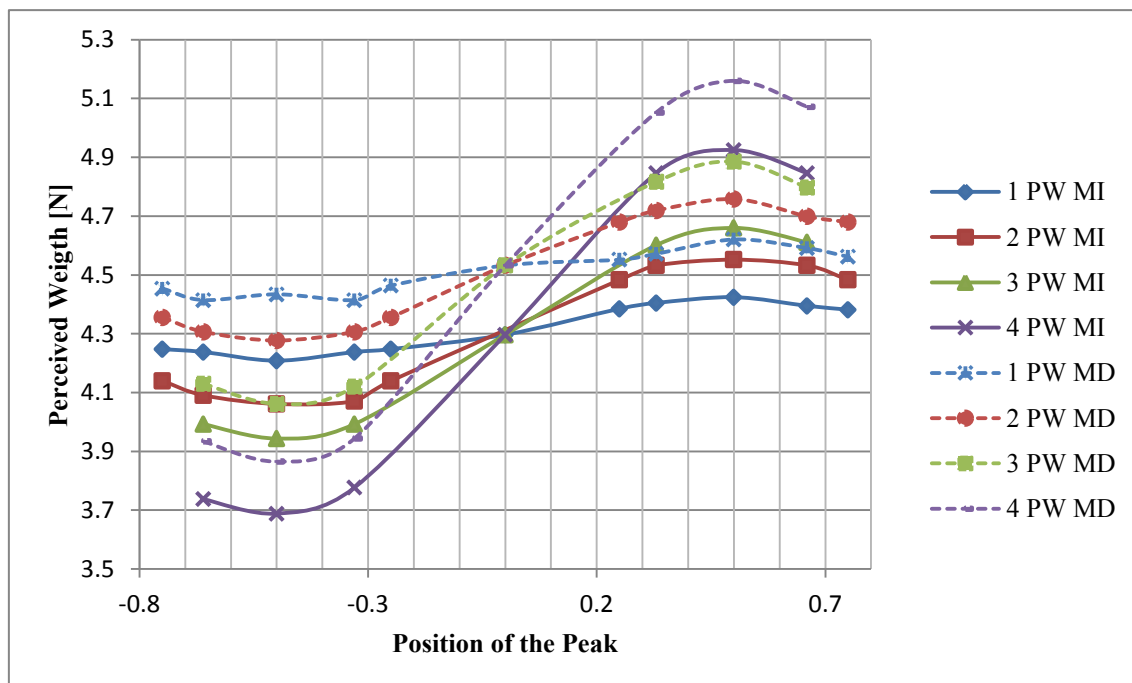


Fig.6.1 Perceived Weight and Position of the Peak (MI and MD,  $m_d=0.45$  kg,  $w_d=4.41$ N)

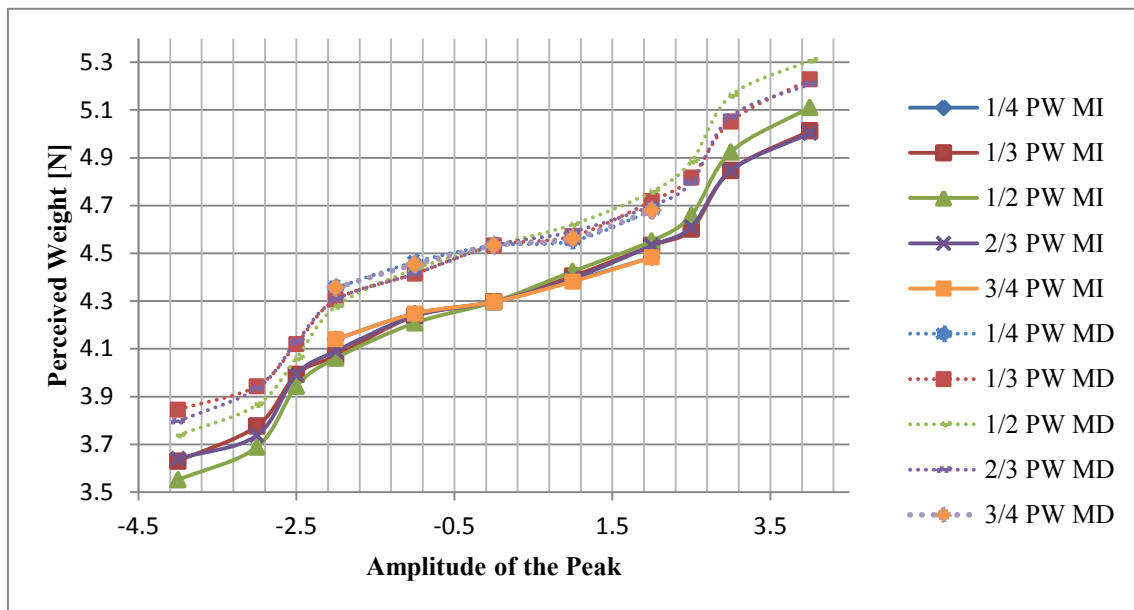


Fig.6.2 Perceived Weight and Amplitude of the Peak (MI and MD,  $m_d=0.45$  kg,  $w_d=4.41$ N)

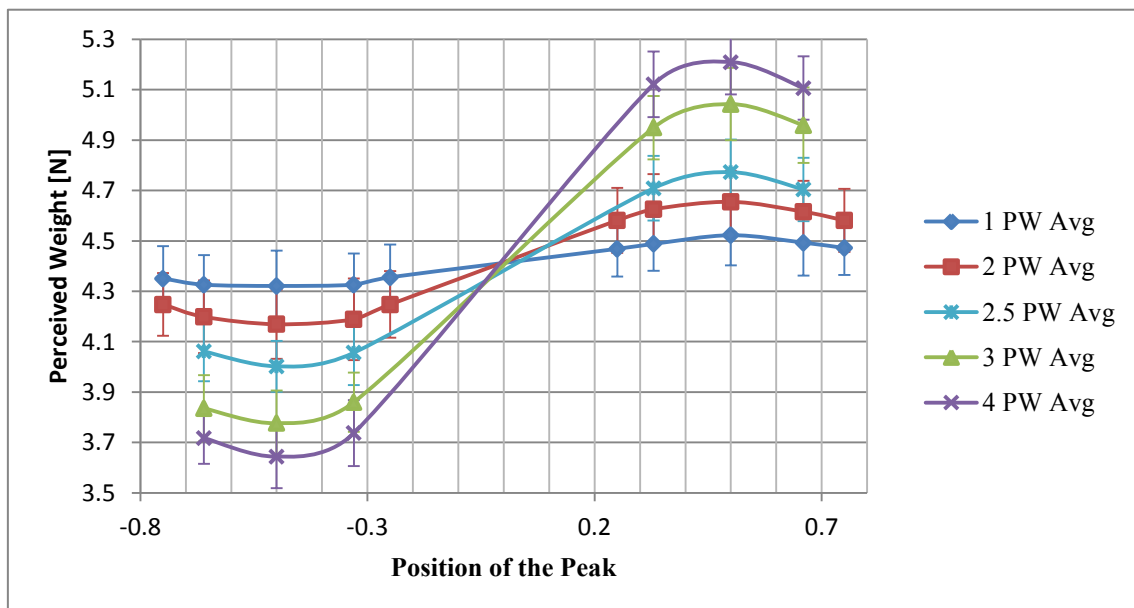


Fig.6.3 Perceived Weight and Position of the Peak (Average,  $m_d=0.45$  kg,  $w_d=4.41$ N)

Fig.6.3 and Fig.6.4 show the average of the trials with MI and MD for all the subjects for the desired mass of 0.45 kg. The vertical axes represent the weight of the guided object. For Fig.6.3 the horizontal axis represents the positions of the peaks tested, the amplitudes of the peaks being the different series. For Fig.6.4 the horizontal axis represents the amplitudes of the peaks tested, the positions of the peaks being the different series. In both cases, the vertical lines represent the standard deviation.

TABLE 6.1 shows the averages from all the subjects for the MI and the MD trials and TABLE 6.2 shows the average of both for the desired mass of 0.45 kg.

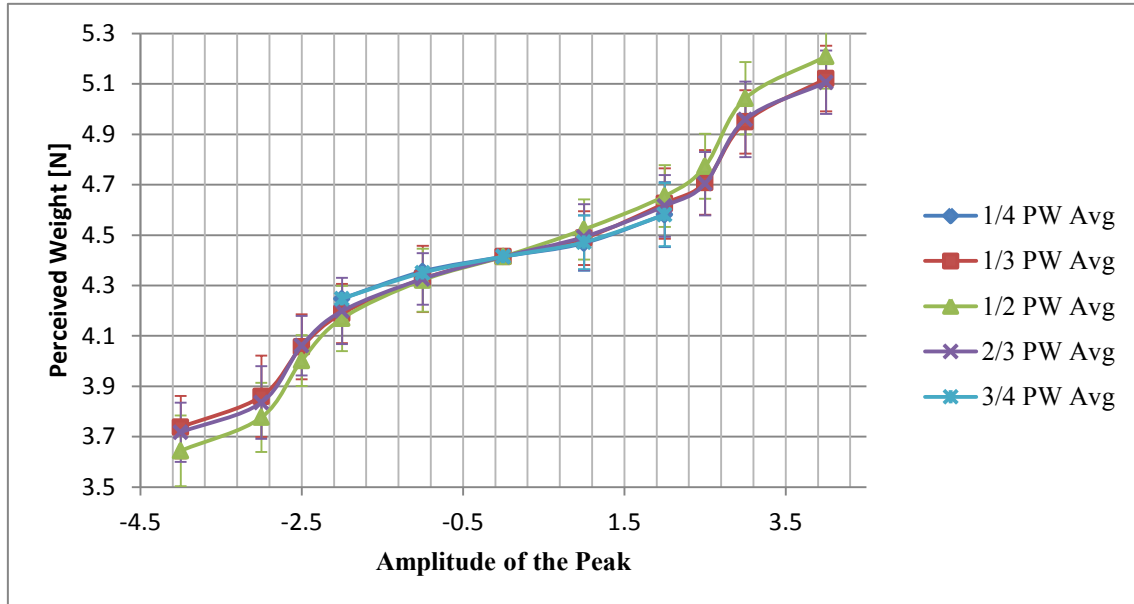


Fig.6.4 Perceived Weight and Amplitude of the Peak (Average,  $m_d=0.45$  kg,  $w_d=4.41$ N)

TABLE 6.1 PERCEIVED WEIGHTS (MI AND MD,  $m_d=0.45$  kg,  $w_d=4.41$ N)

$md$	MI [N]					MD [N]				
Position	1/4	1/3	1/2	2/3	3/4	1/4	1/3	1/2	2/3	3/4
Amplitude										
-4		3.6297	3.5512	3.6395			3.8455	3.7376	3.7964	
-3		3.7768	3.6885	3.7376			3.9436	3.8651	3.9338	
-2.5		3.9926	3.9436	3.9926			4.1202	4.0613	4.1300	
-2	4.1398	4.0711	4.0613	4.0907	4.1398	4.3556	4.3065	4.2771	4.3065	4.3556
-1	4.2477	4.2379	4.2084	4.2379	4.2477	4.4635	4.4145	4.4341	4.4145	4.4537
0	4.2967	4.2967	4.2967	4.2967	4.2967	4.5322	4.5322	4.5322	4.5322	4.5322
1	4.3850	4.4046	4.4243	4.3948	4.3818	4.5518	4.5714	4.6205	4.5910	4.5616
2	4.4831	4.5322	4.5518	4.5322	4.4831	4.6793	4.7186	4.7578	4.6989	4.6793
2.5		4.6008	4.6597	4.6107			4.8167	4.8853	4.7970	
3		4.8461	4.9246	4.8461			5.0521	5.1600	5.0717	
4		5.0129	5.1110	5.0031			5.2287	5.3072	5.2091	

TABLE 6.2 PERCEIVED WEIGHTS (AVERAGE,  $m_d=0.45$  kg,  $w_d=4.41$ N)

$md$	Average [N]					
	Position	1/4	1/3	1/2	2/3	3/4
Amplitude						
-4			3.7376	3.6444	3.7179	
-3			3.8602	3.7768	3.8357	
-2.5			4.0564	4.0024	4.0613	
-2	4.2477	4.1888	4.1692	4.1986	4.2477	
-1	4.3556	4.3262	4.3213	4.3262	4.3507	
0	4.4145	4.4145	4.4145	4.4145	4.4145	
1	4.4684	4.4880	4.5224	4.4929	4.4717	
2	4.5812	4.6254	4.6548	4.6156	4.5812	
2.5			4.7088	4.7725	4.7039	
3			4.9491	5.0423	4.9589	
4			5.1208	5.2091	5.1061	

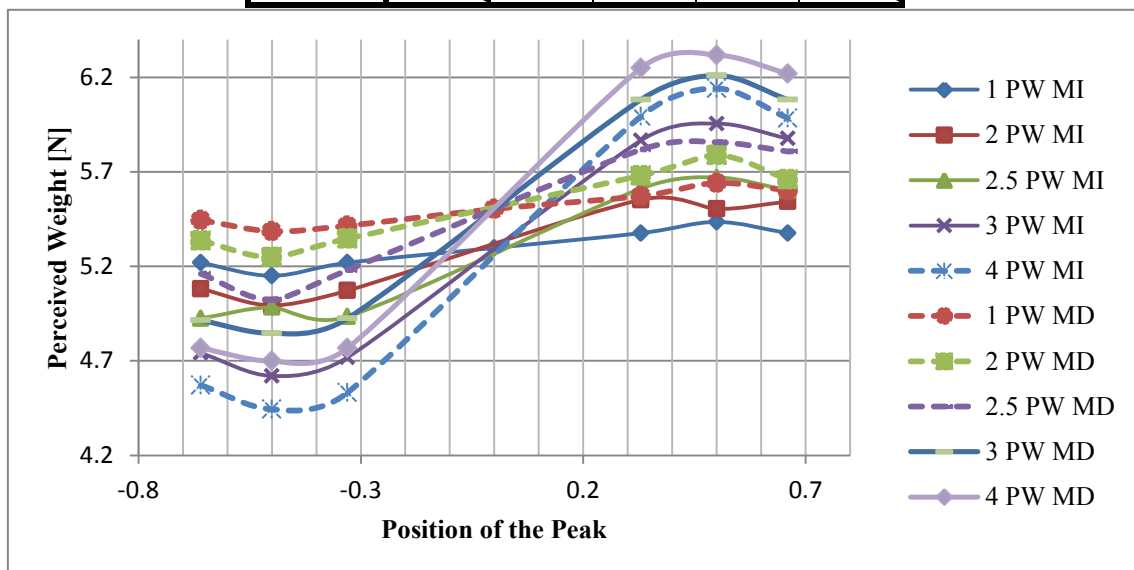
Fig.6.5 Perceived Weight and Position of the Peak (MI and MD,  $m_d=0.55$  kg,  $w_d=5.39$ N)

Fig.6.5 and Fig.6.6 show the average from all the subjects for the desired mass of 0.55 kg (desired weight of 5.39N). The continuous lines correspond to the trials with MI and the dotted lines to the trials with MD. The vertical axes represent the weight of the guided object. For Fig.6.5 the horizontal axis represents the positions of the peaks tested, the amplitudes of the peaks being the different series. For Fig.6.6 the horizontal axis represents the amplitudes of the peaks tested, the positions of the peaks being the different series.

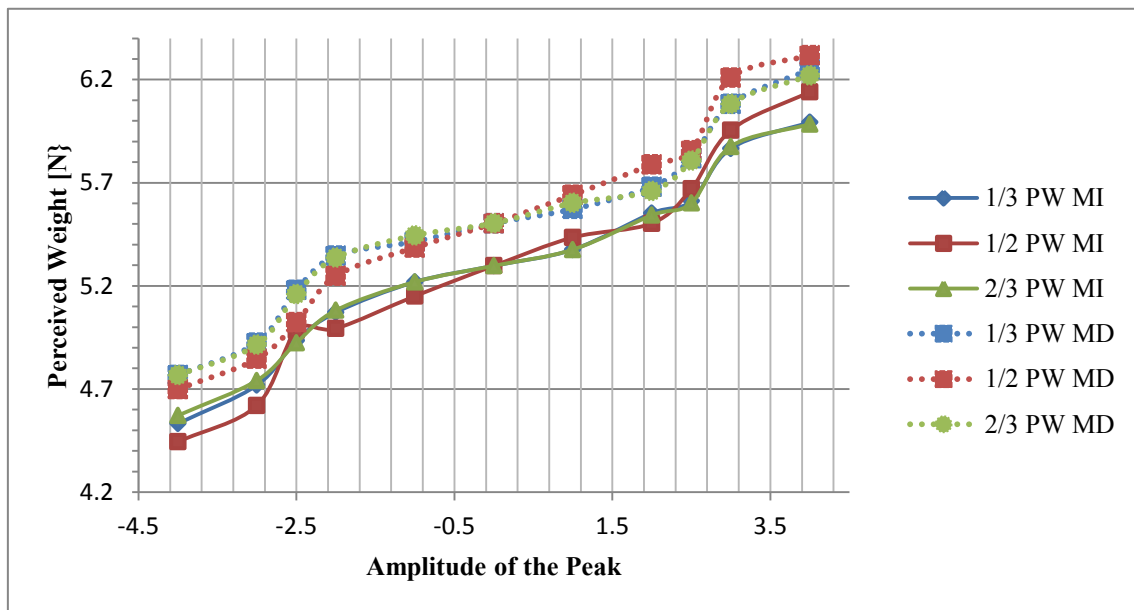


Fig.6.6 Perceived Weight and Amplitude of the Peak (MI and MD,  $m_d=0.55$  kg,  $w_d=5.39$ N)

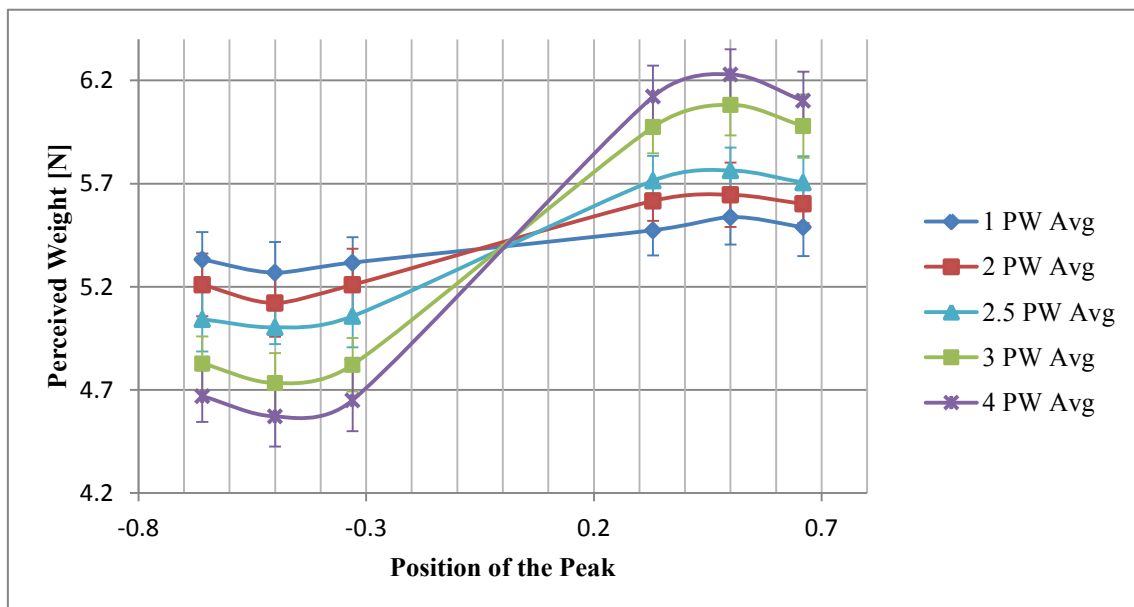


Fig.6.7 Perceived Weight and Position of the Peak (Average,  $m_d=0.55$  kg,  $w_d=5.39$ N)

Fig.6.7 and Fig.6.8 show the average of the trials with MI and MD for all the subjects for the desired mass of 0.55 kg. The vertical axes represent the weight of the guided object. For Fig.6.7 the horizontal axis represents the positions of the peaks tested, the amplitudes of the peaks being the different series. For Fig.6.8 the horizontal axis represents the amplitudes of the peaks tested, the positions of the peaks being the different series. In both cases, the vertical lines represent the standard deviation.

TABLE 6.3 shows the averages from all the subjects for the MI and the MD trials and the average of both for the desired mass of 0.45 kg.

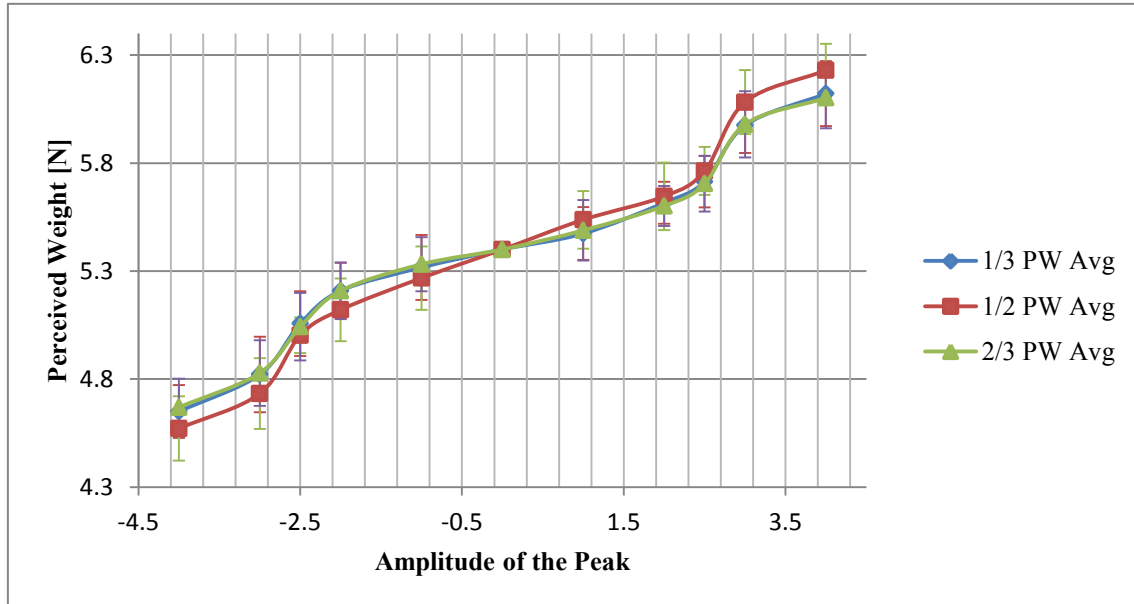


Fig.6.8 Perceived Weight and Amplitude of the Peak (Average,  $m_d=0.55$  kg,  $w_d=5.39$ N)

TABLE 6.3 PERCEIVED WEIGHTS (MI, MD AND AVERAGE,  $m_d=0.55$  kg,  $w_d=5.39$ N)

Position Amplitude	MI [N]			MD [N]			Average [N]		
	1/3	1/2	2/3	1/3	1/2	2/3	1/3	1/2	2/3
-4	4.5322	4.4439	4.5715	4.7677	4.699	4.7677	4.6499	4.5715	4.6696
-3	4.7186	4.6205	4.7415	4.9246	4.8461	4.9148	4.8216	4.7333	4.8282
-2.5	4.9344	4.9835	4.9246	5.1797	5.0227	5.1601	5.0571	5.0031	5.0423
-2	5.0718	4.9933	5.0816	5.3465	5.2484	5.3366	5.2091	5.1208	5.2091
-1	5.2189	5.1503	5.2189	5.4151	5.3857	5.4446	5.317	5.268	5.3317
0	5.2974	5.2974	5.2974	5.5034	5.5034	5.5034	5.4004	5.4004	5.4004
1	5.3759	5.4347	5.3759	5.5721	5.6408	5.6015	5.474	5.5377	5.4887
2	5.5525	5.5034	5.5427	5.68	5.7879	5.6604	5.6162	5.6457	5.6015
2.5	5.6113	5.6702	5.6015	5.8173	5.8566	5.8075	5.7143	5.7634	5.7045
3	5.8664	5.9547	5.8762	6.0822	6.2097	6.0822	5.9743	6.0822	5.9792
4	5.9939	6.1411	5.9841	6.249	6.3176	6.2195	6.1214	6.2294	6.1018

Fig.6.9 and Fig.6.10 show the difference between the mass of the guided object that gave the same PW as the PA object and the desired mass. The continuous lines correspond to the desired mass of 0.55 kg and the dotted lines correspond to the desired mass of 0.45 kg. The vertical axes correspond to the difference of both masses [kg]. For Fig.6.9 the horizontal axis represents the positions of the peaks tested, the amplitudes of the peaks being the different series. For Fig.6.10 the horizontal axis represents the amplitudes of the peaks tested, the positions of the peaks being the different series. The data for these plots is shown in TABLE 6.4.

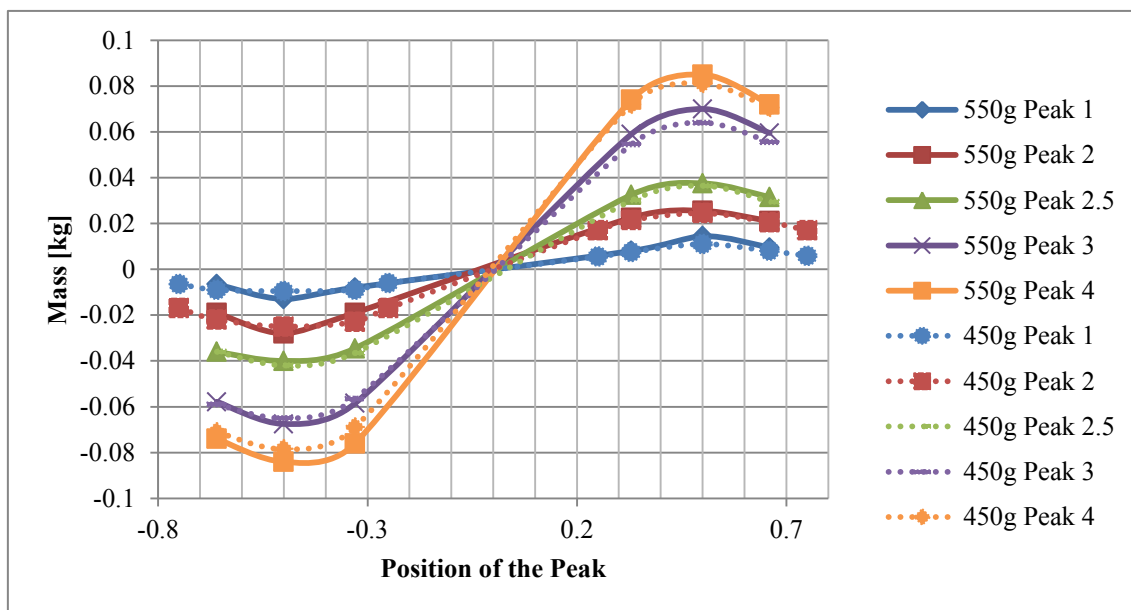


Fig.6.9 Position of the Peak and Difference between the Perceived Mass and the Desired Mass

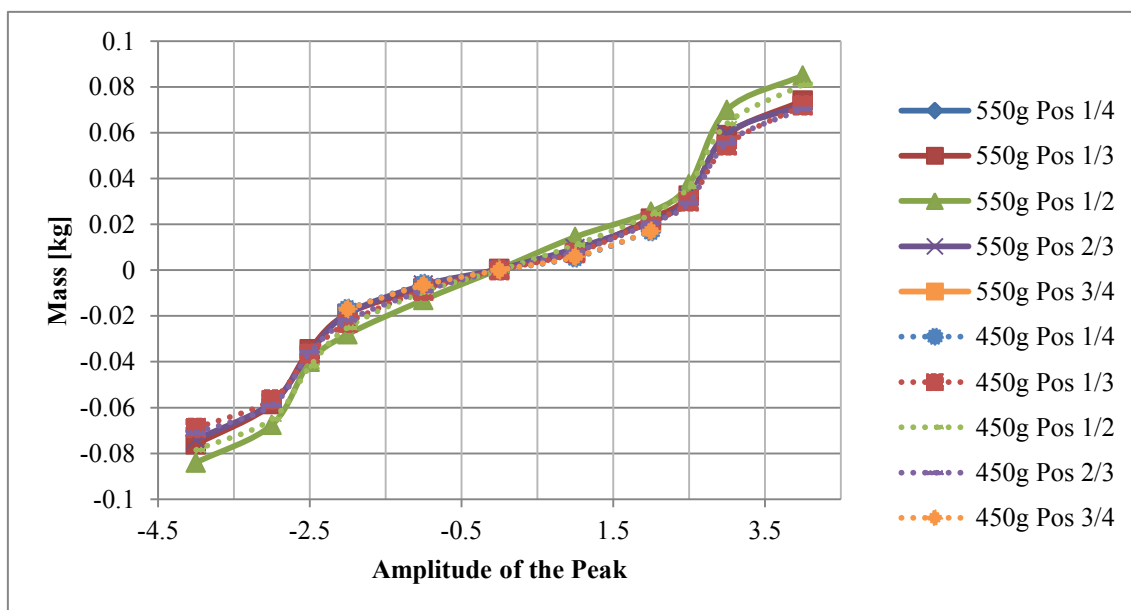


Fig.6.10 Amplitude of the Peak and Difference between the Perceived Mass and the Desired Mass

TABLE 6.4 DIFFERENCE BETWEEN THE REAL MASS AND THE DESIRED MASS

<i>md</i>	0.45 kg					0.55 kg				
Amplitude	1	2	2.5	3	4	1	2	2.5	3	4
Position										
-3/4	0.006	0.017								
-2/3	0.009	0.022	0.036	0.059	0.071	0.006	0.019	0.036	0.057	0.074
-1/2	0.009	0.025	0.042	0.065	0.078	0.013	0.028	0.04	0.067	0.084
-1/3	0.009	0.023	0.036	0.056	0.069	0.008	0.019	0.034	0.058	0.076
-1/4	0.006	0.017								
1/4	-0.005	-0.017								
1/3	-0.007	-0.021	-0.03	-0.054	-0.072	-0.008	-0.022	-0.032	-0.059	-0.074
1/2	-0.011	-0.024	-0.036	-0.064	-0.081	-0.014	-0.025	-0.037	-0.07	-0.085
2/3	-0.008	-0.020	-0.029	-0.055	-0.070	-0.009	-0.021	-0.031	-0.059	-0.072
3/4	-0.005	-0.017								

## 6.2 Data from the Sensors

During the trials, the position and acceleration of the object, the RF, the HF and the PAF were recorded via an oscilloscope. Fig.6.11 shows an example of the recorded data for the desired mass of 0.45 kg with the position of the peak at  $\frac{1}{2}$  and amplitude of 2 for the MI trial. The northeast plot represents the position of the object, the horizontal axis being the time [s] and the vertical axis the height [m]. The northwest plot was for validation purposes; the horizontal axis being the RF [N] and the vertical axis the HF [N]. The lower plot shows the recorded forces, the blue line being the RF, the magenta line the HF and the green line the PAF; the horizontal axis represents the time [s] and the vertical axis the forces [N].

The duration on Fig.6.11 corresponds to the entire recorded length of the trial, that is, 5 s. To calculate the forces on the lifting, the length of the data was limited and the RF was used as a trigger. Fig.6.12 shows the time restriction applied to the same case shown in Fig.6.11. The plots and the axes correspond to those of Fig.6.11.

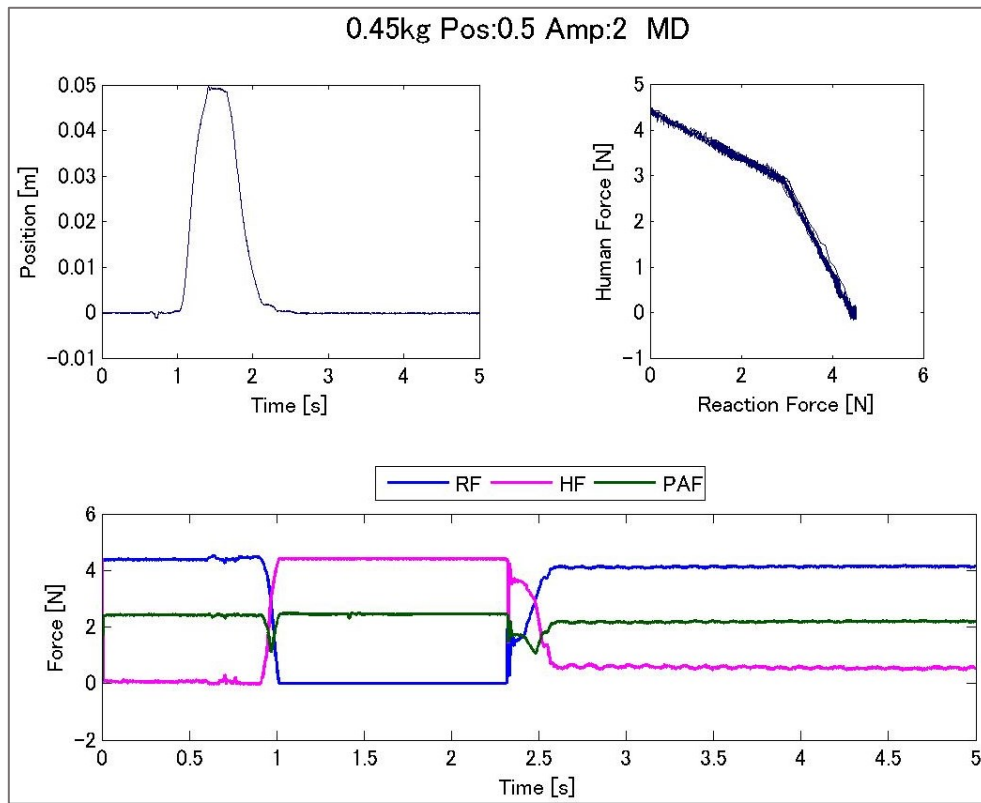


Fig.6.11 Data from the Sensors ( $m_d=0.45$  kg, Entire Recorded Length)

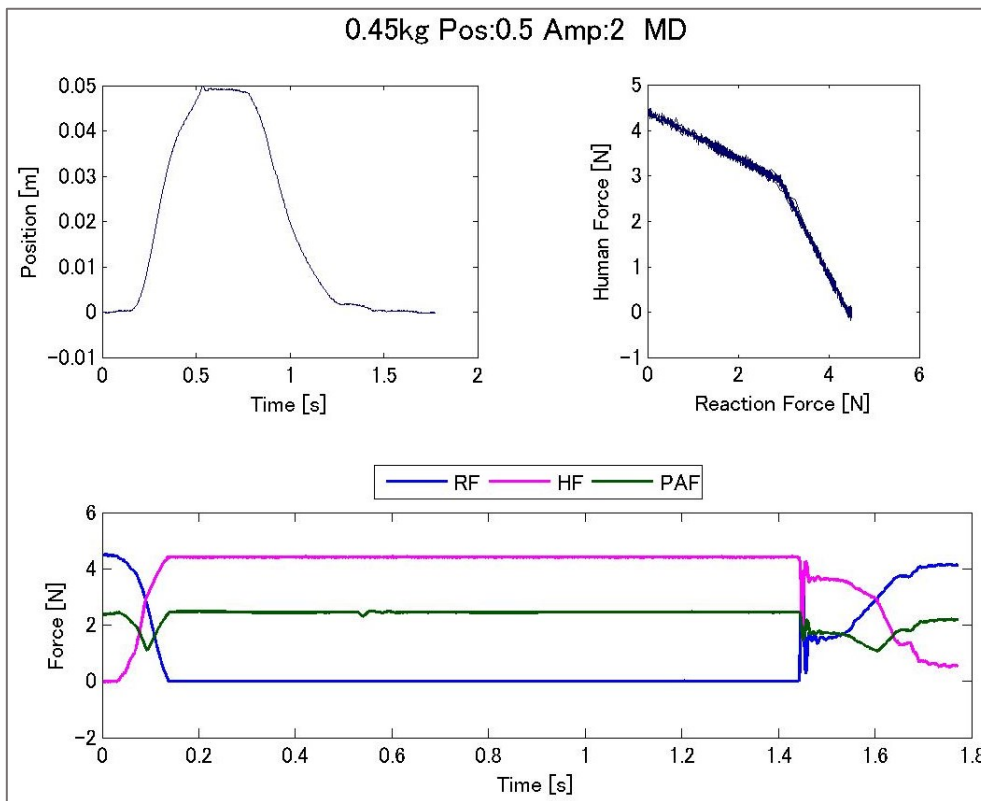


Fig.6.12 Data from the Sensors ( $m_d=0.45$  kg,  $w_d=4.41$ N, Entire Lifting)

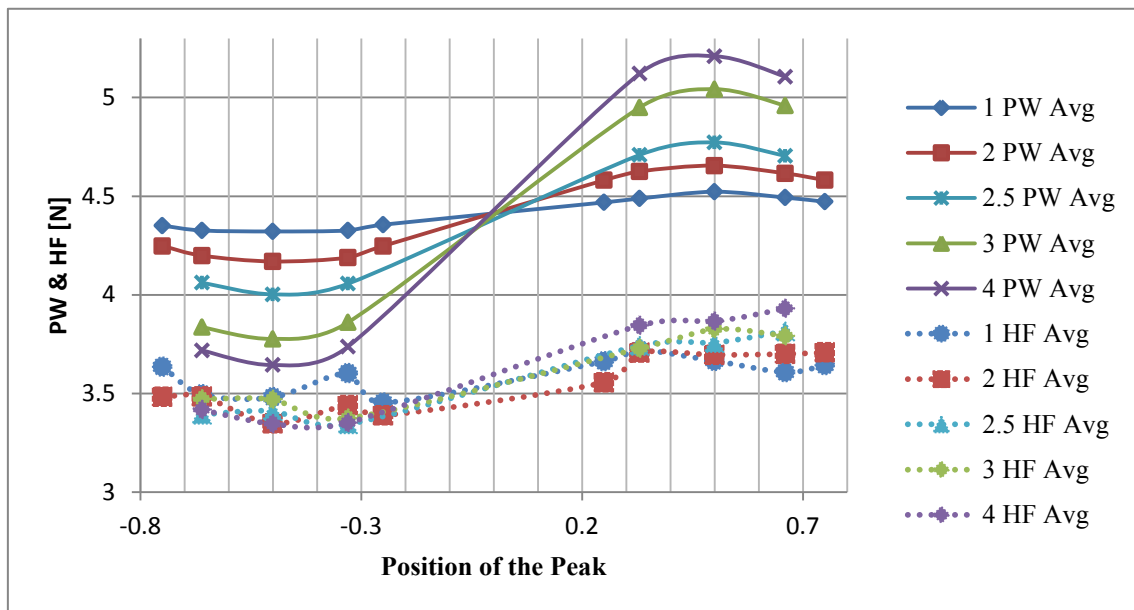


Fig.6.13 PW and HF Arranged by the Position of the Peak ( $m_d=0.45$  kg,  $w_d=4.41$ N, Lifting)

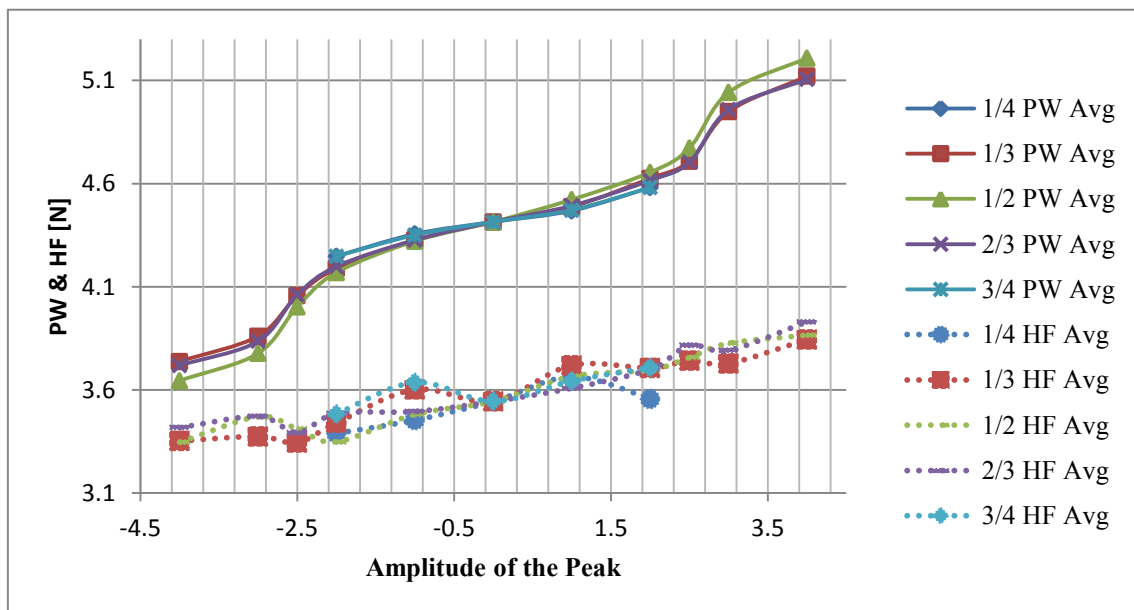


Fig.6.14 PW and HF Arranged by the Amplitude of the Peak ( $m_d=0.45$  kg,  $w_d=4.41$ N, Lifting)

Moreover, the data from the sensors was plotted and compared to the subjective data. Fig.6.13 and Fig.6.14 show the average of the PW and the HF from all the subjects. The vertical axes represent the forces [N]. In Fig.6.13, the horizontal axis corresponds to the positions of the peaks and in Fig.6.14 to the amplitudes of the peaks.

Additionally, the difference between the weight of the object ( $W=m*g$ , in this case  $W=6.87$ N) and the PAF was calculated and plotted against the PW. This is shown in

Fig.6.15 and Fig.6.16, the vertical axes represent the forces [N]. In Fig.6.15, the horizontal axis corresponds to the positions of the peaks and in Fig.6.16 to the amplitudes of the peaks.

Other comparisons made between the PW and the forces recorded during the lifting are shown in Appendix D.

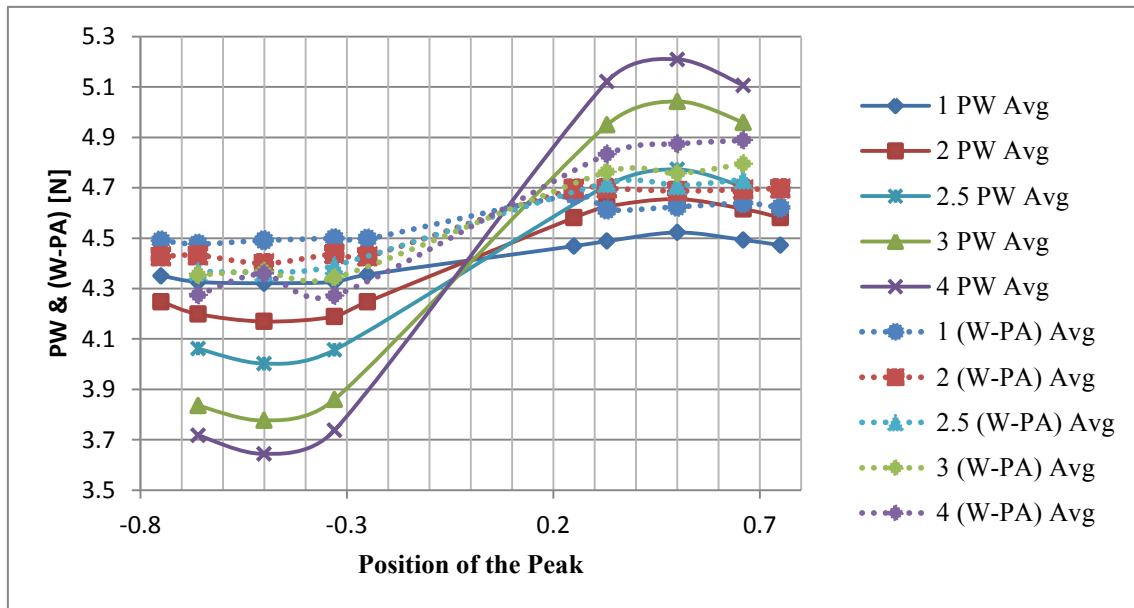


Fig.6.15 PW and (W-PA) Arranged by the Position of the Peak ( $m_d=0.45$  kg,  $w_d=4.41$ N, Lifting)

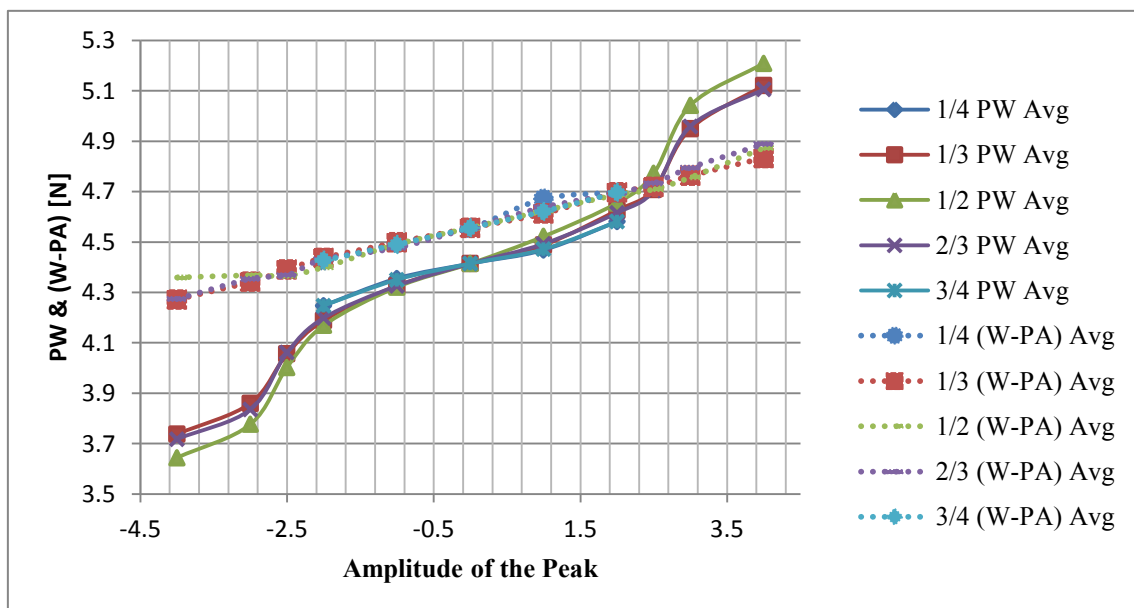


Fig.6.16 PW and (W-PA) Arranged by the Amplitude of the Peak ( $m_d=0.45$  kg,  $w_d=4.41$ N, Lifting)

In the same way as in Fig.6.12, the time length of the trial was limited, now focusing only on the detaching phase. An example of this time restriction is shown in Fig.6.17, the data, order of the plots and axes are the same as for Fig.6.12.

Fig.6.18 and Fig.6.19 are the simile of Fig.6.13 and Fig.6.14 for only the detaching phase. The solid lines correspond to the PW and the dotted lines to the HF. The vertical axes represent the forces [N]. In Fig.6.18, the horizontal axis corresponds to the positions of the peaks and in Fig.6.19 to the amplitudes of the peaks.

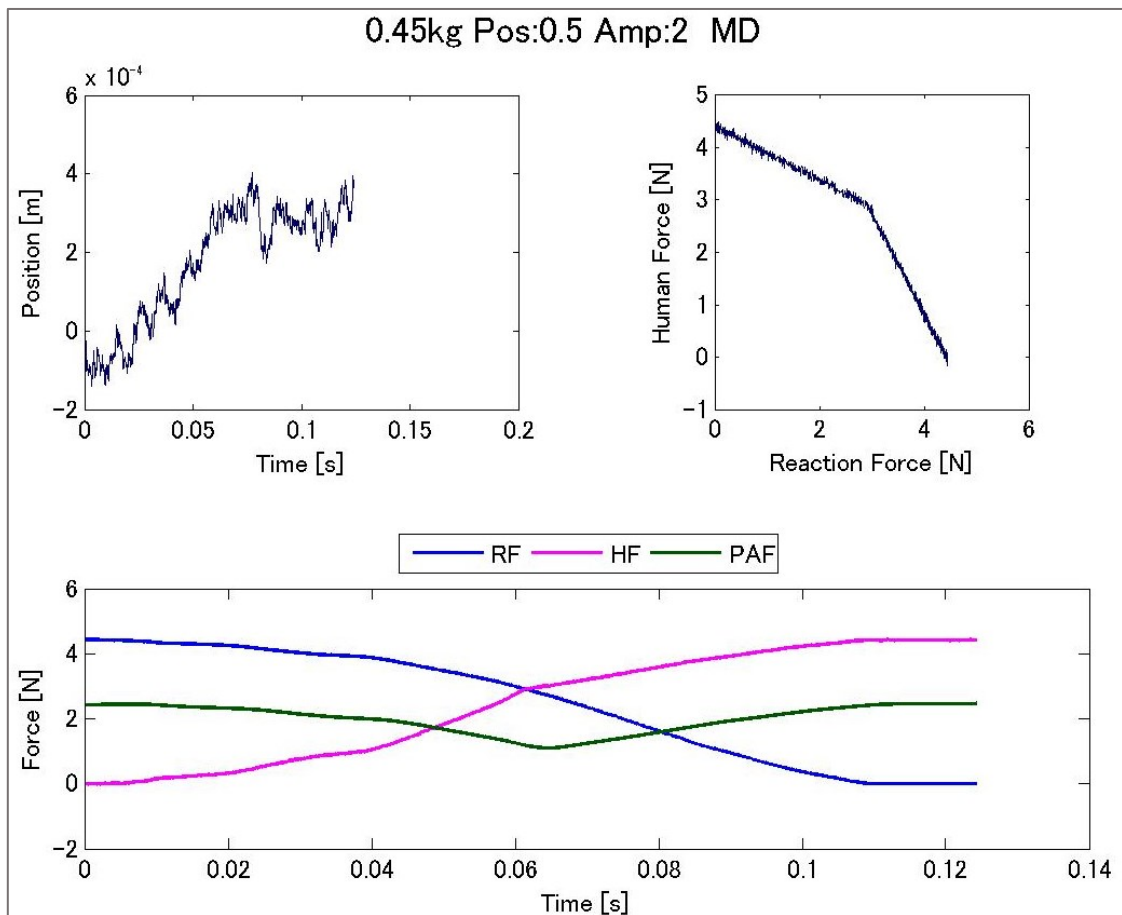


Fig.6.17 Data from the Sensors ( $m_d=0.45$  kg,  $w_d=4.41$ N, Detaching Phase)

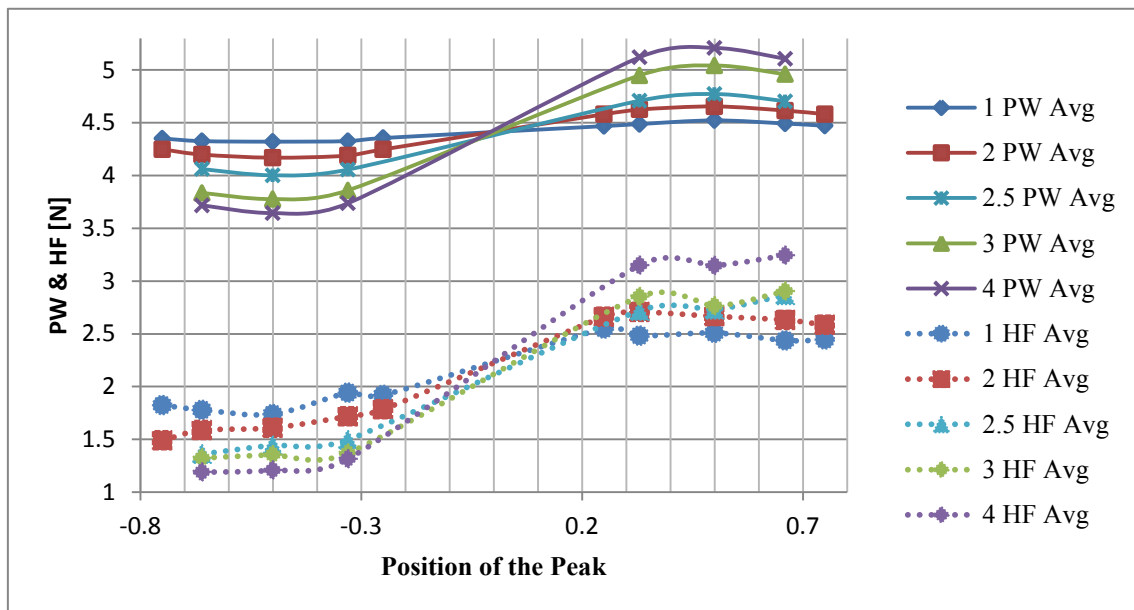


Fig.6.18 PW and HF Arranged by the Position of the Peak ( $m_d=0.45$  kg,  $w_d=4.41$ N, Detaching Phase)

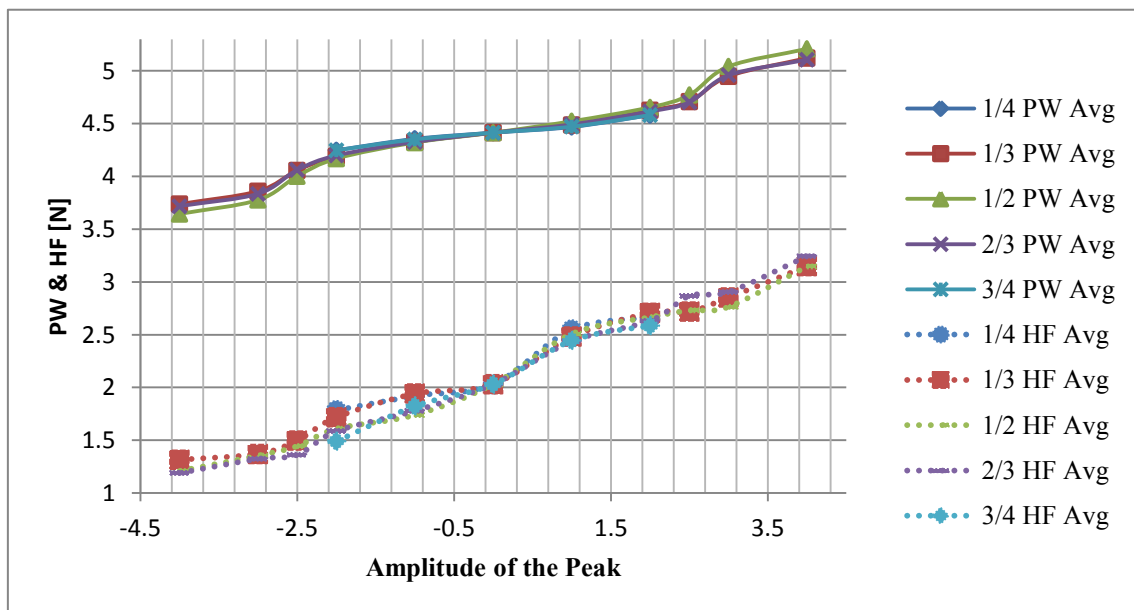


Fig.6.19 PW and HF Arranged by the Amplitude of the Peak ( $m_d=0.45$  kg,  $w_d=4.41$ N, Detaching Phase)

As for the entire length of the lifting, de PW and the difference between the weight and the PAF, for the detaching phase was calculated. This data is shown in Fig.6.20 and in Fig.6.21, the vertical axes represent the forces [N]. In Fig.6.20, the horizontal axis corresponds to the positions of the peaks and in Fig.6.21 to the amplitudes of the peaks.

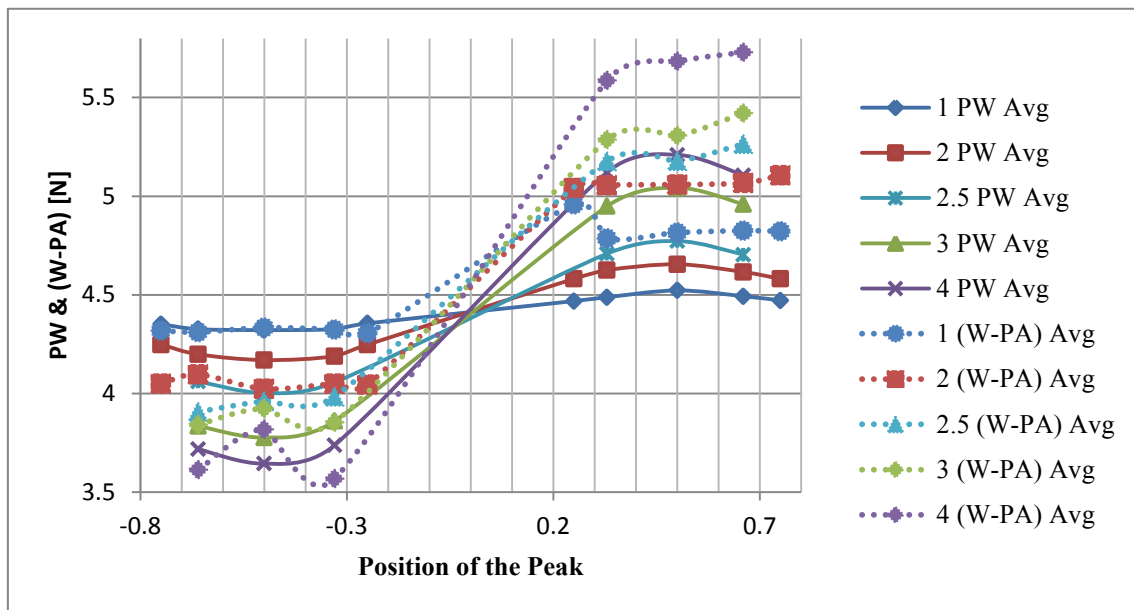


Fig.6.20 PW and (W-PA) Arranged by the Position of the Peak ( $m_d=0.45$  kg,  $w_d=4.41$ N, Detaching Phase)

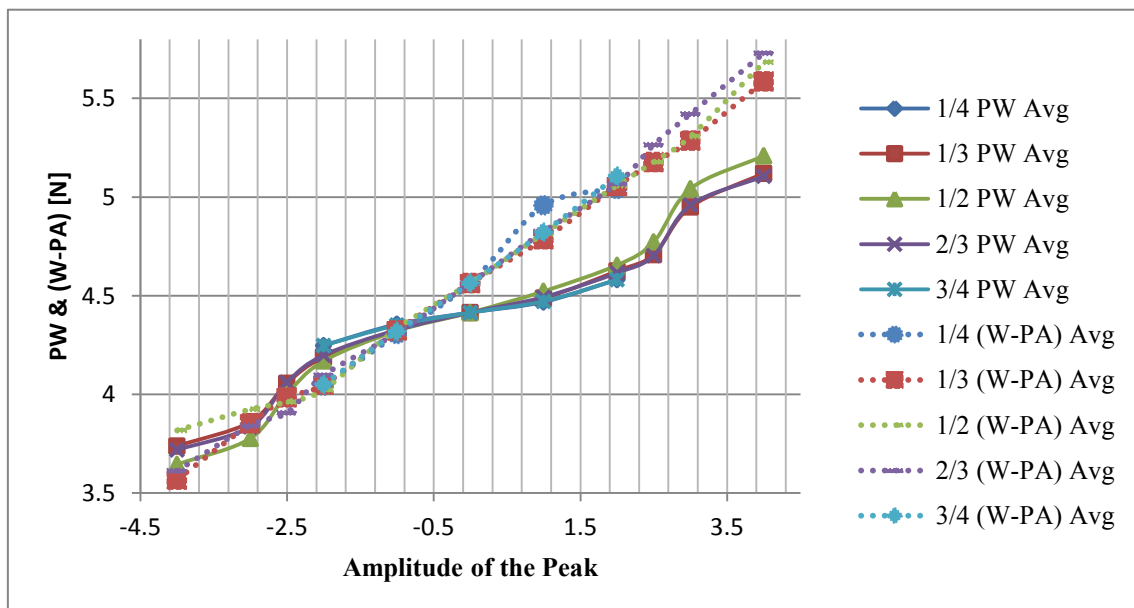


Fig.6.21 PW and (W-PA) Arranged by the Amplitude of the Peak ( $m_d=0.45$  kg,  $w_d=4.41$ N, Detaching Phase)

Other comparisons made between the PW and the forces recorded during the detaching phase are shown in Appendix E.

The process shown above for the sensor's data for the desired mass of 0.45 kg was also followed for the desired mass of 0.55 kg. Fig.6.22 corresponds to the trial of MD with the peak of amplitude 2.5 at position  $-2/3$ . As before, the northeast plot represents

the position of the object, the horizontal axis being the time [s] and the vertical axis the height [m]. The northwest plot was for validation purposes; the horizontal axis being the RF [N] and the vertical axis the HF [N]. The lower plot shows the recorded forces, the blue line being the RF, the magenta line the HF and the green line the PAF; the horizontal axis represents the time [s] and the vertical axis the forces [N].

The duration on Fig.6.22 correspond to the 5 s corresponding to the entire length of the trial. For the determination of the forces during the lifting, this duration was limited to the lifting part. Fig.6.23 shows this time restriction applied to the same case shown in Fig.6.22. The plots and the axes correspond to those of Fig.6.22.

In this case, the PW were also compared to the data from the sensors. The average of the PW and the average of the HF from all subjects are shown in Fig.6.24 and Fig.6.25. The vertical axes represent the forces [N]. In Fig.6.24, the horizontal axis corresponds to the positions of the peaks and in Fig.6.25 to the amplitudes of the peaks

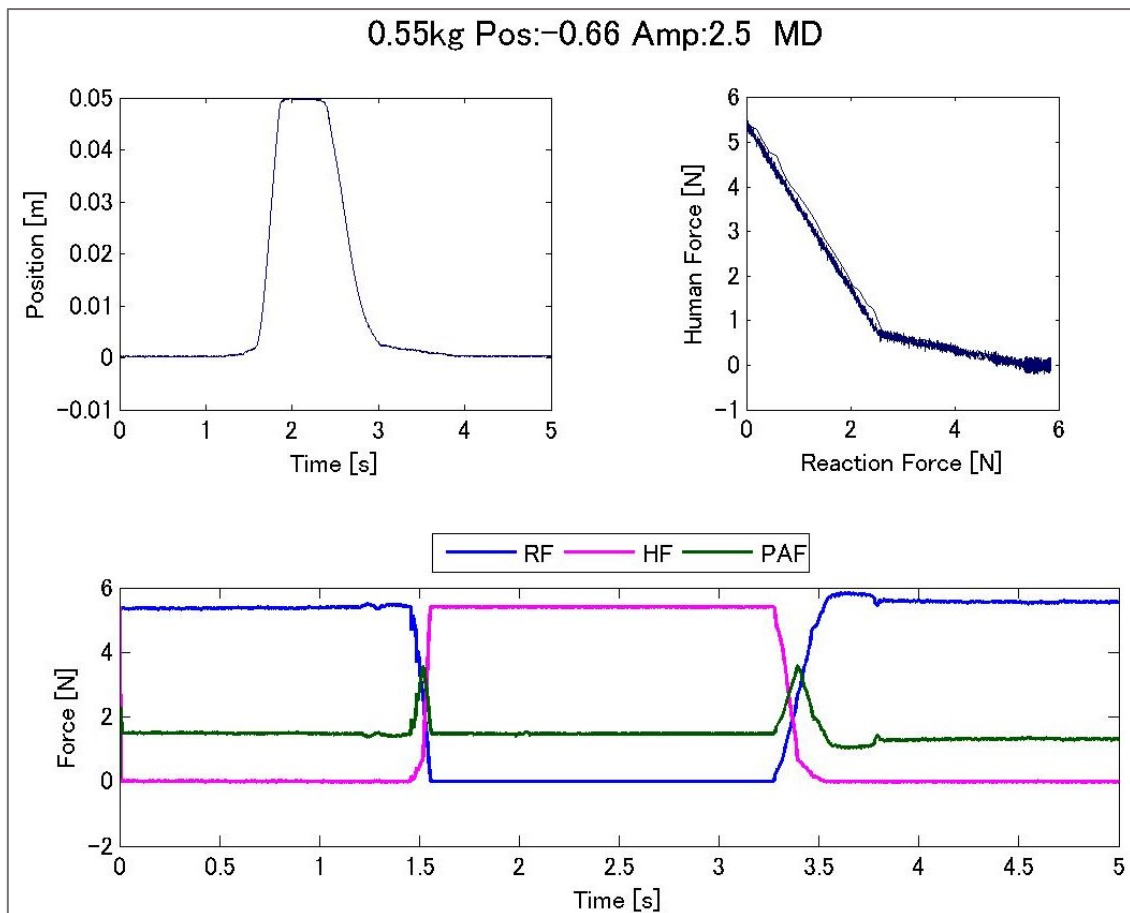


Fig.6.22 Data from the Sensors ( $m_d=0.55$  kg,  $w_d=5.39$ N, Entire Recorded Length)

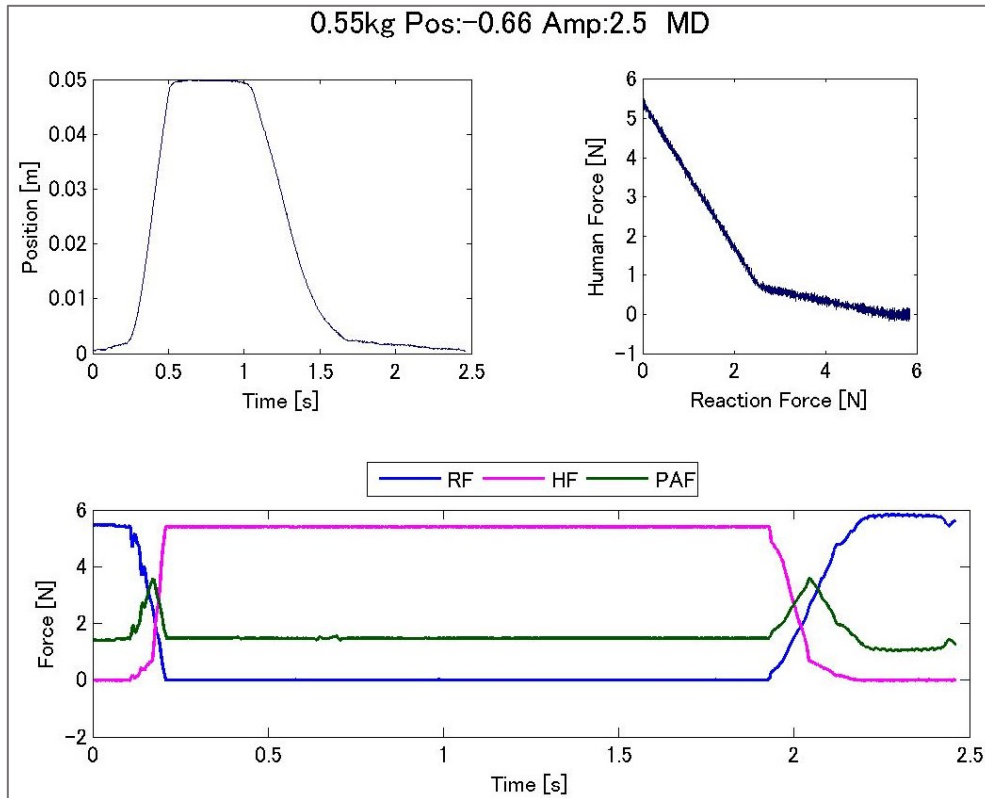


Fig.6.23 Data from the Sensors ( $m_d=0.55$  kg,  $w_d=5.39$ N, Lifting)

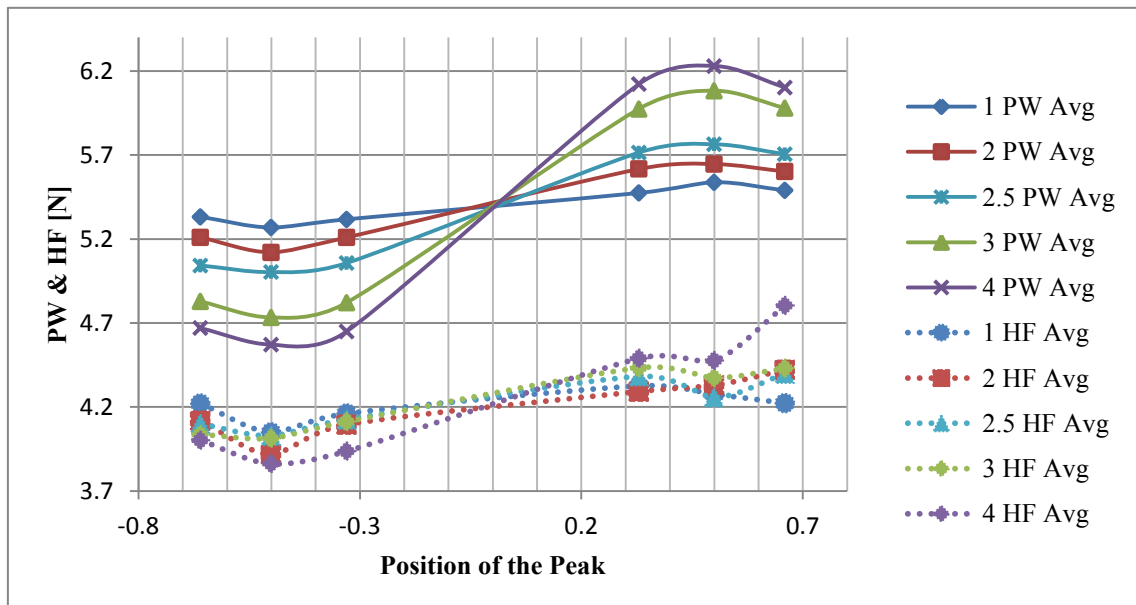


Fig.6.24 PW and HF Arranged by the Position of the Peak ( $m_d=0.55$  kg,  $w_d=5.39$ N, Lifting)

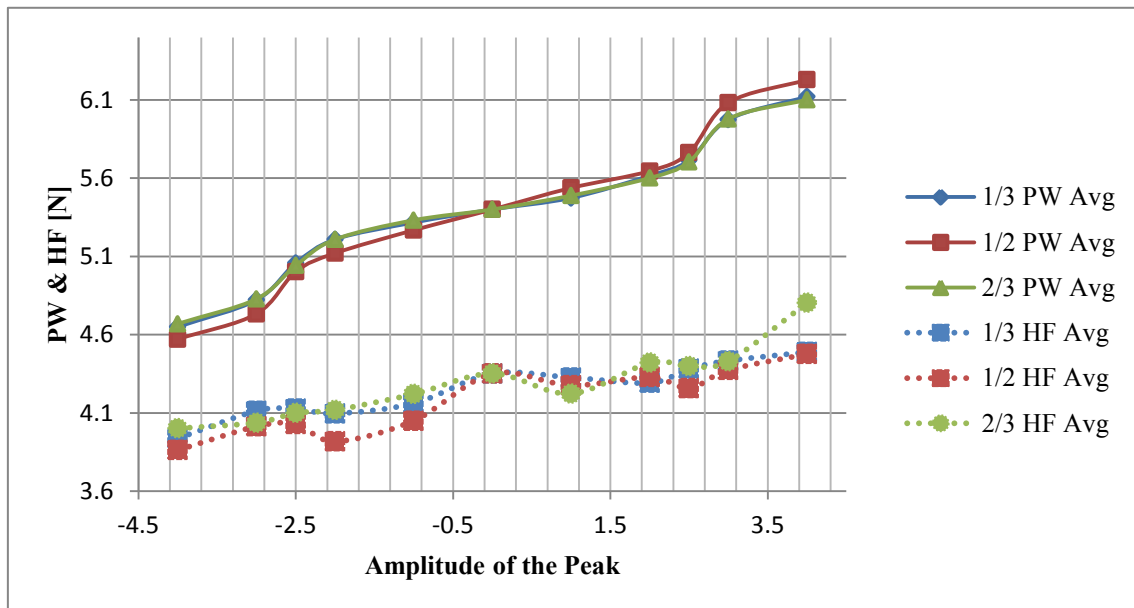


Fig.6.25 PW and HF Arranged by the Amplitude of the Peak ( $m_d=0.55$  kg,  $w_d=5.39$ N, Lifting)

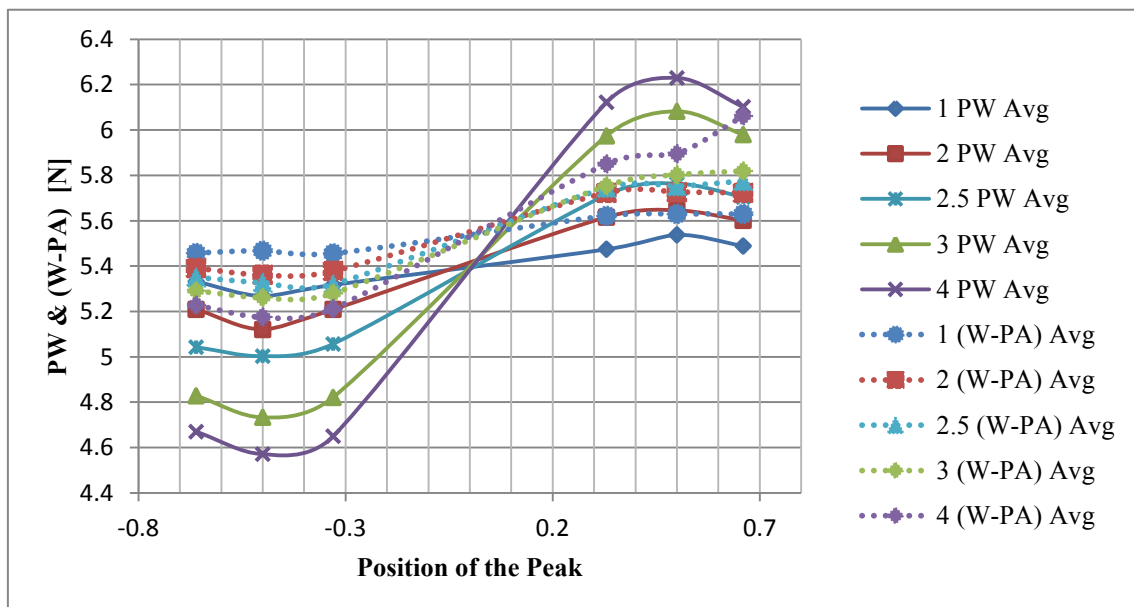


Fig.6.26 PW and (W-PA) Arranged by the Position of the Peak ( $m_d=0.55$  kg,  $w_d=5.39$ N, Lifting)

For this desired mass, the difference between the weight of the object and the PAF was also calculated and plotted against the PW as shown in Fig.6.26 and Fig.6.27. The vertical axes represent the forces [N]. In Fig.6.26, the horizontal axis corresponds to the positions of the peaks and in Fig.6.27 to the amplitudes of the peaks.

Other comparisons made between the PW and the forces recorded during the lifting are shown in Appendix F.

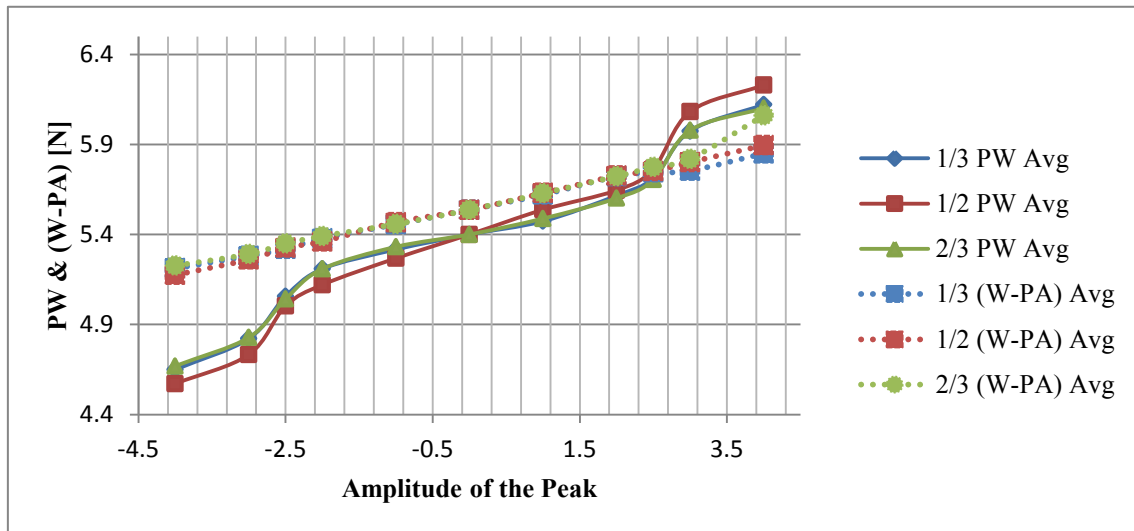


Fig.6.27 PW and (W-PA) Arranged by the Amplitude of the Peak ( $m_d=0.55$  kg,  $w_d=5.39$ N, Lifting)

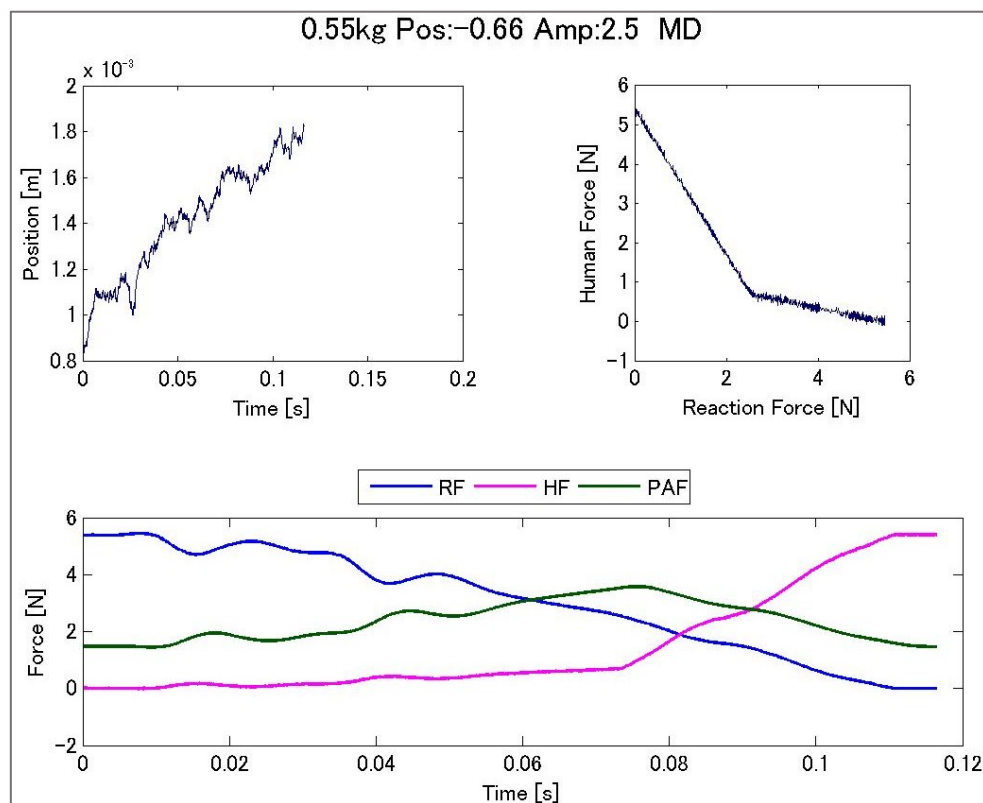


Fig.6.28 Data from the Sensors ( $m_d=0.55$  kg,  $w_d=5.39$ N, Detaching Phase)

As for the entire length of the lifting, the duration of the trial was restricted to the detaching phase. This is shown in Fig.6.28. The data, order of the plots and axes are the same as for Fig.6.22.

For the detaching phase, the PW and the HF were also compared as shown in Fig.6.29 and Fig.6.30. The solid lines correspond to the PW and the dotted lines to the HF. The vertical axes represent the forces [N]. In Fig.6.29, the horizontal axis corresponds to the positions of the peaks and in Fig.6.30 to the amplitudes of the peaks.

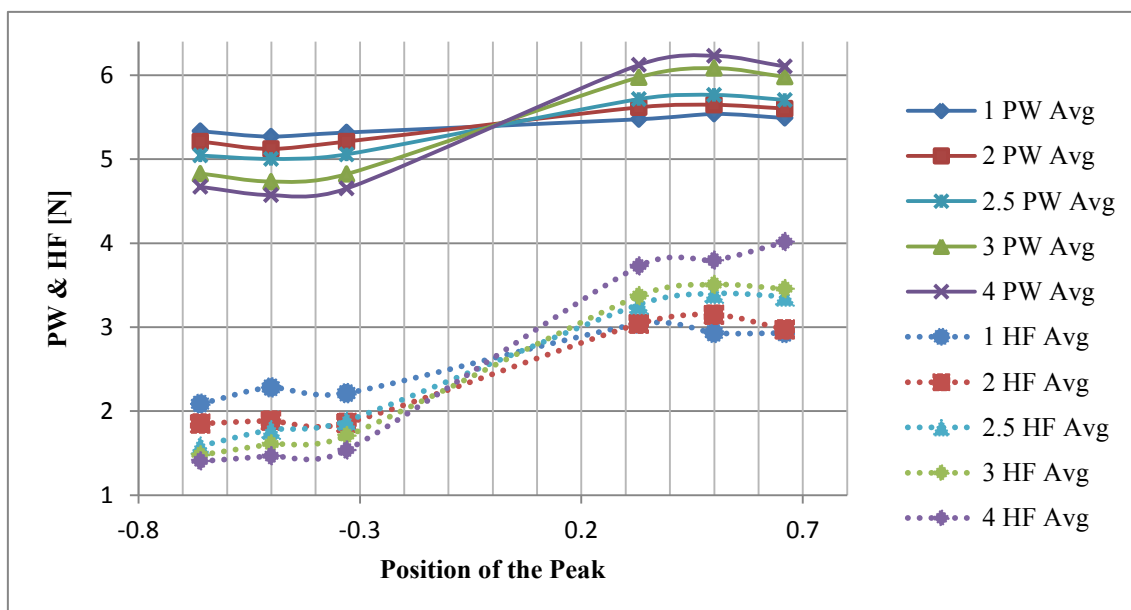


Fig.6.29 PW and HF Arranged by the Position of the Peak ( $m_d=0.55$  kg,  $w_d=5.39$ N, Detaching Phase)

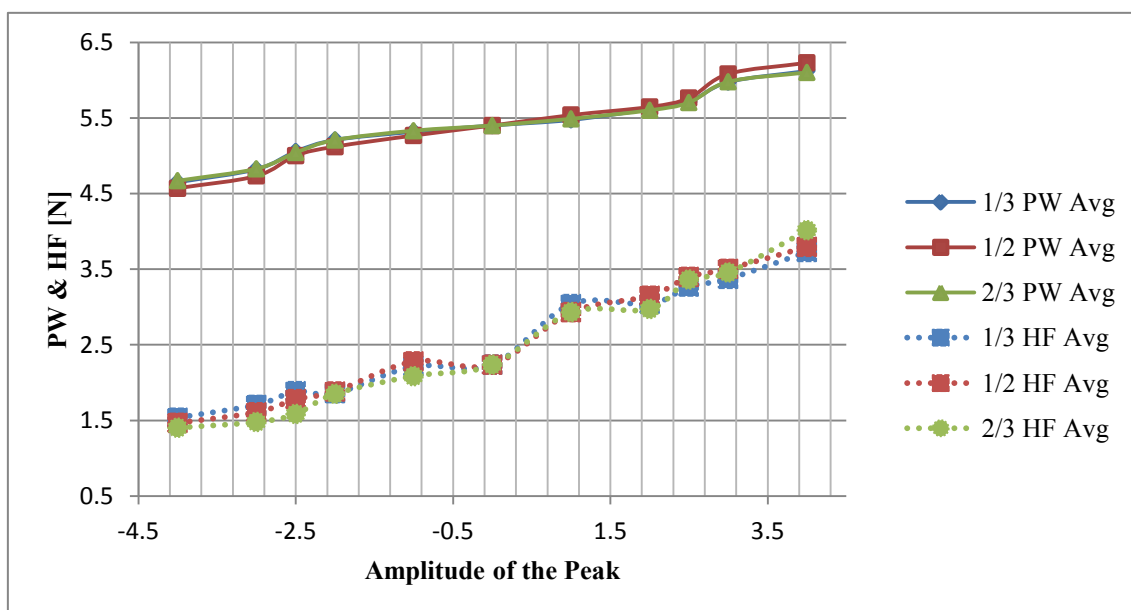


Fig.6.30 PW and HF Arranged by the Amplitude of the Peak ( $m_d=0.55$  kg,  $w_d=5.39$ N, Detaching Phase)

Likewise, the PW and the difference between the weight of the object and the PAF were compared as shown in Fig.6.31 and Fig.6.32. The vertical axes represent the forces [N]. In Fig.6.31, the horizontal axis corresponds to the positions of the peaks and in Fig.6.32 to the amplitudes of the peaks

Other comparisons made between the PW and the forces recorded during the lifting are shown in Appendix G.

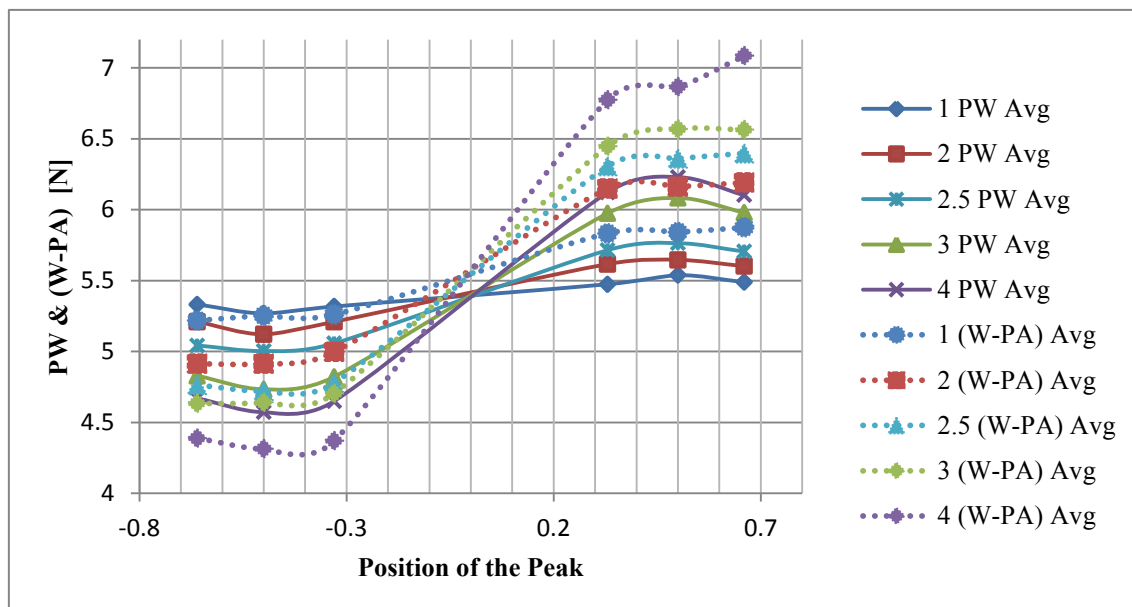


Fig.6.31 PW and (W-PA) Arranged by the Position of the Peak ( $m_d=0.55$  kg,  $w_d=5.39$ N, Detaching Phase)

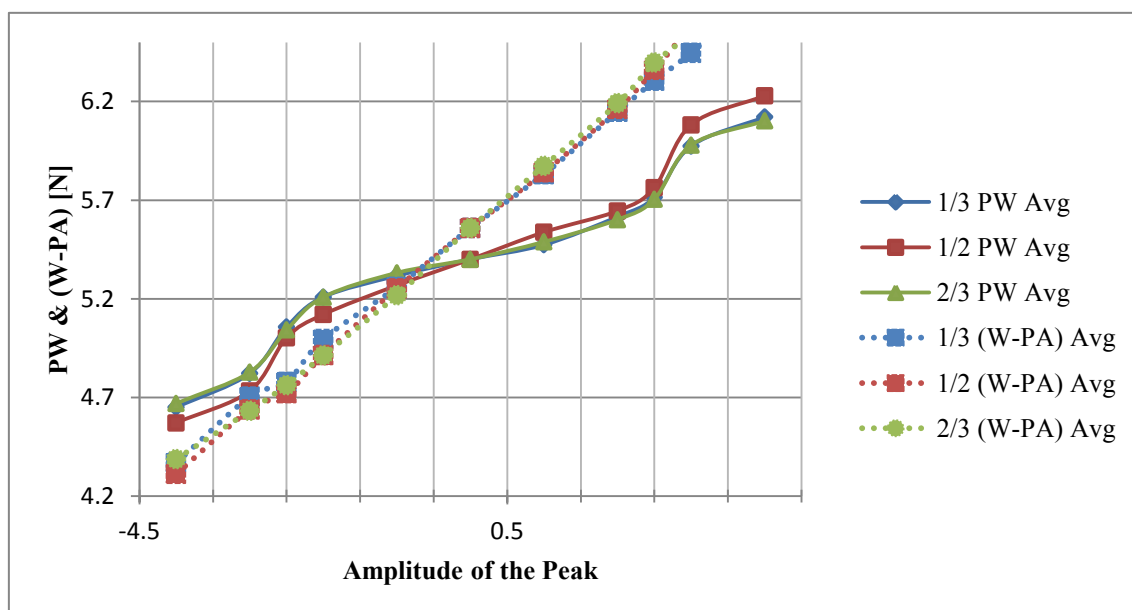


Fig.6.32 PW and (W-PA) Arranged by the Amplitude of the Peak ( $m_d=0.55$  kg,  $w_d=5.39$ N, Detaching Phase)

---

# Chapter 7

## Discussion and Conclusions

---

### 7.1 Discussion

From Fig.6.1, Fig.6.2, Fig.6.5 and Fig.6.6 we observe that the difference between PWs for the MI and the MD trials for both desired masses was approximately of 0.02 kg for all the peaks tested. In psychophysics, a sensory threshold is the weakest stimulus that an organism can detect [17]. Several different thresholds have been defined, among them:

- *Absolute threshold*: the lowest level at which a stimulus can be detected.
- *Recognition threshold*: the level at which a stimulus can not only be detected but also recognized.
- *Differential threshold*: the level at which an increase in a detected stimulus can be perceived.
- *Terminal threshold*: the level beyond which a stimulus is no longer detected.

Therefore, the value of 0.02 kg was the differential sensory threshold determined for both desired masses. One of the uses for this value is that it indicates the “gray-zone” where misperceptions between two different weights are more likely to happen. Nevertheless, this value is not constant for all weights but it is proportional to the baseline of the weight tested as the Weber’s Law indicates.

If we refer to Fig.6.3 and Fig.6.7 we can observe that the position of the peak had almost no effect on the PW. This was consistent to the data shown in Fig.6.13, Fig.6.15, Fig.6.24 and Fig.6.26 where we can see that the average value of the measured HF and the difference between the weight and the PAF weren’t affected by the position of the peak. On the other hand, if we refer to Fig.6.4 and Fig.6.8, we see that the PW did varied depending of the amplitude of the peak tested. Once more, this is consistent to the average value of the measured HF and the difference between weight and PAF as shown in in Fig.6.14, Fig.6.16, Fig.6.25 and Fig.6.27.

The position of the peak was related to the timing at which the maximum force was proportionated while the amplitude of the peak related to the given PAF. Therefore, one possibility is that if the average of the force needed to lift an object is the same, it doesn’t matter the timing at which such force is applied. On the other hand, the PWs

between positions was similar but not exactly the same (Standard Deviation between 0.01 N and 0.04N), maybe if the time difference between peaks were larger, the sensory threshold could change and could impact on the PW.

On Fig.6.9 and Fig.6.10 we can see that the perceived masses were different to the desired masses and that the maximum difference between the desired mass and the perceived mass was of approximately  $\pm 0.08$  kg for both desired masses. The functions used on these experiments were symmetric about the axis formed by the aforementioned non-altered function of the RF and the HF. Further experiments are necessary to confirm this proportionality but the current results indicate that modifications made considering the non-altered function as axis of symmetry could render symmetric PWs.

Moreover, on Fig.6.4 and Fig.6.8 we can appreciate that the PW given by the amplitude 0, that is, the non-altered function, gave a PW corresponding to the desired mass. Hence, confirming that the control implemented produced the desired effect and validating the results of amplitude 0 as control case.

However, from the recorded forces shown in Fig.6.13, Fig.6.14, Fig.6.18, Fig.6.19, Fig.6.24, Fig.6.25, Fig.6.29 and Fig.6.30, we observe that the PW didn't correspond to the HF either for the detaching phase or the entire length of the lift; even if the slope of the PW and the HF were similar. The resemblance on the form of both curves gives reason to think that the PW are to some extent linear to the HF but there is another factor not contemplated on this experiment that is causing the "bump" on the PWs. Moreover, the difference between the PW and the HF was more accentuated when considering only the detaching phase than when considering the entire lifting. Therefore, one possible way to find the factor causing the aforementioned bump is to focus in which factors are present during the lifting but not during the detaching phase and vice versa.

As can be seen in Fig.6.15, Fig.6.16, Fig.6.20, Fig.6.21, Fig.6.26, Fig.6.27, Fig.6.31 and Fig.6.32, the difference between the weight of the object and the applied PAF gave the closer similarity to the PWs. This reinforces the previous hypothesis that there is an external factor affecting the PW. However, the similarity applies for the peaks of amplitude 1 and 2. From Fig.6.15, Fig.6.16, Fig.6.26 and Fig.6.27 we can see that the PW corresponding to the positive amplitudes was closer to the difference between the weight and the PAF when considering the entire length of the lifting. On the contrary, on Fig.6.20, Fig.6.21, Fig.6.31 and Fig.6.32 we can see that the PW corresponding to the

negative amplitudes was closer to the aforementioned difference when considering only the detaching phase. As for the rest of the amplitudes, the value of the PW falls between the value of the aforesaid difference for the detaching phase and the value for the entire length of the lifting. One of the reasons why the bigger amplitudes don't correspond to one of the cases may be that they are big enough to fall in a different sensory threshold. In fact, originally only the peaks at {1,2,3,4} were implemented and it was the difference of PW between the amplitudes that made us add the peak at 2.5 to the experiment. Our suspicion was that the threshold is between the amplitudes of 2 and 3, yet, to prove it further experiments with more divisions between those amplitudes are necessary.

These results indicate that to produce a heavier PW than the desired weight, the focus should be on the average of the proportionated force during the entire length of the lifting whilst to produce a lighter PW, the focus should be on the detaching phase.

## 7.2 Conclusions

The aim of our research was to elucidate the factors that affect the PW and the hypothesis was that focusing on the detaching phase and modifying the relation between the RF and the HF affected the PW. With this objective, we created a 1 DOF PA device and implemented several modifications of the aforementioned relation on the control algorithm. The subjective data and the data from the sensors were recorded.

The difference between the PW and the desired weight were not a surprise since the cases when the amplitude was positive require the subject to proportionate a bigger force to lift the object than the cases of negative amplitude, this according to the laws of motion. However, by how much the PW and the desired weight differ is still to be foreseeable.

We determined the differential sensory threshold for both desired masses as 0.02 kg. This threshold could be used to reduce the range at which misperceptions are more likely to happen and therefore, be on guard to prevent accidents when using PA devices.

Furthermore, the position of the peaks tested was found not to influence the PW, contrary to the amplitude that did affect it. This findings were consistent to the average of the measured force and the average of the difference between weight and PAF. The first one matched with the slope of the PWs while the later matched rather to the values of the PWs. Therefore, the suspicion is that there is another factor than the contemplated in these experiments that is affecting the PW, explaining the offset between the recorded

HF and the PW.

The offset between the desired mass and the perceived mass was of  $\pm 0.08$  kg in the case of both desired masses. More likely, the found symmetry on the PW is also due to the axis of symmetry of the tested functions. Therefore this proportionality could be used as a reference to modify the PW.

Additionally, our control case, i.e. the peak of amplitude 0 was found to produce the PW corresponding to the desired mass, which validated the control algorithm.

For the peaks of amplitude 1 and 2 we may have found a reason for the PW on the difference between the weight of the object and the applied PAF. The cases with a lighter PW than expected, relying on the detaching phase; those with a heavier PW relying on the entire length of the lifting.

However the value of the PW for the rest of the amplitudes was found to be in the middle of the values of the previous difference for the detaching phase and the entire lifting. This suggests that the jump in the amplitude may produce also a change in the sensory threshold, the peak of amplitude 2.5 being near the sensory threshold limit.

In a nutshell, since the PW didn't match to the desired masses or the recorded data, our hypothesis was confirmed: modifying the relation between the HF and the RF does affect the PW. Several probable causes were proposed on this document but further experiments are desirable.

One of the more promising results being that to produce a heavier PW, the focus should be on the average of the proportionated force during the entire length of the lifting whilst to produce a lighter PW, the focus should be on the detaching phase.

### 7.3 Future Work

In these experiments, not only our hypothesis was confirmed but several possible correlations for the PW were proposed. This opens the field to future experiments to validate our results and expand its implications and uses.

In one of such future experiments, it may be worthy to determine the rest of the sensory thresholds to have a more complete view of the weight perception and its limits. Also, to test more desired masses, especially those likely to be lifted in daily and industrial applications.

On other experiments, the position of the peaks could be broadened to include the

entire lifting, using a different basis than the RF as reference. This could enlighten the question of if the position indeed didn't affect the PW or if it was just insufficient to trespass the sensory threshold.

Moreover, the possible factors present on the lifting but not on the detaching phase should be included on the spectrum of the experiments in order to determine the factor producing the offset between the PW and the HF.

On this direction, other amplitudes between 2 and 3 should be tested with these and other desired masses to determine the limit at which the PW stops to match with the difference between the weight and the PAF.

What is more, explore until what point, the chosen axis of symmetry for the tested functions produces symmetric PWs and why the lighter ones rely on the detaching phase and why the heavier ones are based on the entire length of the lifting.

In other words, the work presented here showed some interesting results but it is just the tip of the iceberg, there are still many factors and correlations to be researched and validated.

However one of my stronger suggestions is for the factors affecting the PW to be implemented and tested on commercial devices or in systems that could be used in real life. This way, the research would be more likely to escalate, be implemented and why not, appeal to the public and the enterprises.

# Appendices

## A. Accelerometer's Specifications



### Model 3145

Signal Conditioned Accelerometer  
 0.5 to 4.5 VDC Output  
 Intergral Temperature Compensation  
 High Performance

- Vibration/Shock Monitoring
- Geophysical Monitoring
- Modal Analysis
- Structural Analysis
- Elevator Ride Control



#### FEATURES

- Bolt Mount
- ±0.5% Non-linearity (typical)
- ±4.0% Temperature Performance
- DC Response
- Built-in Damping
- Built-in Overrange Stops
- Low Power

#### STANDARD RANGES

Range	g
±2	•
±5	•
±10	•
±20	•
±50	•
±100	•

#### DESCRIPTION

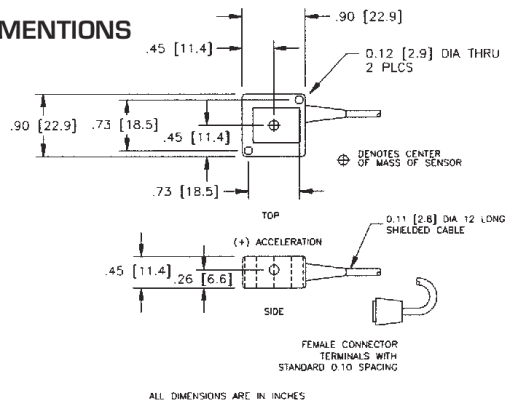
The Model 3145 is a general purpose performance accelerometer intended for instrumentation applications. The 3145 provides a fully signal conditioned output with performance similar to traditional instrumentation accelerometers but at a much lower cost.

The accelerometer consists of a silicon micro machined accelerometer with signal conditioning electronics in a lightweight Valox™ housing that can be easily attached to a mounting surface.

The sensing element is a micro machined silicon mass suspended by multiple beams from a silicon frame. Piezoresistors located in the beams change their resistance as the motion of the suspended mass changes the strain in the beams. Silicon caps on the top and bottom of the device are added to provide over-range stops. This design provides for a very low profile, high shock resistance, durability and built-in damping over a wide usable bandwidth.

A higher performance version of the 3145 is available for critical applications. Please refer to the Model 3140 for additional information.

#### DIMENSIONS



Internet: www.msiausa.com  
 Tel: 1-757-766-1500  
 North America Toll Free: 1-800-745-8008  
 Fax: 1-757-766-4297

## B. Gap Sensor's Specifications

Non-contact displacement measuring system

**GAP-SENSOR**

### AEC-55 Series

Converter : **AEC-55**

Adopted converter : PU model sensor  
 Adopted cables : PC model cable  
 : PCT model cable



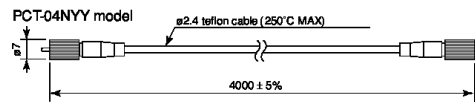
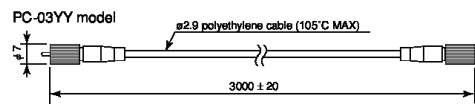
#### Specifications

model	Converter : AEC-55 □□ (□□ symbolize sensor diameter)
output voltage	See each sensor section.
frequency characteristics	DC to 20kHz -2dB
resolution	See each sensor section.
temperature range	-10°C to 55°C
Thermal characteristics	0.1%/°C of drift between -10°C and 55°C
power supply	DC ± 11V to DC ± 17V, ± 40mA max

#### Features and specifications

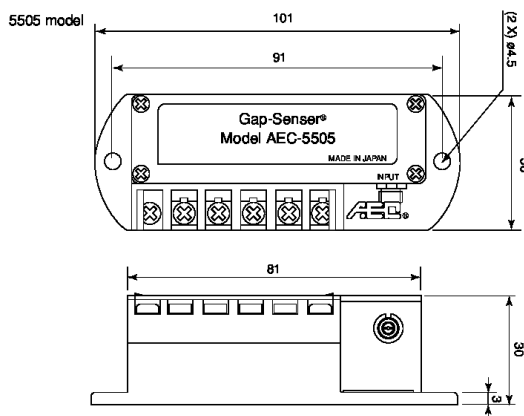
- Optimum miniature converter for installation
- Able to calibrate and adjust sensitivity with a built-in volume control dial
- Able to prepare a converter that is designed to protect from interference noise caused when multiple sensors approach each other
- Able to prepare a specified build-in power supply multi-channel on demand

#### Adopted ordered cables



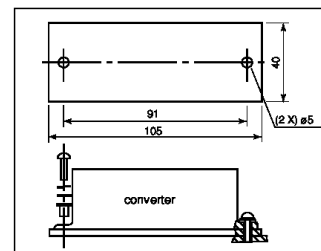
※Acceptable for use with all kinds and lengths of flexible armoured cables

#### Outline view



#### 55 model Converter (option)

Insulating bakelite plate (55IP)



### C. PIC18F4455's Specifications



## MICROCHIP PIC18F2455/2550/4455/4550

### 28/40/44-Pin High-Performance, Enhanced Flash USB Microcontrollers with nanoWatt Technology

#### Universal Serial Bus Features:

- USB V2.0 Compliant
- Low Speed (1.5 Mb/s) and Full Speed (12 Mb/s)
- Supports Control, Interrupt, Isochronous and Bulk Transfers
- Supports up to 32 endpoints (16 bidirectional)
- 1-Kbyte dual access RAM for USB
- On-chip USB transceiver with on-chip voltage regulator
- Interface for off-chip USB transceiver
- Streaming Parallel Port (SPP) for USB streaming transfers (40/44-pin devices only)

#### Power-Managed Modes:

- Run: CPU on, peripherals on
- Idle: CPU off, peripherals on
- Sleep: CPU off, peripherals off
- Idle mode currents down to 5.8  $\mu$ A typical
- Sleep mode currents down to 0.1  $\mu$ A typical
- Timer1 oscillator: 1.1  $\mu$ A typical, 32 kHz, 2V
- Watchdog Timer: 2.1  $\mu$ A typical
- Two-Speed Oscillator Start-up

#### Flexible Oscillator Structure:

- Four Crystal modes including High Precision PLL for USB
- Two External Clock modes, up to 48 MHz
- Internal oscillator block:
  - 8 user-selectable frequencies, from 31 kHz to 8 MHz
  - User-tunable to compensate for frequency drift
- Secondary oscillator using Timer1 @ 32 kHz
- Dual oscillator options allow microcontroller and USB module to run at different clock speeds
- Fail-Safe Clock Monitor
  - Allows for safe shutdown if any clock stops

#### Peripheral Highlights:

- High-current sink/source 25 mA/25 mA
- Three external interrupts
- Four Timer modules (Timer0 to Timer3)
- Up to 2 Capture/Compare/PWM (CCP) modules:
  - Capture is 16-bit, max. resolution 6.25 ns (Tcy/16)
  - Compare is 16-bit, max. resolution 100 ns (Tcy)
  - PWM output: PWM resolution is 1 to 10-bit
- Enhanced Capture/Compare/PWM (ECCP) module:
  - Multiple output modes
  - Selectable polarity
  - Programmable dead time
  - Auto-Shutdown and Auto-Restart
- Enhanced USART module:
  - LIN bus support
- Master Synchronous Serial Port (MSSP) module supporting 3-wire SPI™ (all 4 modes) and I<sup>2</sup>C™ Master and Slave modes
- 10-bit, up to 13-channels Analog-to-Digital Converter module (A/D) with programmable acquisition time
- Dual analog comparators with input multiplexing

#### Special Microcontroller Features:

- C compiler optimized architecture with optional extended instruction set
- 100,000 erase/write cycle Enhanced Flash program memory typical
- 1,000,000 erase/write cycle Data EEPROM memory typical
- Flash/Data EEPROM Retention: > 40 years
- Self-programmable under software control
- Priority levels for interrupts
- 8 x 8 Single-Cycle Hardware Multiplier
- Extended Watchdog Timer (WDT):
  - Programmable period from 41 ms to 131 s
- Programmable Code Protection
- Single-Supply 5V In-Circuit Serial Programming™ (ICSP™) via two pins
- In-Circuit Debug (ICD) via two pins
- Optional dedicated ICD/ICSP port (44-pin devices only)
- Wide operating voltage range (2.0V to 5.5V)

Device	Program Memory		Data Memory		I/O	10-bit A/D (ch)	CCP/ECCP (PWM)	SPP	MSSP		EAUSART	Comparators	Timers 8/16-bit
	Flash (bytes)	# Single-Word Instructions	SRAM (bytes)	EEPROM (bytes)					SPI™	Master I <sup>2</sup> C™			
PIC18F2455	24K	12288	2048	256	24	10	2/0	No	Y	Y	1	2	1/3
PIC18F2550	32K	16384	2048	256	24	10	2/0	No	Y	Y	1	2	1/3
PIC18F4455	24K	12288	2048	256	35	13	1/1	Yes	Y	Y	1	2	1/3
PIC18F4550	32K	16384	2048	256	35	13	1/1	Yes	Y	Y	1	2	1/3

**D. Comparisons between the PW and the Recorded Forces ( $m_d=0.45$  kg,  $w_d=4.41$ N, Time Length: Entire Lifting)**

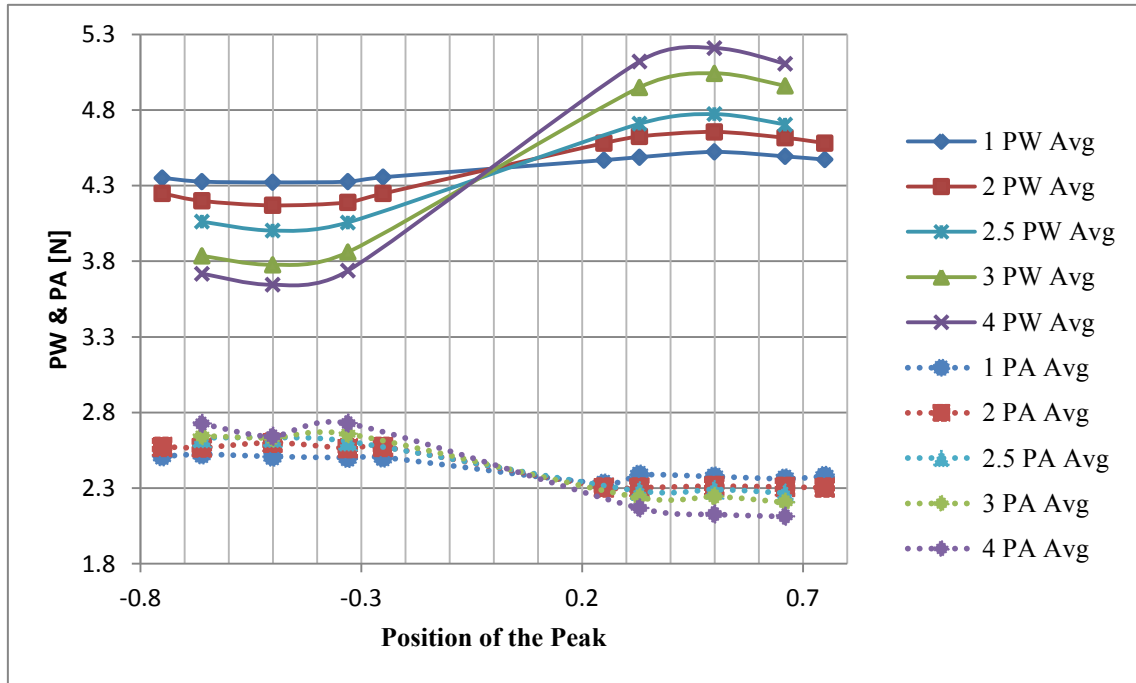


Fig.D.1 PW and PA Arranged by the Position of the Peak ( $m_d=0.45$  kg,  $w_d=4.41$ N, Lifting)

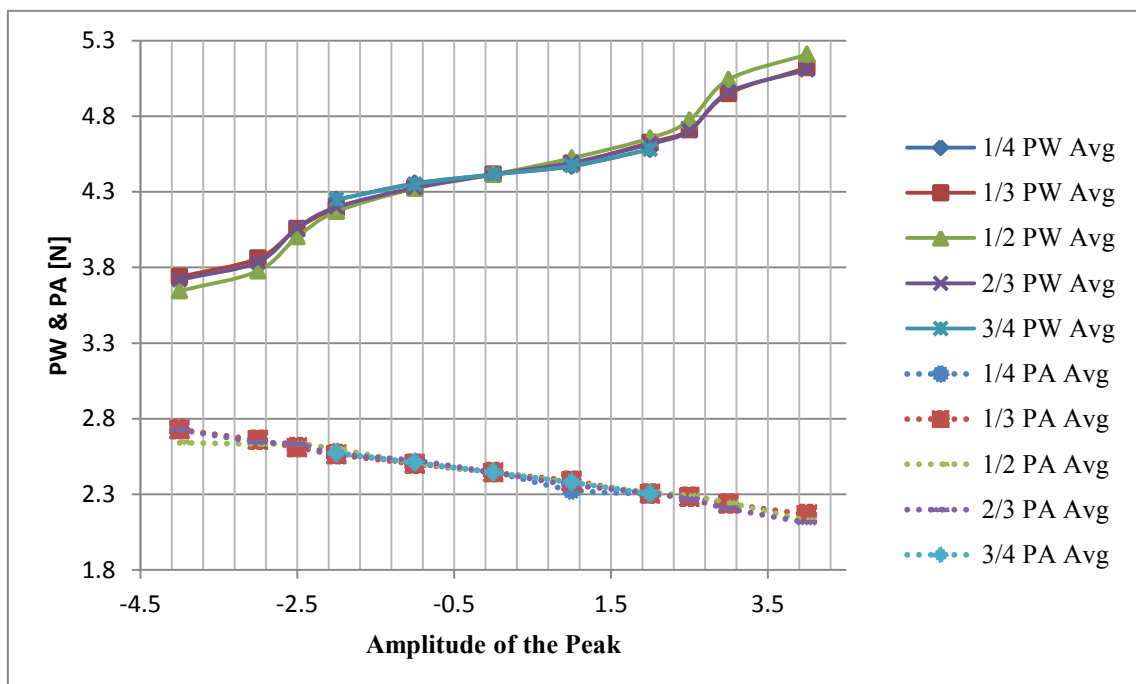


Fig.D.2 PW and PA Arranged by the Amplitude of the Peak ( $m_d=0.45$  kg,  $w_d=4.41$ N, Lifting)

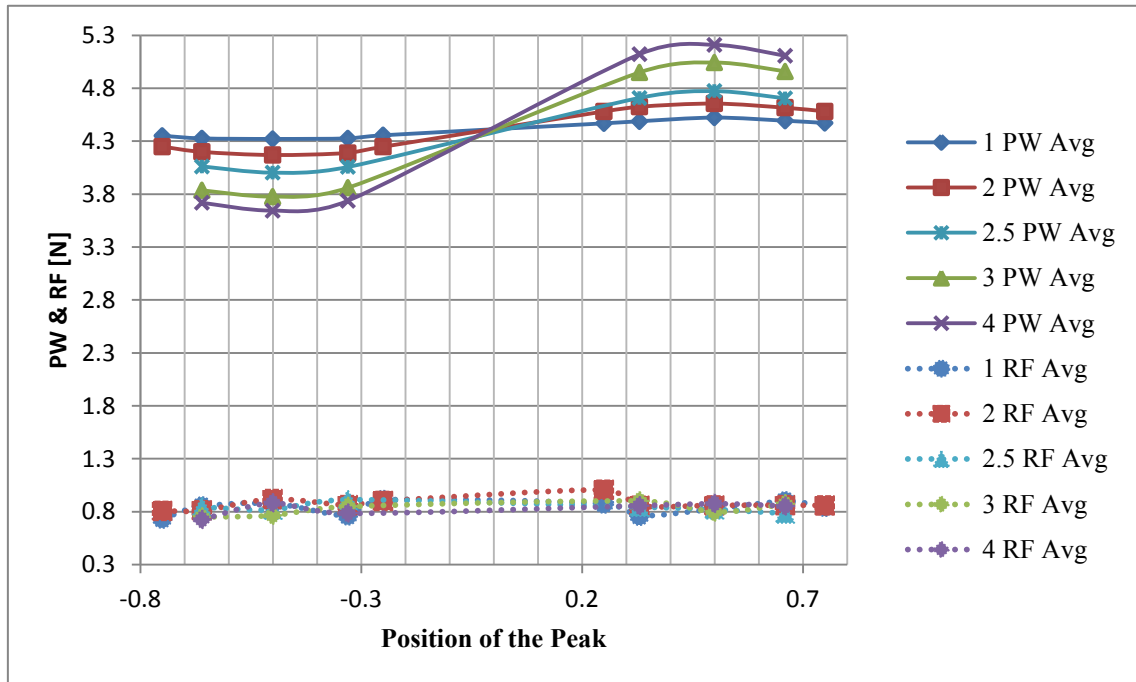


Fig.D.3 PW and RF Arranged by the Position of the Peak ( $m_d=0.45$  kg,  $w_d=4.41$ N, Lifting)

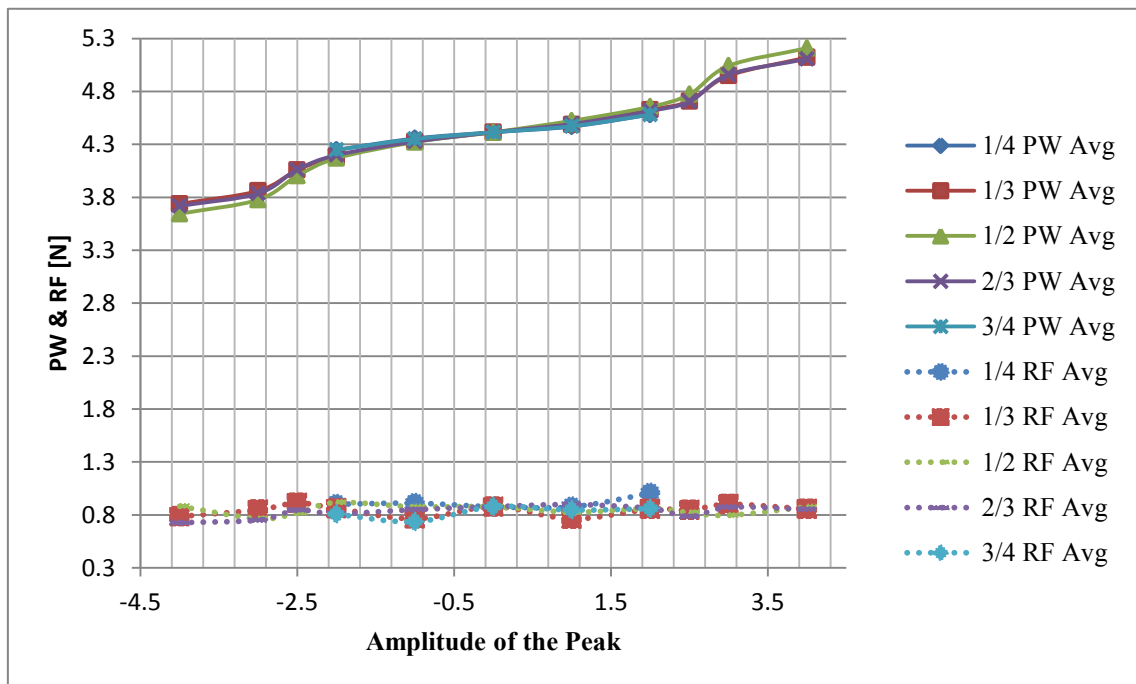


Fig.D.4 PW and RF Arranged by the Amplitude of the Peak ( $m_d=0.45$  kg,  $w_d=4.41$ N, Lifting)

**E. Comparisons between the PW and the Recorded Forces ( $m_d=0.45$  kg,  $w_d=4.41$ N, Time Length: Detaching Phase)**

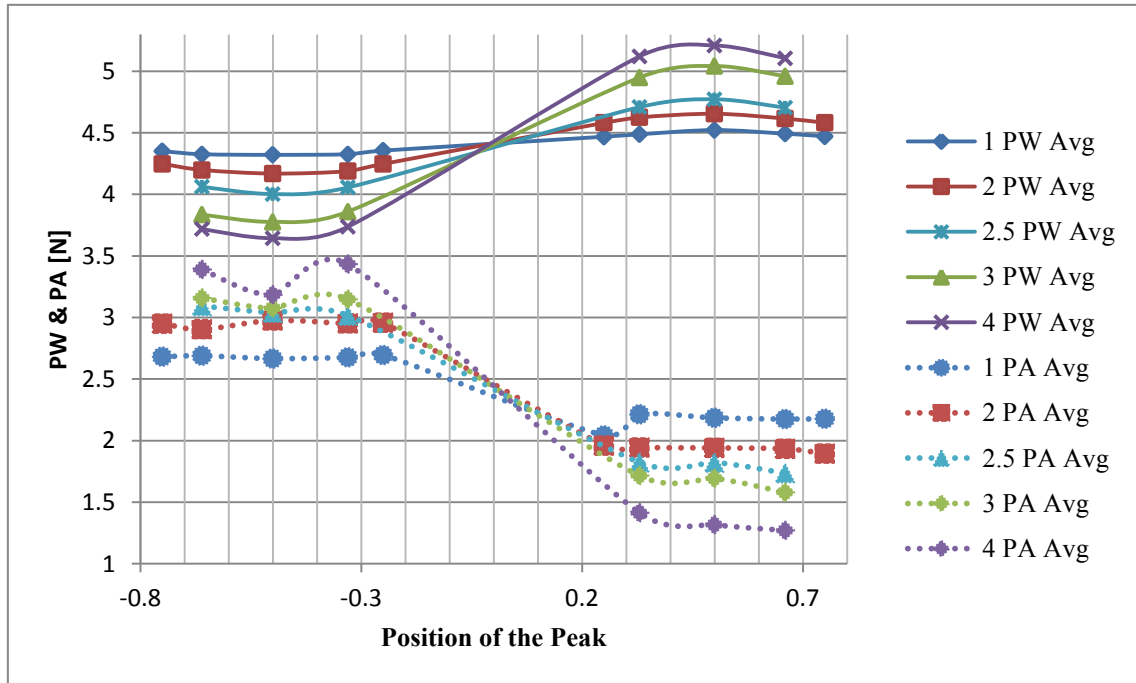


Fig.E.1 PW and PA Arranged by the Position of the Peak ( $m_d=0.45$  kg,  $w_d=4.41$ N, Detaching)

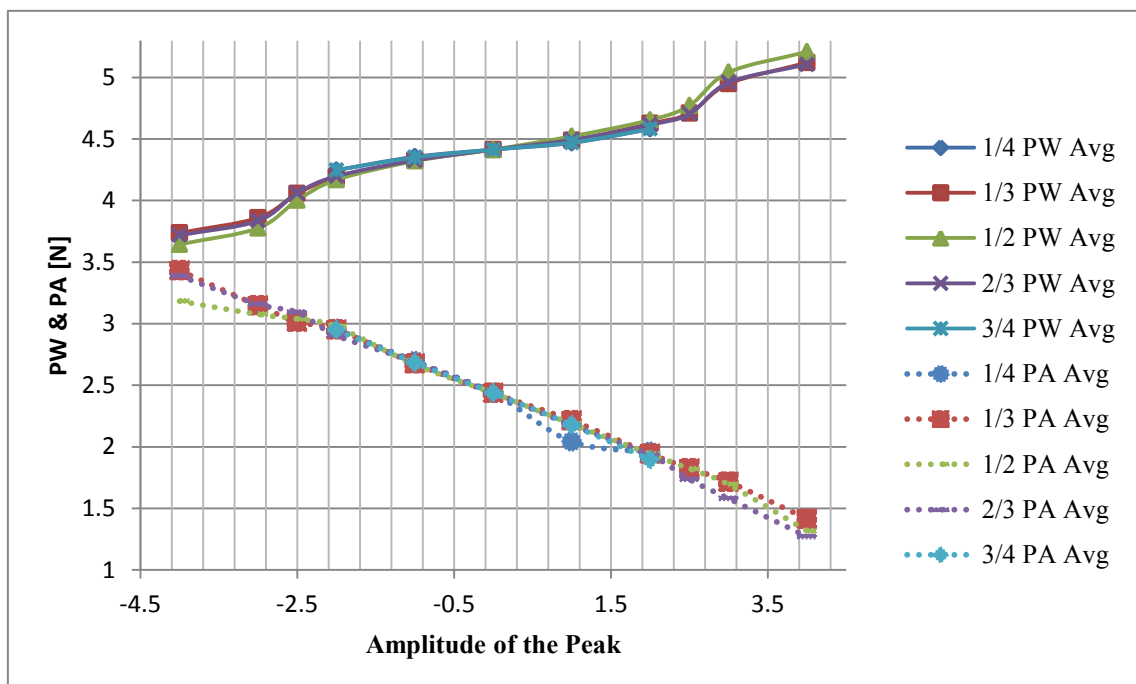


Fig.E.2 PW and PA Arranged by the Amplitude of the Peak ( $m_d=0.45$  kg,  $w_d=4.41$ N, Detaching)

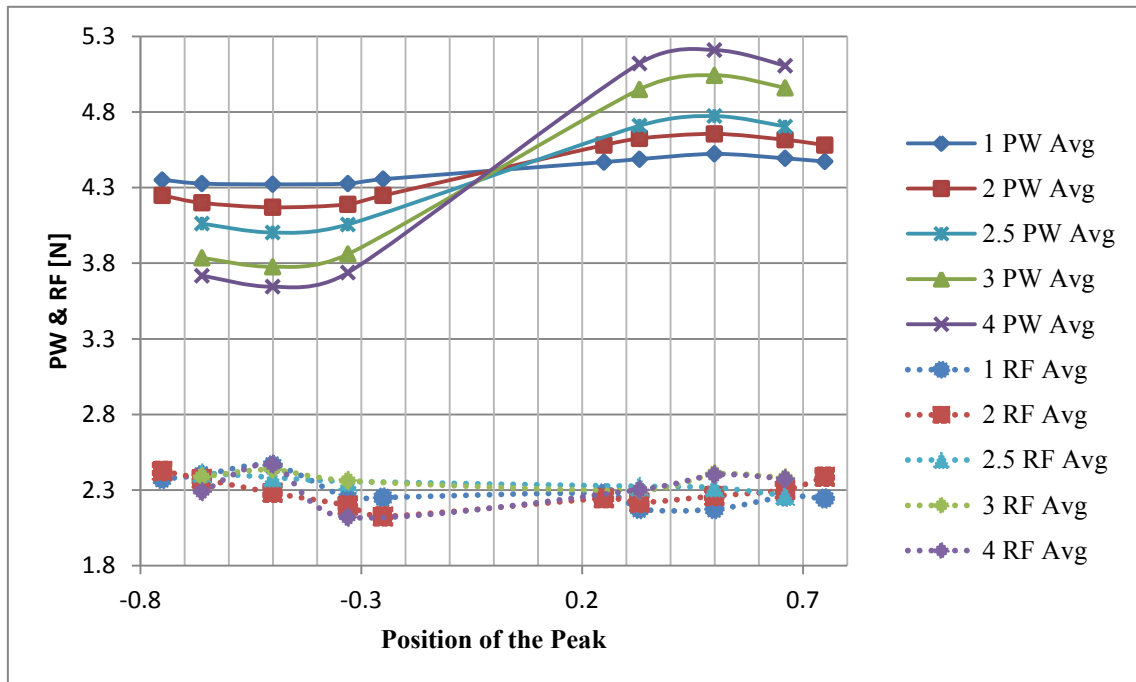


Fig.E.3 PW and RF Arranged by the Position of the Peak ( $m_d=0.45$  kg,  $w_d=4.41$ N, Detaching)

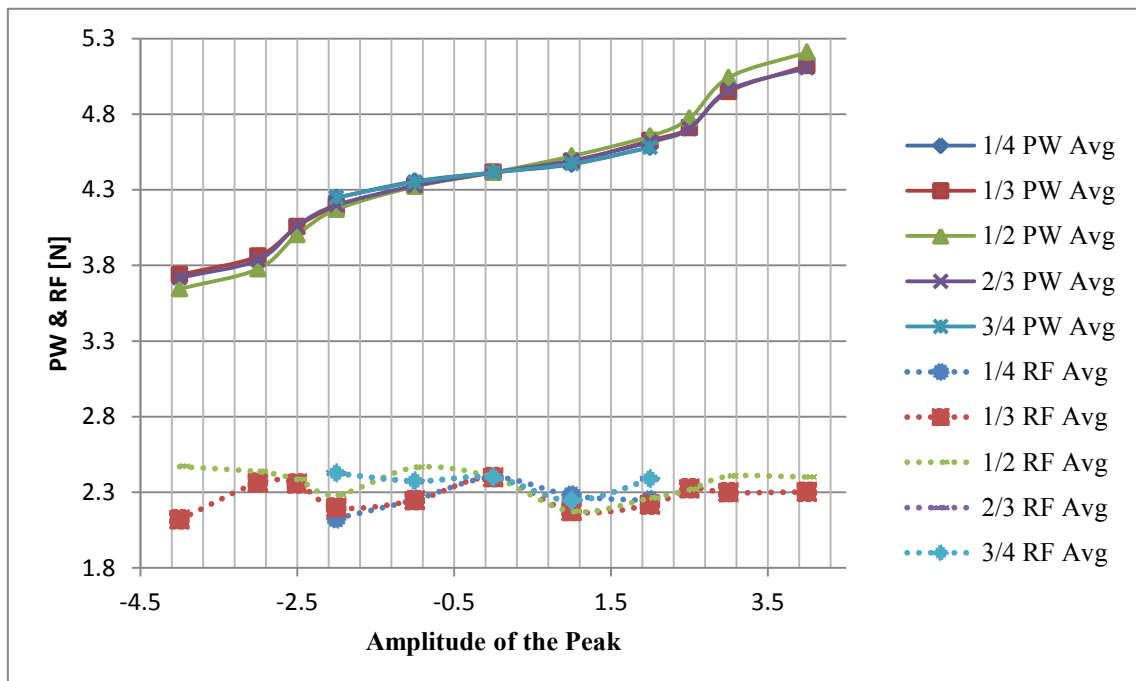


Fig.E.4 PW and RF Arranged by the Amplitude of the Peak ( $m_d=0.45$  kg,  $w_d=4.41$ N, Detaching)

**F. Comparisons between the PW and the Recorded Forces ( $m_d=0.55$  kg,  $w_d=5.39$ N, Time Length: Entire Lifting)**

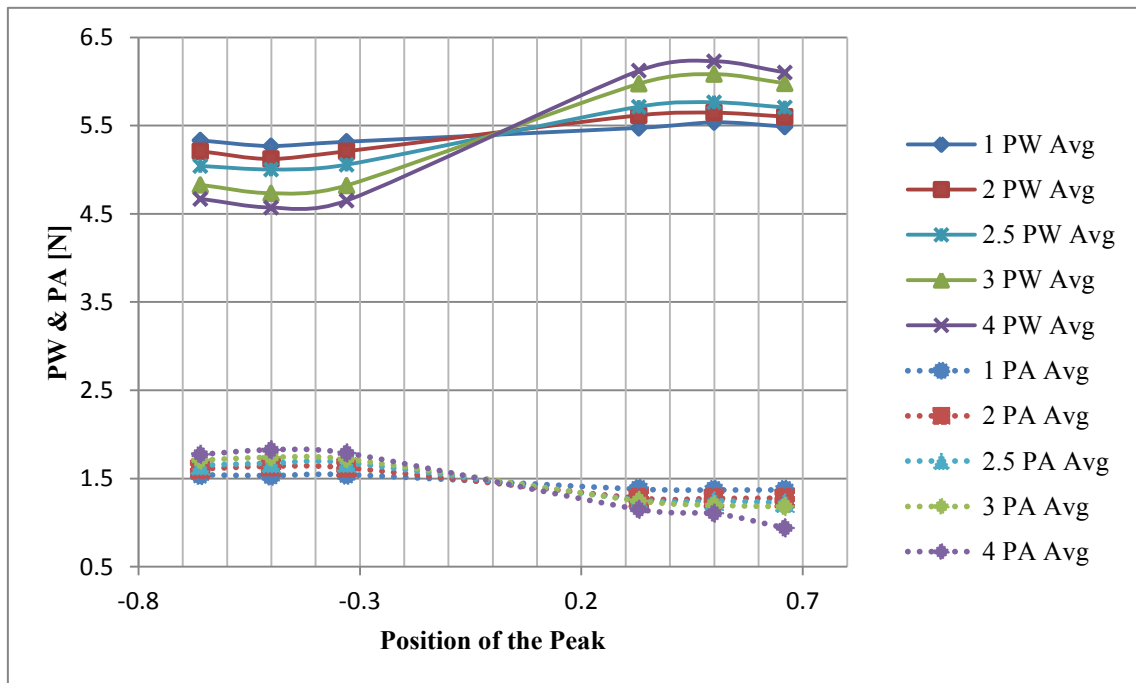


Fig.F.1 PW and PA Arranged by the Position of the Peak ( $m_d=0.55$  kg,  $w_d=5.39$ N, Lifting)

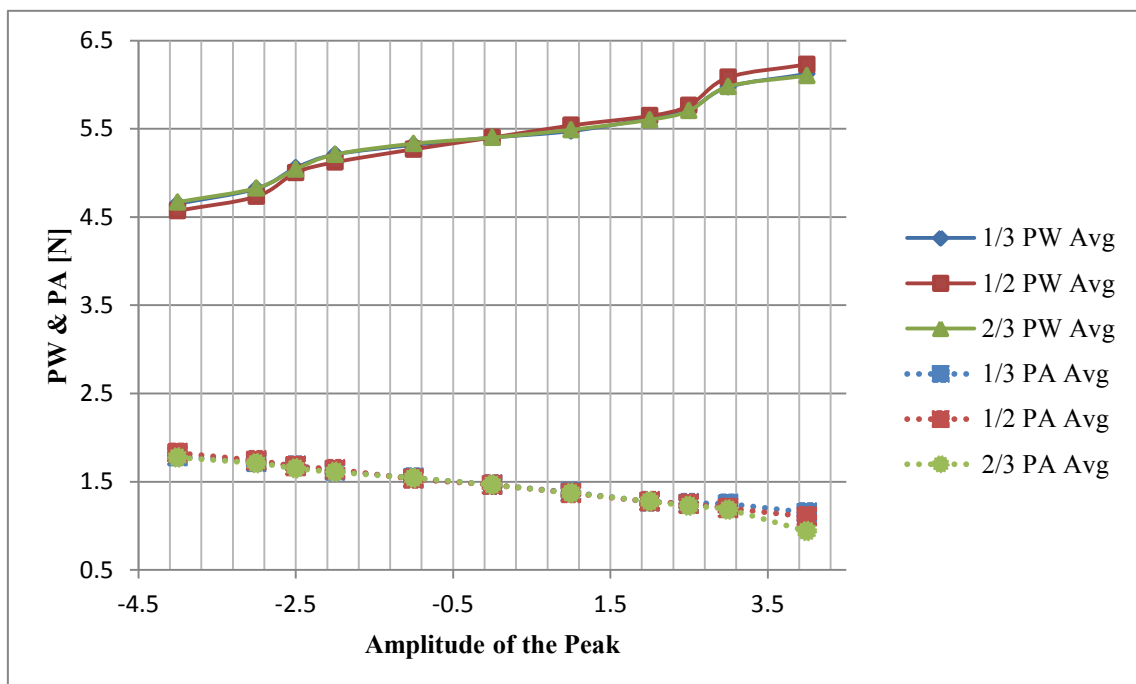


Fig.F.2 PW and PA Arranged by the Amplitude of the Peak ( $m_d=0.55$  kg,  $w_d=5.39$ N, Lifting)

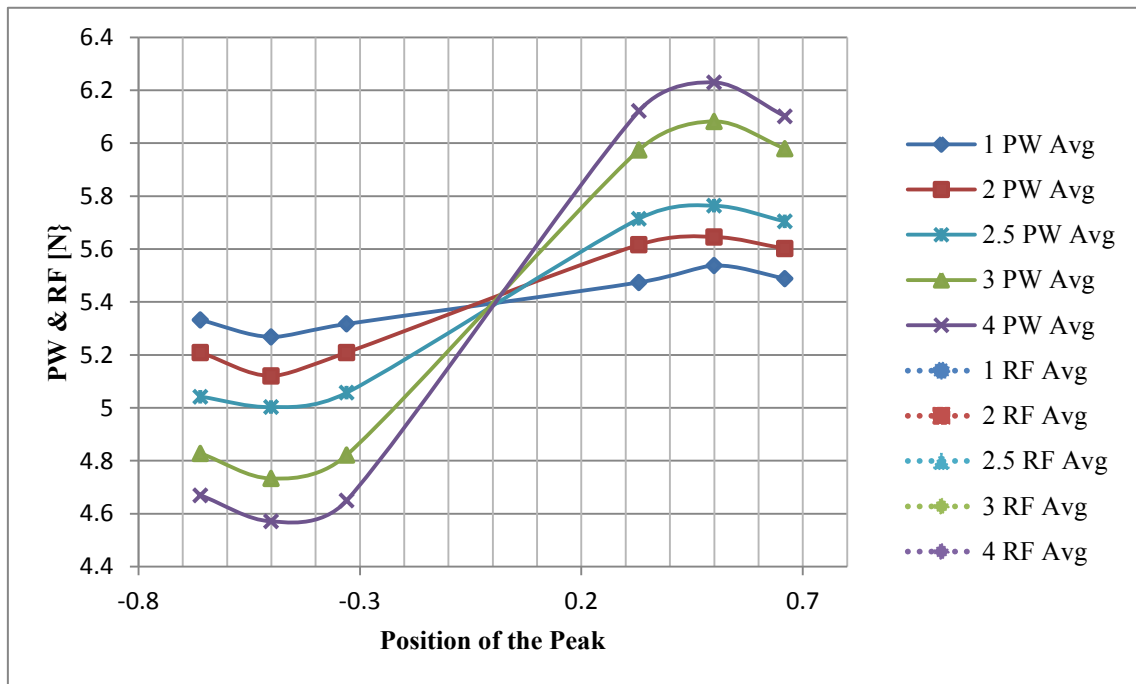


Fig.F.3 PW and RF Arranged by the Position of the Peak ( $m_d=0.55$  kg,  $w_d=5.39$ N, Lifting)

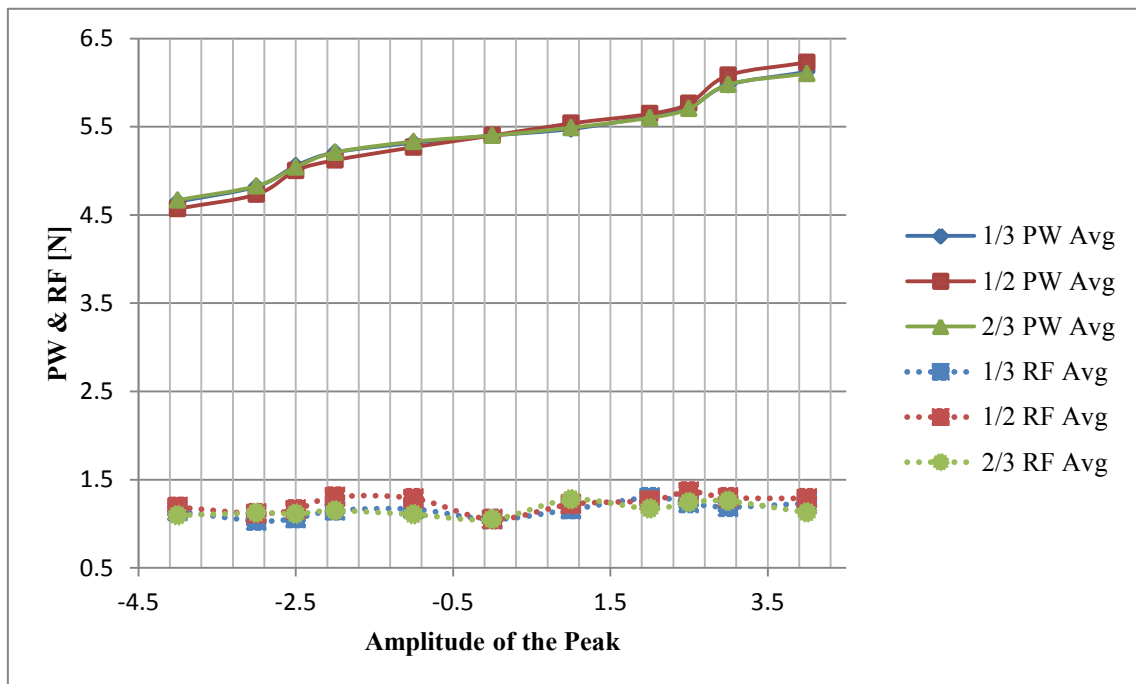


Fig.F.4 PW and RF Arranged by the Amplitude of the Peak ( $m_d=0.55$  kg,  $w_d=5.39$ N, Lifting)

**G. Comparisons between the PW and the Recorded Forces ( $m_d=0.55$  kg,  $w_d=5.39$ N, Time Length: Detaching Phase)**

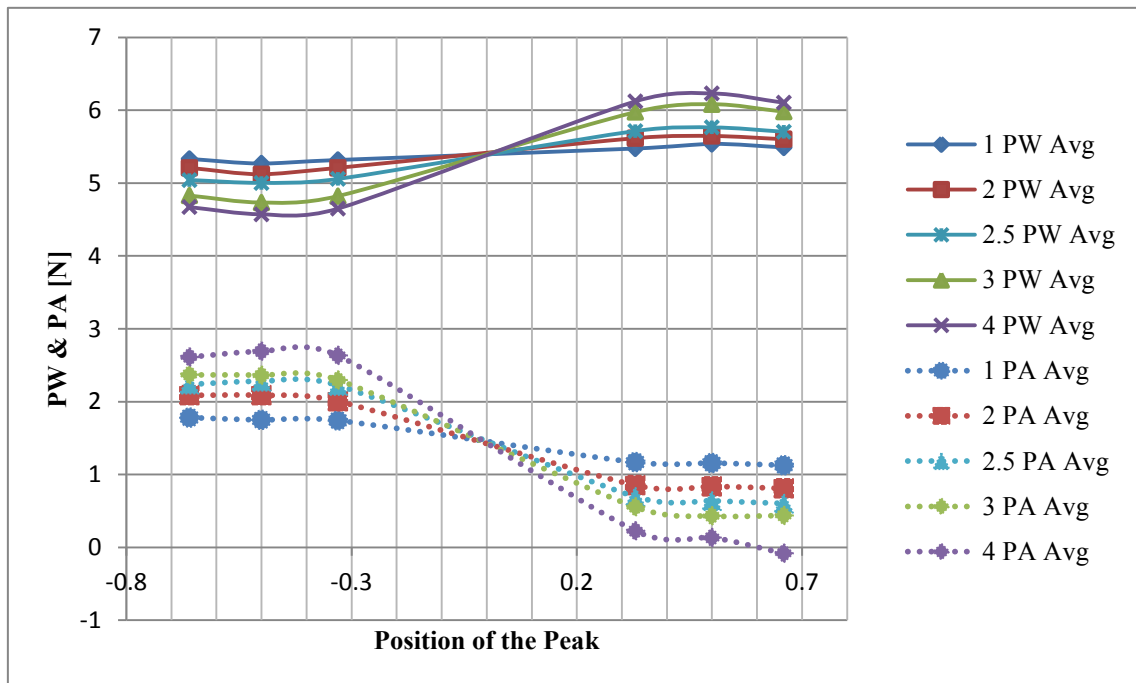


Fig.G.1 PW and PA Arranged by the Position of the Peak ( $m_d=0.55$  kg,  $w_d=5.39$ N, Detaching)

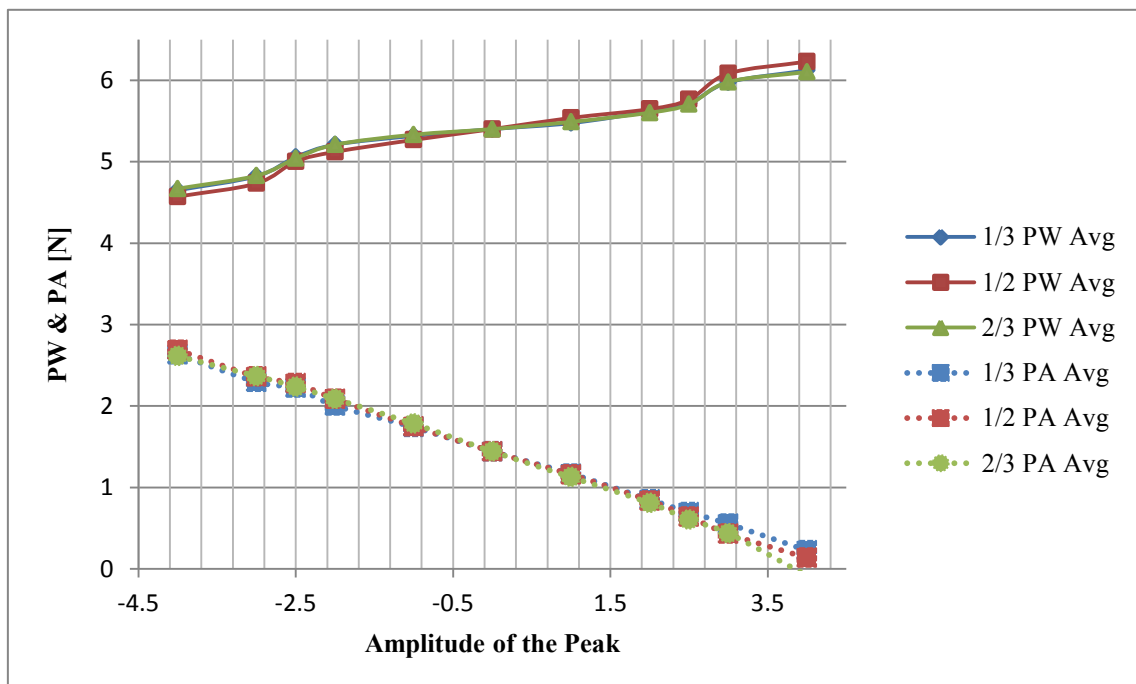


Fig.G.2 PW and PA Arranged by the Amplitude of the Peak ( $m_d=0.55$  kg,  $w_d=5.39$ N, Detaching)

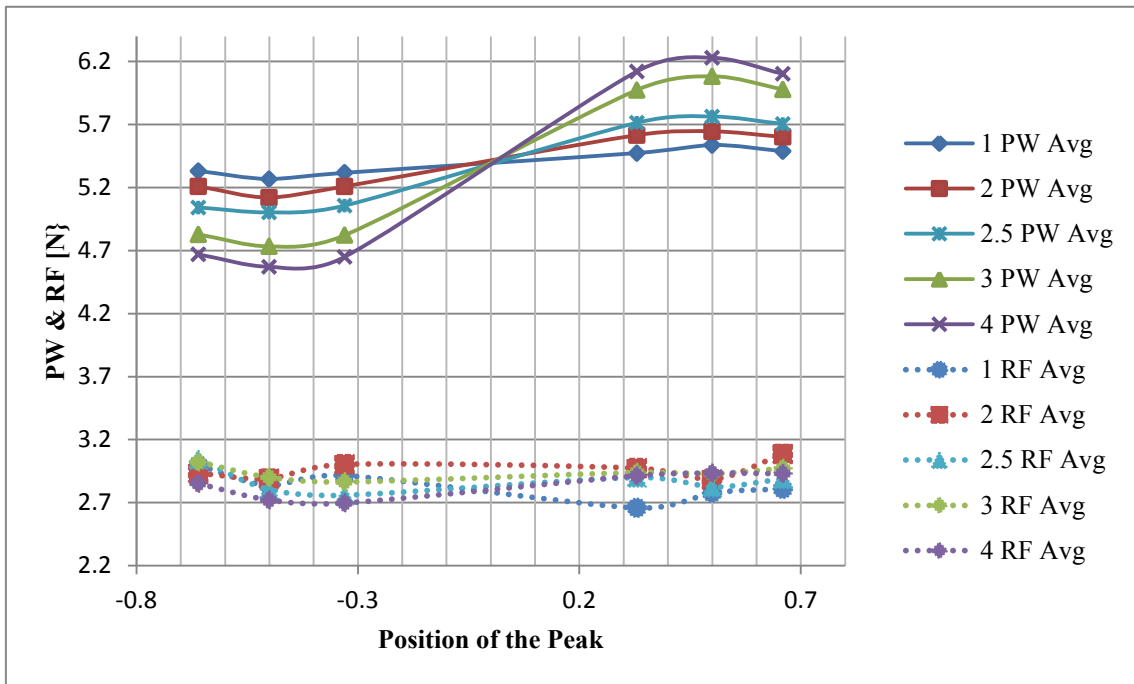


Fig.G.3 PW and RF Arranged by the Position of the Peak ( $m_d=0.55$  kg,  $w_d=5.39$ N, Detaching)

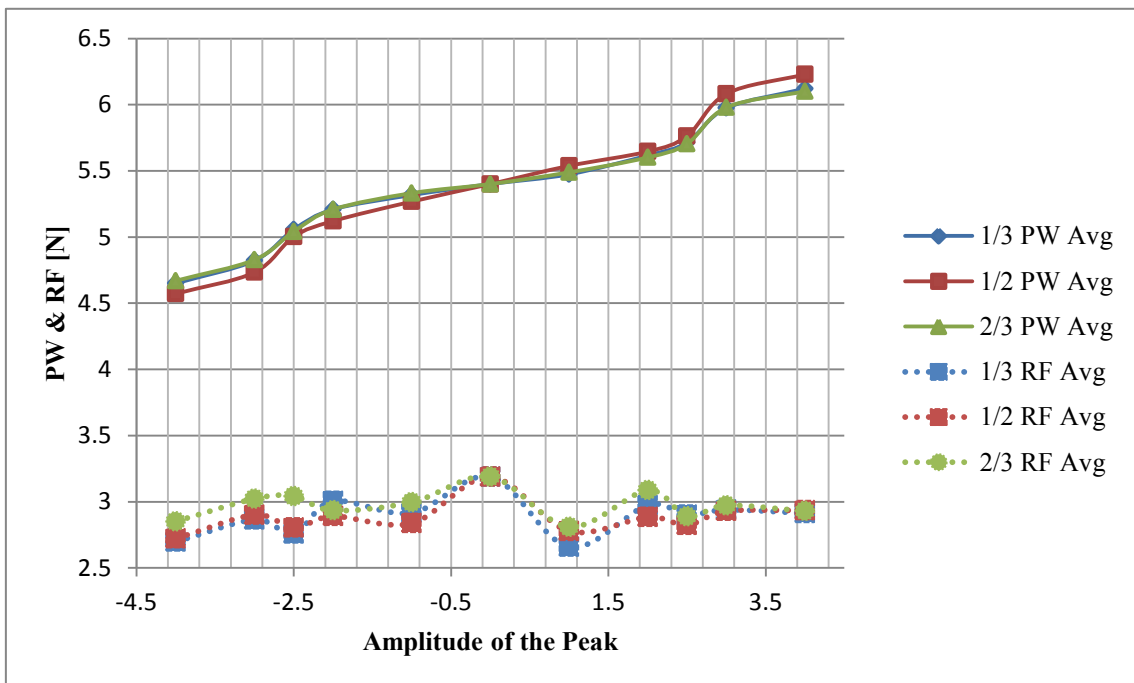


Fig.G.4 PW and RF Arranged by the Amplitude of the Peak ( $m_d=0.55$  kg,  $w_d=5.39$ N, Detaching)

---

## References

---

- [1] M. Hara, N. Ashitaka, N. Tambo, J. Huang and T. Yabuta, "Consideration of Weight Discriminative Powers for Various Weight Changes Using a Haptic Device," *IEEE/RSJ International Conference on Intelligent Robots and Systems Acropolis Nice, France*, September 2008.
- [2] Ph.D. JR. Block. (2002) Sandlot Science [What is an Illusion?]. [Online]. <http://www.sandlotscience.com/EyeonIllusions/whatisanillusion.htm>
- [3] A. Charpentier, "Analyse experimentale de quelques elements de la sensation de poids (Experimental study of some aspects of weight perception)," *Archives de Physiologie Normales et Pathologiques*, vol. 3, pp. 122-135, 1981.
- [4] G. Buckingham, "Getting a grip on heaviness perception: a review of weight illusions and their probable causes," *Exp Brain Res*, no. DOI 10.1007, 2014.
- [5] M. Hara, T. Higuchi, A. Ohtake, J. Huang, and T. Yabuta, "Influence of visually induced expectation on perceived motor effort: A visual–proprioceptive interaction at the Santa Cruz Mystery Spot," *Psychonomic Bulletin & Review*, 2005.
- [6] M. Hara, T. Higuchi, T. Yamagishi, N. Ashitaka, J. Huang and T. Yabuta, "Analysis of Human Weight Perception for Sudden Weight Changes during Lifting Task Using a Force Display Device," *IEEE International Conference on Robotics and Automation*, April 2007.
- [7] M.S Grandy and D.A. Westwood, "Opposite Perceptual and Sensorimotor Responses to a Size-Weight Illusion," *J. Neurophysiol*, no. DOI 10.1152, 2006.
- [8] K. Maruse, S. Kawai, and Y. Kakazu, "Design of Wearable Power-Assist Device for Lower Back Support," *Journal of Robotics and Mechatronics*, vol. 16, no. 5, 2004.
- [9] M. Yokozuka, T. Ogure, Y. Yamada, and K. Ozaki, "パワーアシスト装置のためのオンライン個人識別 [Online User Identification for a Power Assist Device]," *精密工学会誌 [Precision Engineering Journal]*, vol. 75, no. 9, 2009.
- [10] S.M.M. Rahman, R. Ikeura, M. Nobe and H. Sawai, "Design and control of a 1DOF power assist robot for lifting objects based on human operator's unimanual and bimanual weight discrimination," *Proceedings of the IEEE International Conference on Mechatronics and Automation (ICMA '09)*, pp. 3637-3644, August 2009.

- [11] T. Doi, H. Yamada, T. Ikemoto and H. Naratani, "Simulation of a pneumatic hand crane power-assist system," *Journal of Robotics and Mechatronics*, vol. 20, no. 6, pp. 896-902, 2008.
- [12] B. Bridgeman, "Analysis of Weight Perceptual Mechanism Based on Muscular Motion Using Virtual Reality," *IEEE International Conference on Systems, Man and Cybernetics*, 2005.
- [13] S.M.M. Rahman, R. Ikeura, S. Hayakawa and H. Sawai, "Design guidelines for power assist robots for lifting heavy objects considering weight perception, grasp differences and worst-cases," *Int. J. Mechatronics and Automation*, vol. 1, no. 1, 2011.
- [14] S.M.M. Rahman, R. Ikeura, S. Hayakawa and H. Yu, "Manipulating Objects with a Power Assist Robot in Linear Vertical and Harmonic Motion: Psychophysical-Biomechanical Approach to Analyzing Human Characteristics to Improve the Control," *Journal of Biomechanical Science and Engineering*, vol. 6, no. 5, 2011.
- [15] S. Ishibashi, R. Ikeura, S. Hayakawa and H. Sawai, "拘束条件を考慮した物体持ち上げ動作における重量知覚特性 (Characteristics of Weight Perception of Human in Motion of Lifting Objects Considering Restricted Condition)," *電気関係学会東海支部連合大会 (Institute of Electrical and Related Engineers Tokai-Section Joint Conference)*, 2011.
- [16] S.M.M. Rahman and R. Ikeura, "Estimating and Validating Relationships between Actual and Perceived Weights for Lifting Objects with a Power Assist Robot: The Psychophysical Approach," *International Symposium on Robotics and Intelligent Sensors 2012*, 2012.
- [17] C. U. M. Smith, *Biology of Sensory Systems*, 9780470694381st ed.: John Wiley & Sons, Ltd, 2008.

---

## Publications Based on the Contents of this Thesis

---

- I.J. Rodriguez Martinez, R. Ikeura, S. Hayakawa, “Characteristics of the human weight perception when lifting objects with a power assist system”, 2014 IEEE International Conference on Systems, Man and Cybernetics (SMC), 2014.
- T. Arizumi, I.J. Rodriguez Martinez, R. Ikeura, S. Hayakawa and H. Sawai, “Control of weight perception characteristics of lifting an object with a power assist device”, 日本機械学会東海支部第 64 期 総会 [Japan Society of Mechanical Engineers, Tokai Branch 64<sup>th</sup> Period Meeting], 2015.
- I.J. Rodriguez Martinez, R. Ikeura, S. Hayakawa, “Control Based on the Modification of the Relation between the Reaction Force and the Human Force and its Effects on the Weight Perception”, 2015 IEEE The 24th International Symposium on Robot and Human Interactive Communication (RO-MAN), Workshop [Social HRI: Overcoming Barriers Through Appearance, Behavior and Context-Based Design], 2015.